Dact genes in mouse kidney development

Wen-Chin Lee

Submitted for the degree of

Doctor of Philosophy

The University of Edinburgh

2008

TABLE OF CONTENTS

Declaration

I declare that:

(a) this thesis was composed by me;

(b) the work presented here is my own unless otherwise clearly stated; and

(c) the work has not been submitted for any other degree or professional qualification

_____

Wen-Chin Lee

Acknowledgements

There are many people to whom I would like to express my deepest appreciation. Without them, the PhD project would have been impossible. Firstly, I would like to thank my supervisor Prof. Jamie Davies, for his invaluable guidance, inspiration and encouragement throughout the course of this study. Special thank must go to Jamie for encouraging me to present my work in the well-known international conferences and for his great advice during the write up of the thesis. I would also like to show my appreciation to Dr. John West and Dr. Cathy Abbott, who is my second supervisor, for their insightful comments on my thesis committee meeting.

I am grateful to all members in Davies group who create such a friendly and warm atmosphere at work. To Darren, Derina, Marc, Shelagh, Markus, Janes, Sue, Chris, Mathieu, Shrobona, Nils, Veronica for the informative discussion on kidney development, the technical consultations and enjoyable chats on life, on Edinburgh, on Europe, on India and on Taiwan.

Thanks will go to people who helped me with the wide-range of techniques involved in this study: Ms. Linda Wilson and Ms. Trudi Gillespie for the help of confocal microscopy; Dr. Paul Perry and Dr. You-Ying Chau for the never ending willingness to help in time-lapse imaging and Grace for the tissue embedding.

I have to say a big Thank You to all my colleagues in Taiwan for the encouragement of doing basic scientific research, for looking after my patients, and for the prompt and high standard medical service to my family when they need.

Finally, I would like to take this opportunity to thank my parents for the encouragement and support; thank my wife, Chia-Ping, for her love and emotional support when I needed to be cheered up and thank my lovely daughter, Yun-Chien, for the patience on my absence in the past three months.

List of Abbreviations

2D	two dimensional
3D	three dimensional
ADP	adenosine diphosphate
ANOVA	analysis of variance
APC	adenomatous polyposis coli
ARF	ADP-ribosylation factor
ASD	Alternative Splicing Database
ASTD	Alternative Splicing and Transcript Diversity
ATRA	all-*trans* retinoic acid
BAC	bacterial artificial chromosome
BCIP	5-bromo-4-chloro-3'-indolyl phosphate p-toluidine salt
BMP	bone morphogenetic protein
bp	base pair
BrdU	bromodeoxyuridine
BSA	bovine serum albumin
CAT	collective amoeboid transition
CC	cap condensates
cDNA	complementary deoxyribonucleic acid
CHAPS	3-[(3-cholamidopropyl)dimethyl-ammonio]-1-propanesulfonate
CLF	cytokine-like factor
CLC	cardiotrophin-like cytokine
DEPC	diethyl pyrocarbonate
DIG	digoxigenin
DMEM	Dulbecco's modified Eagle's medium
DNA	deoxyribonucleic acid
dNTP	deoxyribonucleotide triphosphate
DTT	dithiotretol
E	embryonic day
E. coli	*Escherichia coli*
ECM	extracellular matrix

EDTA	ethylenediaminetetraacetic acid
EGF	epidermal growth factor
EpCAM	epithelial cell adhesion molecule
ERK	extracellular signal-regulated kinase
EST	expressed sequence tag
FGF	fibroblast growth factor
FITC	fluorescein isothiocyanate
GAPDH	glyceraldehyde-3-phosphate dehydrogenase
GDF	growth differentiation factor
GDNF	glial derived neurotrophic factor
GFP	green fluorescent protein
Gfrα	glial derived neurotrophic factor receptor alpha
GSK	glycogen synthase kinase
GUDMAP	The GenitoUrinary Development Molecular Anatomy Project
HGF	hepatocyte growth factor
HSPG	heparan sulfate proteoglycan
IF	immunofluorescence
IGF	insulin-like growth factor
JNK	c-Jun N-terminal kinase
LB	Laria-Bertani
LDL	low-density lipoprotein
LEF	lymphoid enhancer factor
LIF	leukaemia inhibitory factor
LRP	LDL receptor-related protein
LM	loose mesenchyme
MAB	maleic acid buffer
MABT	maleic acid buffer Tween-20
MAP	mitogen-activated protein
MDCK	Madin-Darby canine kidney
MEM	Eagle's minimum essential medium
MET	mesenchyme-to-epithelia transition
mIMCD	murine inner medullary collecting duct

MMP	matrix metalloproteinase
mRNA	messenger ribonucleic acid
NBT	nitro-blue tetrazolium chloride
NC	negative control
NCBI	National Center for Biotechnology Information
NKCC	sodium-potassium-chloride cotransporter
NTC	no template control
PCNA	proliferating cell nuclear antigen
PCR	polymerase chain reaction
PDGF	platelet-derived growth factor
PFA	paraformaldehyde
PhD	Doctor of Philosophy
PI3K	phosphatidylinositol 3-kinase
PRKX	protein kinase X
RA	retinoic acid
Rar	retinoic acid receptor
RARE	retinoic acid response element
RISC	RNA-induced silencing complex
RNA	ribonucleic acid
RNAi	RNA interference
ROCK	Rho-associated protein kinase
rpm	revolutions per minute
RT	reverse transcriptase
SDS	sodium dodecyl sulfate
SEM	standard error of the mean
sFRP	secreted frizzled-related protein
Shh	sonic hedgehog
shRNA	short-hairpin RNA
siRNA	small interfering ribonucleic acid
SP	splicing pattern
SSC	saline sodium citrate
Taq	*Thermus aquaticus*

TBE	tris-borate-EDTA
TBS	tris-buffered saline
TCF	T-cell factor
TEA	triethanolamine
TGF	transforming growth factor
TRITC	tetramethyl rhodamine iso-thiocyanate
tRNA	transfer ribonucleic acid
UB	ureteric bud
URL	uniform resource locator
UTR	untranslated region
UV	ultraviolet

List of Tables

List of Figures

Gene symbol nomenclature

In this thesis, mouse gene and protein symbols are written according to the guidelines published on the Mouse Genome Informatics website (http://www.informatics.jax.org/mgihome/nomen/short_gene.shtml). These guidelines follow the rules established by the International Committee on Standardized Genetic Nomenclature for Mice and are implemented through the Mouse Genomic Nomenclature Committee. Mouse gene symbols begin with an uppercase letter followed by all lowercase letters and are italicised. Protein symbols use all uppercase letters and are not italicised. Human genes are stated by using all uppercase letters and are italicised.

Preface

Mammalian kidney development was one of the sections in anatomy and embryology, which was the central medical discipline I learnt in the medical college. It offered me fundamental knowledge behind renal physiology and pathology to enable me better to manage the diverse clinical problems of nephrology. However, every time that I encounter patients with end stage renal disease, renal cancer or a congenital anomaly of the urinary system, I can only offer them medical services specified by current treatment guidelines. Unfortunately, even the most up-to-date treatment guidelines are a compromise between existing knowledge and the clinical facilities developed so far. In order to do something more than simply following treatment guidelines, I feel the key in extending the knowledge we have about diseases and hence improving the methods of treatment lies in basic medical research. Mammalian kidney development is central to the pathomechanisms of all three of these miserable diseases and this therefore brought me from the bedside back to the bench.

Abstract

Mammalian kidney development proceeds through a series of interactions among metanephric mesenchyme, ureteric bud, extracellular matrix, growth factors and various other signalling molecules. These complex, but well integrated, networks control cell proliferation, differentiation, migration and survival and thus orchestrate kidney development. More and more molecules in these networks have been identified since the past few years. Therefore, it is crucial to explore their functions and the mechanisms by which they work to fill the research gaps. DACTs have recently been reported as pathway-specific regulators in WNT signalling, known to be important in kidney development, but their expressions and functions in mammalian kidneys are yet to be elucidated. The aims of this thesis are to describe the expression patterns of these two new genes, *Dact1* and *Dact2*, in mouse embryonic kidneys and to further investigate their functional roles by applying RNAi to cell culture-based models. The first goal of this thesis is to establish the temporospatial expression patterns of *Dact1* and *Dact2* in kidneys by conventional end-point RT-PCR, quantitative real time PCR and RNA *in situ* hybridisation. Based on the expression patterns and preliminary observations in cell cultures, I hypothesize that *Dact1* regulates cell proliferation while *Dact2* governs cell migration. Experiments including siRNA transfection, BrdU proliferation assay, generation of stable cell lines expressing *Dact2* shRNA and wound assay, are designed to test these hypotheses and the results may offer implications of functional roles of both molecules in kidney development. The results obtained are as follows.

- *Dact1* and *Dact2* show different temporal expression patterns in mouse kidneys. In adult kidneys, *Dact1* is greatly downregulated while *Dact2* is still expressed at a comparable level to that at E14.5.
- *Dact1* is initially expressed in metanephric mesenchyme and, as development proceeds, shows a characteristic pattern of renal stroma whilst *Dact2* is exclusively expressed in ureteric buds throughout embryonic stages.
- *Dact1* and *Dact2* expressions are regulated by known regulators of kidney development including retinoic acid and chlorate.

- Silencing of *Dact1* facilitates proliferation of embryonic cells.
- Silencing of *Dact2* hinders migration of renal collecting duct cells.

Taken together, I have characterised temporospatial expression patterns of *Dact1* and *Dact2* in kidneys and provided evidences of functional roles of both novel molecules in cell cultures. Based on this thesis, further studies on *Dact1* and *Dact2* using either *in vitro* or *in vivo* mammalian kidney models will offer more insights into their functions and regulations in renal organogenesis.

Chapter 1

Literature review

1.1 Introduction

There has been a growing body of research on kidney development since the nineteenth century. Mammalian kidney development can be approached from several angles such as anatomical structure, genetics, mechanisms, and signalling pathways. During the past two decades, more and more novel molecules in kidney development have been identified. The trend of research in this field is to move towards its molecular basis. Great efforts have been made to integrate these emerging results into a public online database, GUDMAP (The GenitoUrinary Development Molecular Anatomy Project), which can be found at the URL: http://www.gudmap.org/ (Little et al., 2007).

This thesis is about two novel genes, *Dact1* and *Dact2*, in mouse kidney development. The aim of this thesis is to characterise the expression patterns and the functional roles of these two genes in mouse kidney development. Therefore, as an introduction, I will present an overview of mammalian kidney development, describe its basic mechanisms including cell proliferation, differentiation, migration and survival, review crucial molecules and signalling pathways and finally introduce background knowledge of these two genes.

1.2 Overview of mammalian kidney development

During mammalian kidney development, three types of kidneys develop successively. They are the pronephros, mesonephros and the metanephros (Figure 1-1). All of them are derived from the intermediate mesoderm. The first two are transient structures while the metanephros eventually differentiates into the permanent kidney. The pronephros forms as early as embryonic day eight (E8) in the mouse and E22 in the human (O'Rahilly and Muecke, 1972; Saxen, 1987). The pronephric duct originates from the cranial region of the intermediate mesoderm just ventral to the somites. As the cells of this duct migrate caudally, the anterior portion of the duct induces the adjacent mesenchyme to form the pronephric tubules. The pronephros is characterised by its vascularised structure, the glomus, which filters waste into the

coelomic cavity. The pronephric tubules and most of the pronephric ducts degenerate but the caudal portion of the duct becomes part of the later excretory system and is referred to as the Wolffian duct (Kuure *et al.*, 2000; Vize *et al.*, 2003).

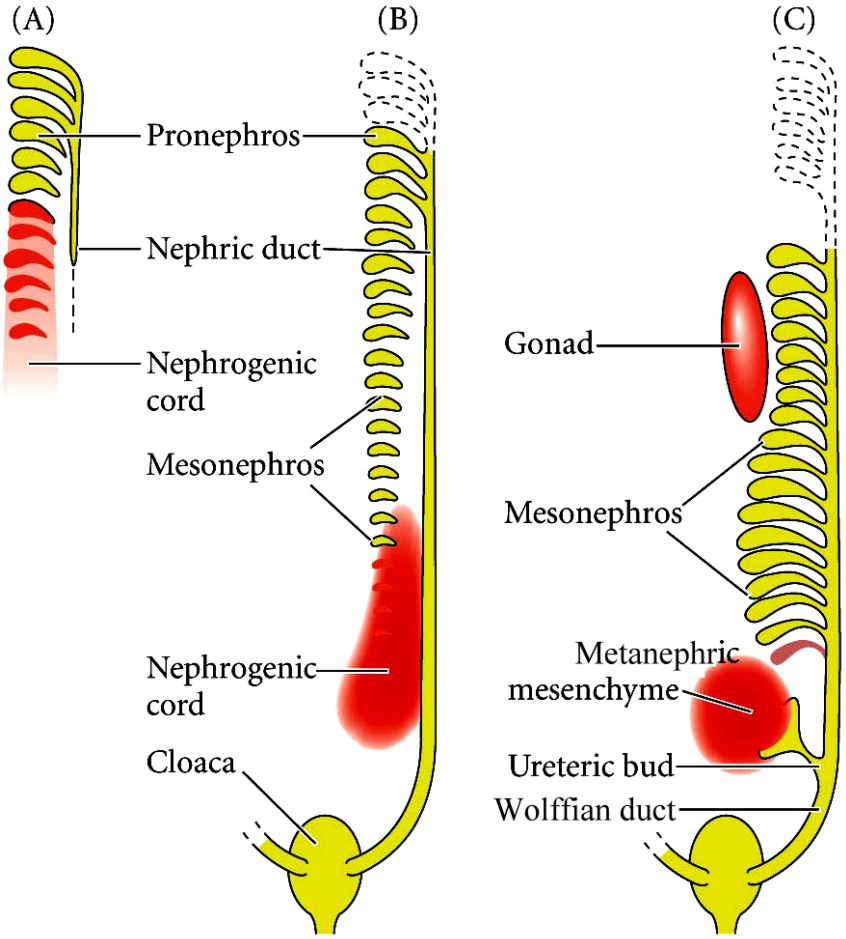

Figure 1-1 Mammalian kidney development. (A) Kidney development starts from pronephros formation. (B) As nephric duct migrates caudally and induces mesonephric tubule formation, the pronephros degenerates. (C) The metanephros is induced by the ureteric bud originating from the outgrowth of the Wolffian duct (Modified from Gilbert, 2006).

As the pronephric tubules degenerate, the middle portion of the nephric duct induces the presumptive mesonephric mesenchyme to condense and form a new set of tubules constituting the mesonephros (Saxen, 1987). This process begins at E9 in the mouse and E24 in the human (O'Rahilly and Muecke, 1972; Saxen, 1987). Mammalian mesonephric nephrons consist of glomeruli-like structures and proximal

and distal tubules. In humans, mesonephric nephrons are functional excretory organs during embryogenesis whereas the murine mesonephros is a non-excretory organ (Smith and Mackay, 1991). As development proceeds, more tubules form caudally but the anterior ones degenerate through apoptosis. In female mammals, mesonephroi eventually disappear whilst in male mammals some of the mesonephric tubules remain and form the vas deferens and efferent ducts of the testes (Sainio, 2003a; Saxen, 1987).

The metanephros begins to form at E10.5 in the mouse and E32 of human gestation (O'Rahilly and Muecke, 1972; Saxen, 1987). At this stage an unbranched epithelial tube called the ureteric bud (UB) sprouts from the posterior end of the Wolffian duct at the level of the hindlimb. The UB extends towards and invades a distinct region of the intermediate mesoderm called the metanephric mesenchyme. On invasion, reciprocal induction happens between these two primordia. The UB is induced to branch dichotomously and undergoes branching morphogenesis within the metanephric mesenchyme. The branching ureteric buds finally form a tree-like arrangement, which is the collecting system of the kidney. The tips of the branching tree send out inductive signals to the surrounding mesenchyme. Once induced, the metanephric mesenchyme condenses at the tips of the ureteric buds. These condensed mesenchymal cells then form cell aggregates and undergo mesenchyme-to-epithelia transition (MET) to form renal vesicles, comma-shaped and S-shaped bodies. The S-shaped bodies will further differentiate and also they fuse with the ureteric bud-derived collecting ducts to form the nephrons, the functional units of the kidney (Bard, 2003; Saxen, 1987). This process is depicted in Figure 1-2. In addition to epithelisation, some mesenchymal cells die via apoptosis and others follow the fates of endothelial cells, smooth muscle cells, neuronal cells and renal stroma (Sariola et al., 2003a).

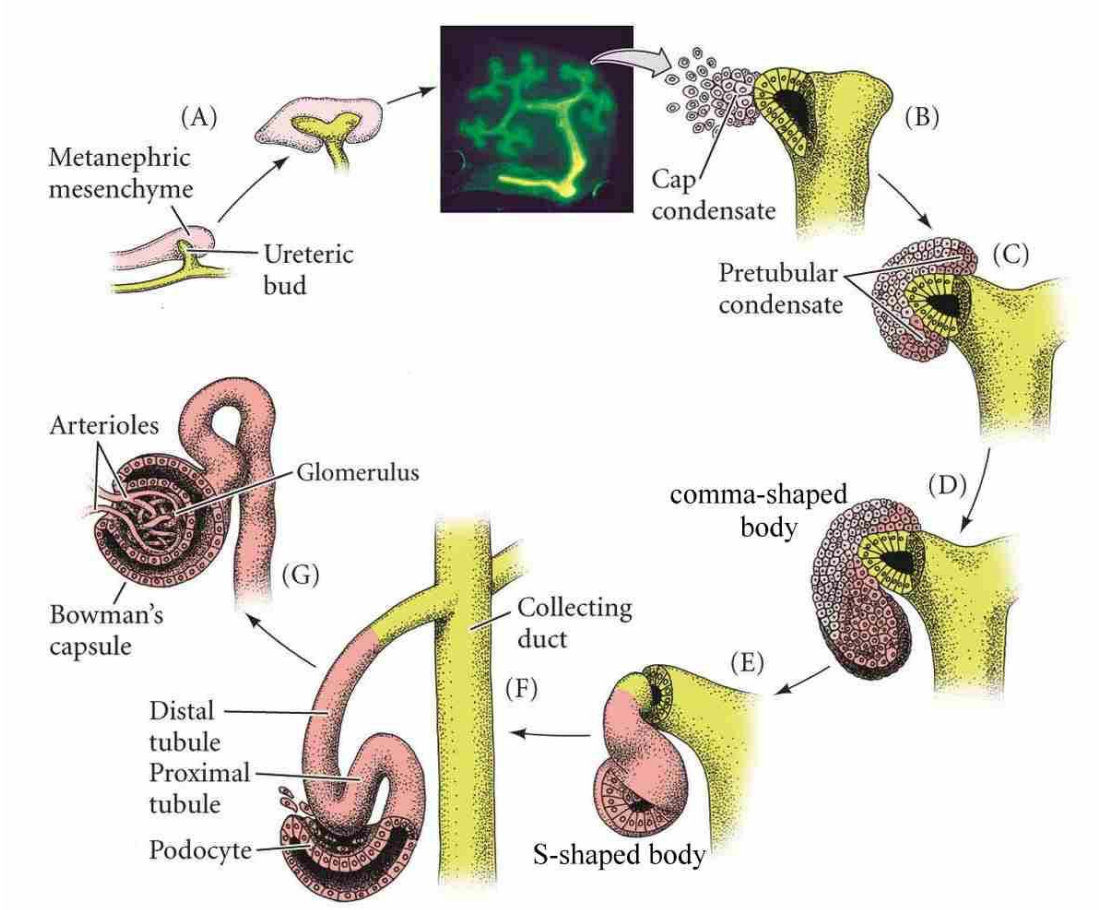

Figure 1-2 Development of metanephroi. The development of metanephros occurs from the reciprocal induction between the UB and the metanephric mesenchyme (A). As the development proceeds, some of the induced mesenchymal cells form the cap condensate at the UB tips (B) and turn into pretubular condensate (C), comma-shaped body (D), and S-shaped body (E). The distal end of the S-shaped body fuses with the collecting duct (F) and the whole structure eventually differentiated into a a mature nephron (G) (Modified from Gilbert, 2006).

This overview section has outlined the three phases of mammalian kidney development by describing their anatomical structures in a temporal sequence. The development of the three major compartments of the metanephric kidney (*i.e.* the UB, metanephric mesenchyme and renal stroma) is described in more detail in the following sections. Furthermore, as knowledge of kidney development has been greatly extended from anatomical structures into molecular bases over the last two decades, developmental biologists have been devoting much time to characterising expression of these molecules, exploring their functions and investigating the mechanisms by which they work to render a coordinated process for kidney

development. For the better understanding of key developmental events within and between each compartment, the following sections will describe them on a molecular level. This background knowledge is central to the study of new genes (*i.e. Dact1* and *Dact2* in this thesis) that may play roles in these developmental events.

1.2.1 UB development

UB development consists of a series of developmental events. Anatomically, these events include the outgrowth of the UB from the Wolffian duct, the elongation of the UB and the iterative branching. Genetic studies and data from *in vitro* systems have offered great understanding into the functions of specific molecules in these events. The accumulating data from these studies have elucidated a delicate molecular network that underlies development. Table 1-1 summarises principal molecules involved in UB development.

Table 1-1 Principal molecules involved in UB development

Molecules	Function in UB development	References
GDNF/Ret/GFRα1	Induction of UB outgrowth from Wolffian duct and maintenance of UB branching	(Cacalano *et al.*, 1998; Moore *et al.*, 1996; Pichel *et al.*, 1996; Schuchardt *et al.*, 1994)
BMP2, BMP7	BMP2 and high doses of BMP7 inhibit branching whilst low doses of BMP7 simulate branching	(Piscione *et al.*, 1997)
Activin A	Inhibits branching	(Ritvos *et al.*, 1995)
TGFβ	Delays branching while allowing elongation	(Bush *et al.*, 2004; Ritvos *et al.*, 1995)
HGF	Supports elongation (but transgenic knockout is normal)	(Davies et al., 1995; Uehara et al., 1995; Woolf et al., 1995)
HSPG	Required for branching and elongation	(Davies et al., 1995)
Integrins	Required for branching and elongation	(Kreidberg et al., 1996; Muller et al., 1997)
MMP9	Required elongation (but transgenic knockout is normal)	(Andrews et al., 2000; Lelongt et al., 1997)
MAP-kinase	Positive regulator of branching; downstream of GDNF	(Fisher et al., 2001)
Protein kinase A	Negative regulator of branching	(Gupta et al., 1999)
Protein kinase C	Positive regulator of branching	(Araki et al., 2003; Davies et al., 1995)

In parallel to studies on the molecular network, by analyzing the morphometric parameters, Cebrian *et al.* found that both the UB tip numbers and the branching events increased rapidly from E11.5 to E15.5 and then slowed down until birth (Cebrian et al., 2004). This would suggest that there may be distinct regulatory mechanisms for UB branching during different developmental stages. In addition, microarray data suggest that global gene expression patterns change in concert with specific developmental stages (Stuart et al., 2001; 2003). Therefore, as some investigators have suggested, the UB development can be considered as several discrete stages. These stages could be classified as the initial outgrowth of the UB (Stage I), early rapid branching (Stage II), late branching and maturation (Stage III) and branching termination (Stage IV) (Figure 1-3) (Sampogna and Nigam, 2004; Shah et al., 2004). Although how many stages ought to be considered is still debatable (Monte et al., 2007), this staging system, together with studies that aim to define the functional roles of specific molecules, (Table 1-1) help to provide a deeper insight into factors that control UB development.

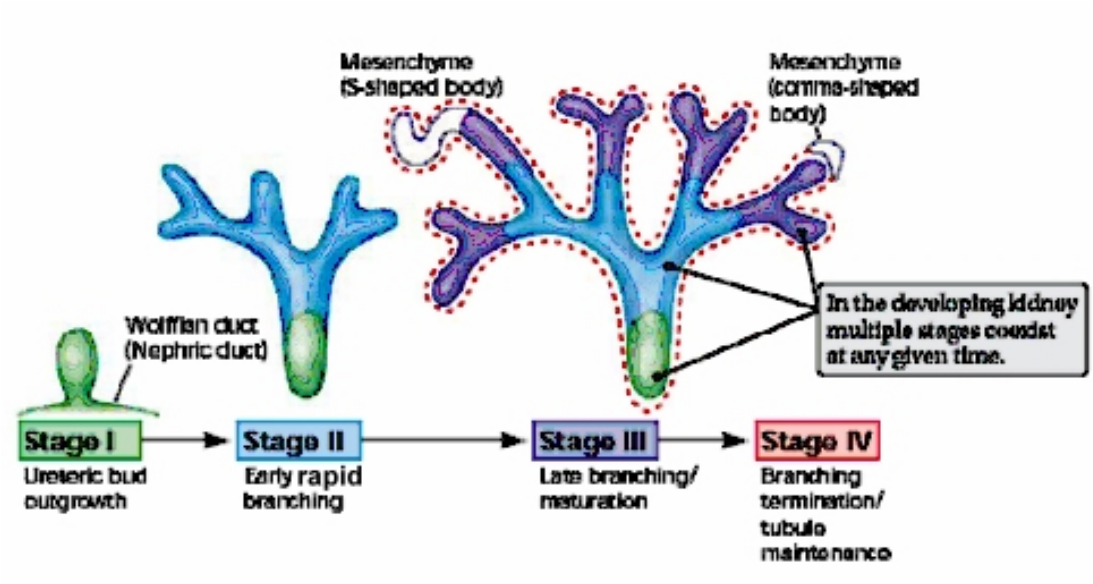

Figure 1-3 Stages of UB development (Adapted from Sampogna and Nigam, 2004).

In this staging system, stage I is characterised by the outgrowth of the UB from the Wolffian duct. Many genes required for this developmental event are linked to GDNF signalling. Examples include *Eya1*, *Pax2*, *Hox11, Six1* and *Sall1*. *Six1* and

Sall1 mutant embryos show reduced *Gdnf* expression and incomplete UB outgrowth (Nishinakamura et al., 2001; Xu et al., 2003). Embryos mutant for *Eya1*, *Pax2* or *Hox11* paralogous genes show loss of *Gdnf* expression and thus have no UB (Brophy et al., 2001; Wellik et al., 2002; Xu et al., 1999).

Stage II is characterised by rapid branching of the ureteric buds. In this stage, factors that promote growth and branching are thought to be highly active. Stage III is the period when growth and branching are slowed down by predominantly inhibitory molecules that offer negative feedback information. Principal molecules involved in stage II and III are summarised in Table 1-1 and depicted in Figure 1-4. In addition to these molecules, a wealth of genes has been reported to control the iterative branching and elongation and is reviewed comprehensively elsewhere (Shah et al., 2004). Finally, in stage IV when the ureteric tree reaches certain size and maturity, branching is terminated probably by the inhibitory molecules such as TGFβ (Bush et al., 2004).

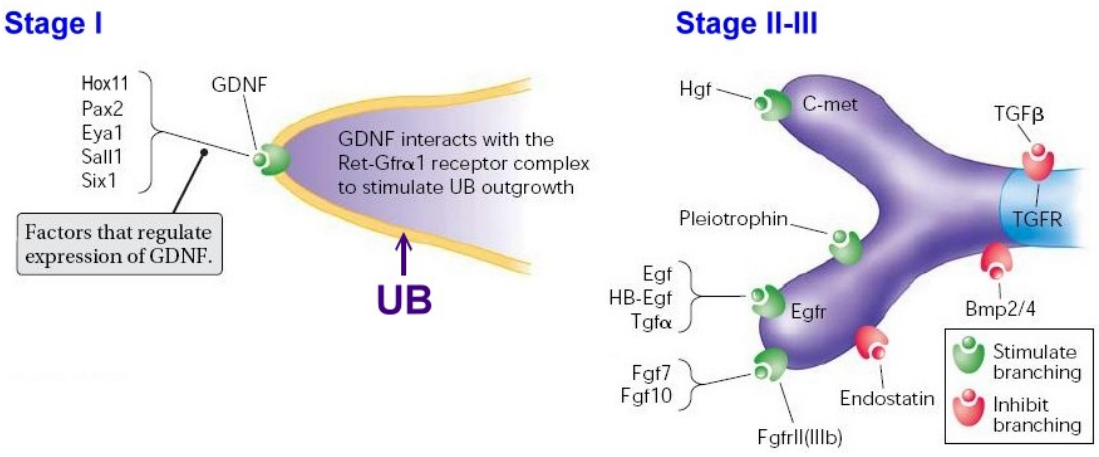

Figure 1-4 Factors involved in UB development. At stage I, genes that regulate the expression of GDNF are required for the UB outgrowth. GDNF binds to the Ret/Gfrα1 receptor complex to stimulate this developmental event. During stage II-III, many molecules and pathways are involved. Branch-stimulating factors (green) favour a feed-forward iterative branching state (stage II); increasing expression of branching inhibitors (red) slows down branching via negative-feedback mechanisms (stage III). Signals to stop branching at stage IV are yet to be defined. Some branching inhibitors such as TGFβ may be involved (Adapted from Sampogna and Nigam, 2004).

1.2.2 Nephron induction and differentiation

The metanephric mesenchyme consists of numerous morphologically similar cells which show different gene expression patterns and may eventually follow different fates to form secretory nephrons, endothelial cells, juxtaglomerular complex, vascular smooth muscle cells, neuronal cells and embryonic renal stroma (Sariola et al., 2003b). When the UB invades the metanephric mesenchyme, it sends out inductive signals to the surrounding mesenchyme. In response to these inductive signals, a subset of mesenchymal cells condenses, undergoes MET and eventually differentiates into nephrons following an intrinsic differentiation programme in the metanephric mesenchyme. The induction and differentiation of nephrons happen repeatedly throughout the whole process of metanephric kidney development and eventually generate adequate number of nephrons, which is about 1600 nephrons in newborn mice (Yuan et al., 2000).

As research in kidney development has progressed into a molecular level, a key question about nephron induction is what these inductive signals are. One strategy to find the inductive molecules is to culture the metanephric mesenchyme together with cells expressing various WNT proteins or other potential inducers and look for nephron formation (details of WNT signalling is described in section 1.4.1). Combined data from these cellular assays with *Wnt* genes' expression patterns in developing kidneys have identified WNT6 and WNT9b as probable inducers (Carroll et al., 2005; Itaranta et al., 2002; Kispert et al., 1998). Another strategy is to purify factors from rat UB cell lines. This approach identifies a cocktail of factors including leukaemia inhibitory factor (LIF), TGFβ2, TGFα, and fibroblast growth factor 2 (FGF2) (Barasch et al., 1999; Karavanova et al., 1996; Plisov et al., 2001). A new strategy is built on microarray analysis to find out UB tip-derived secreted molecules. This method led to the discovery of CLF-1, which is capable of inducing nephron formation in cultured mesenchyme by binding its ligand, CLC (Schmidt-Ott et al., 2005).

In addition to the inductive signals, nephron induction also relies on many genes expressed by the mesenchyme including *Pax2*, *Wt1* and *Six1*. Metanephric mesenchyme mutant for *Pax2*, *Wt1*, or *Six1* completely fail to form nephrons in tissue recombination experiments (Brophy et al., 2001; Donovan et al., 1999; Xu et al., 2003). A schematic diagram for this induction process is shown in Figure 1-5 (A).

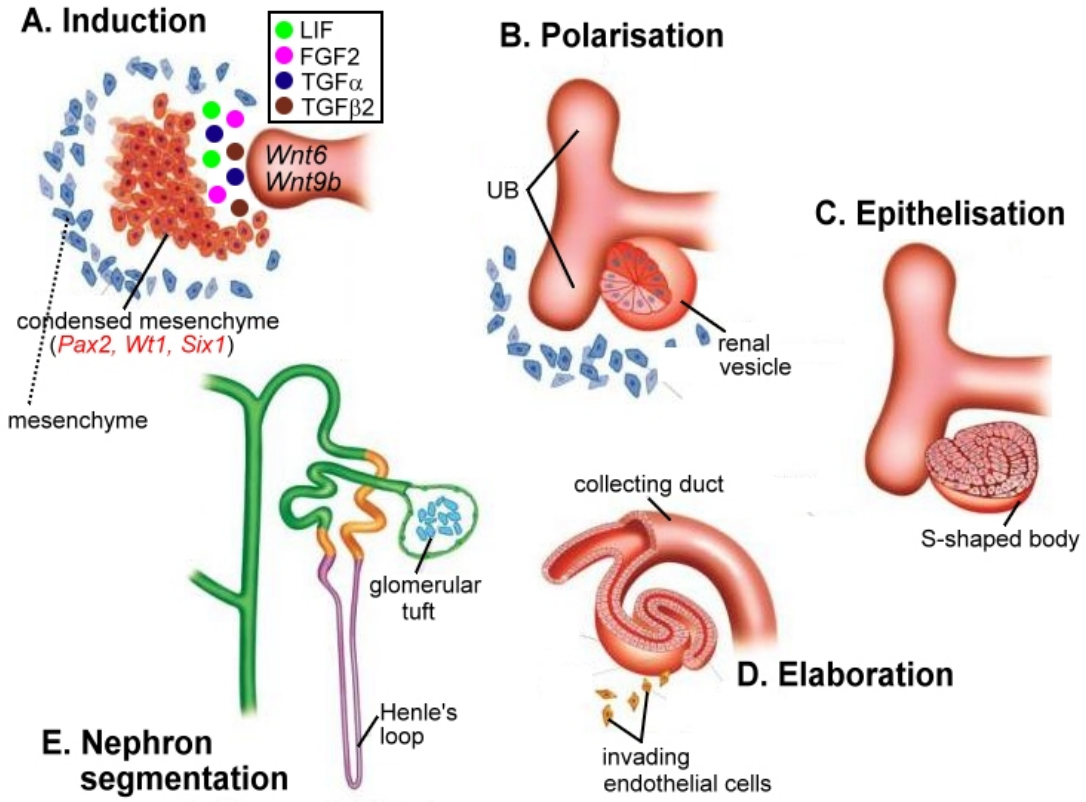

Figure 1-5 Nephron development. Schematic diagram outlines the process of nephron development. Nephron induction (A) depends on inductive signals and several mesenchymal genes. Once induced, cells begin to show signs of epithelial polarisation and form the renal vesicle (B). The polarised renal vesicle elongates and forms the S-shaped body (C). At the stage of elaboration (D), endothelial cells infiltrate the distal end of the S-shaped body. Finally, segmentation occurs along the proximal-distal axis of tubular epithelia (E) (Adapted from Cho and Dressler, 2003).

Once induced, the metanephrogenic mesenchymal cells undergo MET and eventually differentiate into nephrons. This process consists of several developmental events including polarisation, epithelisation, elaboration and segmentation of the nephron (Figure 1-5). By changing cell adhesion properties, cells are able to aggregate around

the ureteric bud tips. These cell aggregates proliferate and begin to show signs of epithelial cell polarity. They begin to express proteins associated with adherens and tight junctions, adopt a more columnar shape, and form a small lumen. The whole structure at this stage is called a renal vesicle. An epithelial basement membrane is then laid down around the growing vesicle, which remains associated with the UB epithelia. The vesicle develops clefts and changes into comma- and S-shaped bodies. By the S-shaped body stage, the distal end of the developing nephron has fused to the epithelium of the collecting duct to form a continuous lumen. Factors that drive MET include those that control cell aggregation and adhesion and cell-matrix interactions. For example, in kidney organ culture, the exogenous Fab fragment of antibody against cadherin6 inhibits cell adhesion and thus blocks the formation of comma- and S-shaped bodies (Cho et al., 1998). At the stage of S-shaped body, its distal end is invaded by endothelial precursor cells. As the nephron develops further, segmentation occurs along the proximal-distal axis of tubular epithelia. This is demonstrated by segment-specific gene expression of cadherins, integrins and laminins (Cho and Dressler, 2003). The factors controlling nephron segmentation probably include the regional expression of transcriptional factors (e.g. *Lim1* and *Brn1*) along this axis and the Notch signalling pathway (Cheng et al., 2007; Kobayashi et al., 2005; Nakai et al., 2003).

1.2.3 Development of renal stroma

When the mesenchymal cells around the ureteric tip condense, some subsets of mesenchymal cells adopt the fate of forming the renal stroma. The condensed cap mesenchymal cells express *Pax2* and finally differentiate into nephrons. By E11, a region peripheral to the condensed cap mesenchyme forms as a looser domain of cells. These cells express *Foxd1* and are presumptive stromal progenitor cells (Hatini et al., 1996). By E12-13, in addition to the stromal progenitor cells which are located in the nephrogenic zone, stromal cells surround the epithelial components of the developing kidney. These stromal cells are characterised by their large fibroblastic spindle shape with clear cytoplasm and are referred to as the primary interstitium (Sariola et al., 2003a). Primary interstitial cells express the cell surface glycolipid

GD3 (Sariola et al., 1988), Tenascin C (*Tnc*) (Ekblom and Weller, 1991) and *Foxd1* (Hatini et al., 1996). By E14, stromal cells are grouped into the cortical and medullary stroma (Cullen-McEwen et al., 2005). Both groups of stromal cells comprise the secondary interstitium. Stromal cells in these two groups show distinct gene expression patterns. For example, *Rarb2* is expressed in both groups of stromal cells whilst *Foxd1* is expressed predominantly in cortical stroma (Mendelsohn et al., 1999). By birth, many of the medullary stromal cells have regressed by apoptosis (Coles et al., 1993). When growth and differentiation of the kidney is complete, the primary interstitium differentiates into adult interstitium.

Renal stromal cells synthesize and secrete extracellular matrix (ECM) to offer a structural support to developing ureteric buds and nephrons. They also play active roles in UB branching and nephrogenesis. Targeted mutation in stromal genes *Foxd1* (Hatini et al., 1996), *Pod1* (Quaggin et al., 1999) or *Pbx1* (Schnabel et al., 2003) generates similar kidney phenotypes which exhibit defects in stromal cells, failure to expand the condensing mesenchymal cells around the tips and impaired branching. Another important stromal signal that regulates branching morphogenesis and nephrogenesis is the interplay between retinoids and Ret. This pathway will be described in section 1.4.4.

1.3 Mechanisms that underlie kidney development

Branching morphogenesis, nephrogenesis and stromal development are accomplished by well-controlled cellular proliferation, differentiation, migration and death. Deregulation of these mechanisms in the developing kidney causes diverse malformations including hypoplasia, dysplsia and agenesis (Woolf and Welham, 2002). This section reviews literature on these four fundamental mechanisms in each compartment of the developing kidney. It covers known signalling factors, growth factors and molecules responsible for these four key mechanisms in the developing kidneys because they are likely to be the components with which the genes studied in this thesis (*Dact1* and *Dact2*) interact. This review is crucial to the exploration of gene functions when using conventional two-dimensional (2D) cell culture and

advanced cell culture-based model for kidney development. Biological functions of the genes identified in cell culture models may offer insights into kidney development.

1.3.1 Proliferation

Proliferation is a simple engine of morphogenetic change and is a key mechanism for normal kidney development. BrdU incorporation assay has demonstrated that there is considerable proliferation throughout the developing mouse kidney, especially in the nephrogenic zone locating at the periphery of the developing kidney (Coles et al., 1993). Mesenchymal cells in this zone have to proliferate to expand the whole nephrogenic zone outwards while receiving signals from the invading ureteric buds. The expansion of the mesenchymal population is controlled at least in part by BMP4 which is made by developing tubules and stroma (Miyazaki et al., 2000). In this way, the more mesenchymal cells differentiate into developing nephrons, the more BMP4 is produced, which in turn signals to the remaining mesenchyme to proliferate so that the nephrogenic mesenchyme will not be exhausted (Davies and Fisher, 2002).

In the branching ureteric buds, cell proliferation is responsible for branching and elongation of the buds. Michael and Davies identified a high proliferation zone in the very tips of the branching epithelium and found it present at UB tips only when they are undergoing active morphogenesis (Michael and Davies, 2004). Stromal cells also regulate the normal growth control of both metanephric mesenchyme and ureteric buds. In mice lacking *Foxd1*, which is only expressed in the renal stroma, reduced growth and branching of the ureteric buds are noted. The *Foxd1* knockout mice also show that the condensed mesenchyme stops epithelialising but grows to a large size (Hatini et al., 1996). The developmental implications of this phenotype remain unclear, but suggest that rapid growth is inhibited in the early stages of nephrogenesis. Another example of stroma derived factor is FGF7. In FGF7 null mice, the size of the collecting system is reduced. Exogenous FGF7 is able to increase the cell number of the UB in organ culture (Qiao et al., 1999). Many

molecules have been found to regulate cell proliferation in developing kidneys. Examples are listed in Table 1-2.

Table 1-2 Examples of molecules controlling cell proliferation in developing kidneys.

Molecules	Functions	References
FGF7	cell proliferation within collecting duct system	(Qiao et al., 1999)
GDNF	ureteric bud cell proliferation	(Pepicelli et al., 1997; Sanchez et al., 1996)
VEGF	endothelial cell proliferation and differentiation	(Kitamoto et al., 1997; Tufro, 2000)
PDGF-B	mesangial cell proliferation and differentiation	(Lindahl et al., 1998; Wagner et al., 2007)
Notch2	mesangial cell proliferation and migration, endothelial migration	(McCright et al., 2001)
IGF I/II	cell proliferation in many compartments of developing kidneys	(Lindenbergh-Kortleve et al., 1997; Liu et al., 1997)
RA	cell proliferation in many compartments of developing kidneys including stroma	(Batourina et al., 2001; Mendelsohn et al., 1999)
Glypican-3	inhibit cell proliferation in many compartments of developing kidneys	(Cano-Gauci et al., 1999)
N-myc	cell proliferation in metanephric mesenchyme and ureteric bud	(Bates et al., 2000)

1.3.2 Cell survival

In addition to proliferation, normal kidney development requires a strict control of programmed cell death through apoptosis (Coles et al., 1993). Increased apoptosis may result in polycystic and dysplastic kidney diseases (Veis et al., 1993; Winyard et al., 1996). Apoptosis occurs in all the three compartments of the developing kidney. One of the first tasks of the UB invasion is to send out signals to rescue the surrounding mesenchyme from apoptosis. One of these UB-derived molecules is FGF2 as it is able to promote survival of isolated mesenchyme in culture (Barasch et al., 1997). In early nephrogenesis, cells on the borders of mesenchymal aggregates show a high rate of apoptosis. This process may limit the number of cells being incorporated into nascent nephrons (Coles et al., 1993). Apoptosis in the UB is mediated at least in part by BMP2 because BMP2 has been shown to promote apoptosis in the UB in kidney organ culture system (Gupta et al., 1999). Apoptosis

also happens in the stroma cells of the medulla towards the end of development (Koseki et al., 1992). Cell loss in this area is to generate space for the extension of the Henle's loop and blood vessels (Bard, 2002; Loughna et al., 1996). Several molecules have been reported to regulate apoptosis in developing kidneys. I have summarised a list of examples (Table 1-3). In addition to these molecules, however, environmental factor such as maternal diet has recently been suggested an important factor controlling apoptosis of metanephric progenitor cells at stages glomeruli have yet to form (Welham et al., 2005).

Table 1-3 Examples of molecules controlling apoptosis in developing kidneys.

Molecules	Functions	References
FGF2	Promote mesenchymal cell survival and lead to differentiation	(Barasch et al., 1997; Perantoni et al., 1995)
EGF receptor and ligands	Prevent apoptosis in cultured metanephric mesenchyme without leading to differentiation	(Koseki et al., 1992; Weller et al., 1991)
BMP2	Promote apoptosis in the UB	(Gupta et al., 1999)
BMP4	Prevent apoptosis in cultured metanephric mesenchyme without leading to differentiation	(Miyazaki et al., 2003)
BMP7	Prevent apoptosis in cultured metanephric mesenchyme without leading to differentiation	(Dudley et al., 1999)
Bcl2	Protect cells from apoptosis in all compartments of the developing kidneys but mainly in the mesenchyme	(Nagata et al., 1996; Sorenson et al., 1995)
AP-2β	Protect cells of distal tubules and collecting ducts from apoptosis	(Moser et al., 1997)
Pax2	Protect UB cells from apoptosis	(Porteous et al., 2000; Torban et al., 2000)

1.3.3 Migration

Cell migration is an important mechanism for kidney morphogenesis. To date, research on cell migration in developing kidneys have focused on nephrogenesis and the branching morphogenesis. In early nephrogenesis, mesenchymal cells migrate and aggregate in response to signals emanating from the UB tips. This process is followed by the condensation of the mesenchymal cells at the UB tips. Signalling by

Rho-GTPase via ROCK has been reported to reduce the migratory activity of the mesenchymal cells at this early stage (Meyer et al., 2006). WNT signalling seems to control the appropriate size of mesenchymal condensates. On receiving signals from the UB tips, mesenchymal cells start to secrete WNT4 as they condense. When the local concentration of WNT4 is high enough to cross the threshold, it will drive the mesenchymal cells to undergo MET. This idea is supported by the *Wnt4* knockout phenotype in which cells migrate and aggregate while waiting for a cross-threshold WNT4 level that can never be achieved in these mice and therefore form large, diffuse groups of mesenchymal cells (Stark et al., 1994). On the contrary, treating the mesenchyme with lithium ions, which activate the WNT/β-catenin canonical pathway, seems to mimic enough WNT signals and force the cells undergo MET earlier. This can explain why lithium treatment results in the formation of small nephrons that have abnormally few cells (Davies and Garrod, 1995). sFRP1 is an inhibitor of WNT signalling and is secreted by stromal cells. Mesenchymal cells away from a forming condensate may use sFRP1 to antagonise WNT4 that diffuses from the condensate (Davies, 2005).

At the stage of comma- and S-shaped bodies, the epithelial cell adhesion molecule (EpCAM) is expressed by these structures (Trzpis et al., 2007). Although the function of EpCAM in nephrogenesis is yet to be determined, it is able to modulate migration in breast epithelial cell lines (Osta et al., 2004). In late nephrogenesis, platelet-derived growth factor (PDGF) B-chain has been shown to act in a paracrine fashion to stimulate the migration of mesangial cell precursors from metanephric mesenchyme to the mesangial area (Arar et al., 2000).

In branching morphogenesis, when the UB invades the mesenchyme, UB cells proliferate and migrate to generate an ampullae that branches to form new buds. These processes of proliferation, migration and branching repeat for several times and eventually generate a complex arborised epithelial tree. The pattern of arborisation depends on positive regulators to promote proliferation and migration and negative regulators to inhibit excessive budding and bifurcation. One insightful study to show the extensive cell migration within the branching ureteric buds has

been performed by using time-lapse imaging of *Hoxb7*-GFP kidneys in organ culture (Shakya et al., 2005). However, the mechanisms underlying this cell migration within the ureteric buds are yet to be determined.

To further investigate the intracellular mechanism regulating UB cell migration and branching morphogenesis, most research is carried out using cell culture based models. Commonly-used approaches include migration assays and three-dimensional (3D) matrices. By using these approaches, the GDNF/Ret pathway has been found to be required for migration of MDCK cells through a chemotactic mechanism (Tang et al., 1998). This GDNF/Ret-mediated chemotaxis is suppressed by PTEN, which antagonises a downstream effector, phosphatidylinositol 3-kinase (PI3K) (Kim and Dressler, 2007). Protein kinase X (PRKX) stimulates epithelial branching morphogenesis by activating cAMP-dependent collecting duct cell migration (Li et al., 2005). H-Ras, expressed in the collecting systems of the late embryonic kidneys from E17.5, is shown to encourage cell migration and generation of elongated tubules in cell culture-based models (Pozzi et al., 2006).

1.3.4 Differentiation

Cell differentiation occurs in every compartment and stage of the developing kidneys. During differentiation, numerous aspects of cell physiology including shape, polarity and responsiveness to signals will change and the differentiated cells finally develop specific structures and may have specific functions. When the reciprocal induction between the UB and the metanephric mesenchyme starts, the mesenchymal cells will differentiate and eventually turn into mature nephrons, stroma, endothelial cells and neuronal cells (Sariola et al., 2003a). The process of nephron differentiation has been reviewed in section 1.2.2. UB cells will develop into different types of specialised cells. For example, UB tip cells express *Wnt11* (Kispert et al., 1996) and *Ret* (Pachnis et al., 1993) whereas non-tip cells do not. At later stages, collecting duct cells differentiate into a major population of ‘principal’ cells and a minor population of ‘intercalated’ cells. Principal cells are characterised by a single cilium and round mitochondria and are able to recover sodium from urine and secrete potassium.

Intercalated cells have copious microvilli and large mitochondria and are responsible for acid/base balance. The zone of differentiation into these specific cell types lies a short distance behind the ampullary tip of the developing collecting duct (Davies, 2003). Cell differentiation in developing kidneys has been comprehensively reviewed elsewhere (Davies, 2006; Ribes et al., 2003; Sariola et al., 2003a). The accumulating molecular data for the differentiation of the developing genitourinary system can be found at the online database GUDMAP (Little et al., 2007). Reviewing the literature on cell differentiation in detail is beyond the scope of this thesis because the work involved in my PhD only touches briefly in the area of cell differentiation in developing kidneys. Nevertheless, the genes studied in this thesis might have undiscovered functional roles in cell differentiation within the developing kidneys.

1.4 Key molecules in kidney development

When describing developmental events (section 1.2) or the cellular mechanisms (section 1.3) of developing kidneys, I have already mentioned some molecules important in those processes. The details of the interactions between these key molecules in kidney development have been comprehensively reviewed in the literature (Davies and Fisher, 2002). Also a growing list of genes and proteins in kidney development can be found at the GUDMAP database (Little et al., 2007). Some signalling pathways and crucial molecules that are highly relevant to *Dact1* and *Dact2* have been reported in different developmental contexts. Interestingly, these signalling and molecules are indeed critical in kidney development and therefore are reviewed in detail in this section. Once the developmental events and/or cellular mechanisms modulated by *Dact1* or *Dact2* are identified, this review may further help to delineate the specific known signalling in which these two genes are involved.

1.4.1 WNT signalling molecules

WNT proteins comprise a large family of secreted glycoproteins that are responsible for the development of many organs including the kidneys. WNT proteins initiate several distinct signalling pathways, which can be classified into β-catenin-dependent (canonical) and β-catenin-independent (non-canonical) pathways. The non-canonical pathways include diverse pathways that are yet to be fully characterised. As *Dact* genes have been implicated in the canonical WNT/β-catenin pathway in the current literature, it is worth reviewing this pathway (Figure 1-6). In the cytoplasm, the tumour suppressors adenomatous polyposis coli (APC), Axin, casein kinase I (CKI) and glycogen synthase kinase 3 (GSK3) constitute a protein complex termed destruction complex. In the absence of WNT ligands, APC and Axin within the destruction complex will bind to the newly synthesised β-catenin. CKI and GSK3 will phosphorylate β-catenin. The phosphorylated β-catenin will recruit a β-TrCP containing E3 ubiquitin ligase leading to its degradation by proteasome. The canonical signalling is initiated when WNT ligands bind to their cognate receptor complex, consisting of a serpentine receptor of the Frizzled family and a member of the LDL receptor family, LRP5/6. The binding of WNT ligands to receptors inhibits the kinase activity of the destruction complex. Consequently, β-catenin accumulates in the cytoplasm and translocates into the nucleus where it binds to DNA-binding proteins of the TCF/LEF family and converts them into transcriptional activators (Gordon and Nusse, 2006; Reya and Clevers, 2005).

Key intermediates that determine which WNT pathway is used in a given developmental context are the Dishevelled (DSH or DVL in mammals) proteins and their associated proteins (Wharton, 2003). DVL proteins have three highly conserved domains which contribute to signalling: an amino terminal DIX domain, a central PDZ domain and a carboxyl terminal DEP domain (Boutros and Mlodzik, 1999; Semenov and Snyder, 1997). A growing body of DVL-associated proteins has been identified. Each of these binds to one of the conserved domains of DVL and activates a downstream signalling cascade (Wharton, 2003). DACT has been reported to bind directly to the PDZ domain of the DVL (Cheyette et al., 2002). DACT may be thus

involved in the WNT signalling by regulating DVL but its function is yet to be explored.

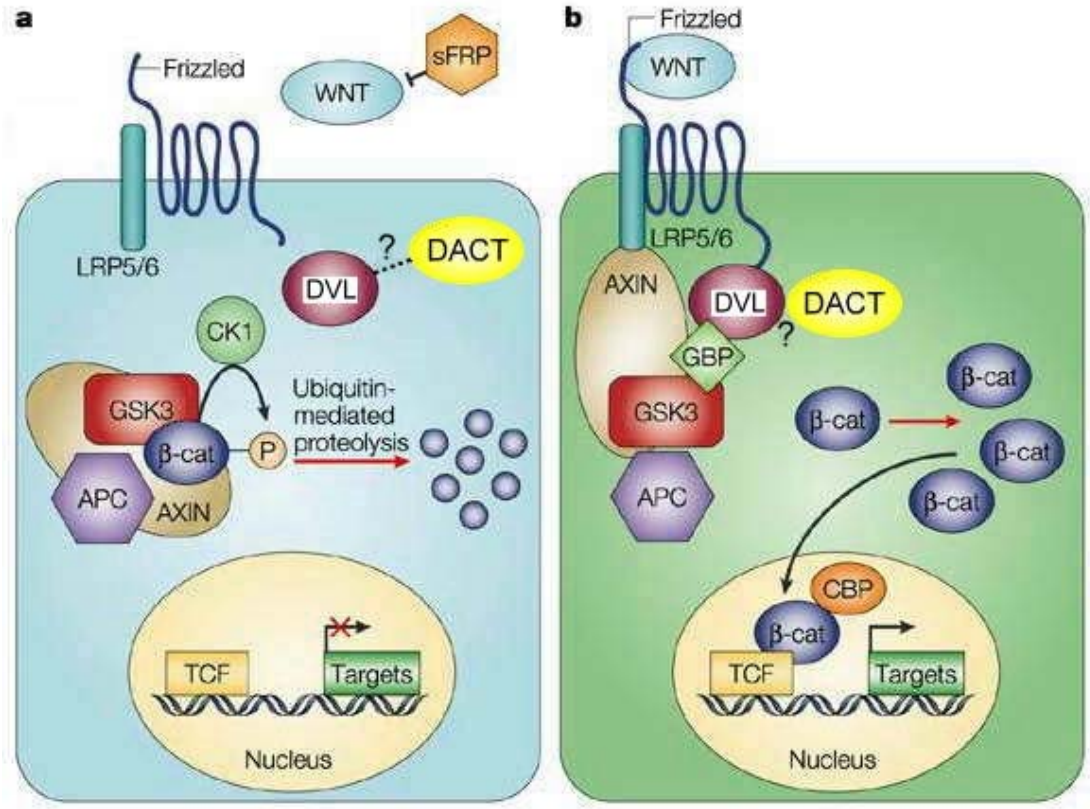

Figure 1-6 The canonical WNT/β-catenin pathway. In the absence of WNT ligand or when it binds to its inhibitor (*i.e.* sFRP) (a) the newly synthesized β-catenin is removed by the GSK3-APC-AXIN destruction protein complex via ubiquitin-mediated proteolysis whereas when WNT engages its receptor complex (*i.e.* Frizzled-LRP 5/6) (b), DVL binds to the destruction complex and thus stabilises β-catenin and activates the transcription factors (e.g. TCF). The roles of DACT in both cellular states are yet to be determined (Modified from Moon et al., 2004).

Six *Wnt* genes are expressed in developing kidneys. *Wnt6*, *Wnt7b*, *Wnt9b*, and *Wnt11* are expressed exclusively by the UB. *Wnt6* is expressed as early as E10.5 in the Wolffian duct and the UB and is expressed more strongly in the UB tips than in the stalk. *Wnt9b* is expressed as early as E9.5 in the Wolffian duct and as development proceeds, it shows stronger expression at the UB tips than stalks (Carroll et al., 2005; Itaranta et al., 2002). *Wnt11* expression is restricted to the UB tips (Christiansen et al., 1995; Kispert et al., 1996). *Wnt7b* expression is restricted to the maturing collecting

ducts from E13.5 (Kispert et al., 1996). *Wnt4* is expressed by the condensing mesenchyme, comma- and S-shaped bodies of the developing nephrons (Kispert et al., 1998; Stark et al., 1994). *Wnt2b* is expressed in the perinephric mesenchymal cells (Lin et al., 2001). Cell lines expressing *Wnt4*, *Wnt6*, *Wnt7b* and *Wnt9b* are capable of inducing isolated mesenchyme to form nephrons in culture. Cell lines expressing *Wnt11* do not have this ability though *Wnt11* is expressed in the UB tips (Carroll et al., 2005; Itaranta et al., 2002; Kispert et al., 1998). *Wnt6*-expressing fibroblasts are able to induce nephrons even in *Wnt4*-/- mesenchyme but *Wnt9b*-expressing fibroblasts are not able to do so. Taking together the expression patterns and the cellular assay results, WNT6 and WNT9b are likely to be inducers for nephron formation. However, whether *Wnt9b*, *Wnt6* and *Wnt4* act in a hierarchy or they signal through distinct receptors to induce nephrons is yet to be determined.

Wnt4 is expressed by the condensing metanephric mesenchyme and the periureteric stroma in the medullary region of the embryonic kidney (Stark et al., 1994). This protein is critical for regulating MET in the cortical region for nephrogenesis (Kispert et al., 1998). Besides, WNT4 signalling regulates the fate of smooth muscle cells in the developing medullary region (Itaranta et al., 2006). *Wnt2b* is expressed by the perinephric mesenchymal cells in the region of the presumptive stroma in the developing kidney at E11.5. Cells expressing *Wnt2b* fail to induce tubulogenesis in cultured mesenchyme but instead they can promote UB survival and growth in a co-culture experiment (Lin et al., 2001).

Although the expression patterns and functions of these *Wnt* genes in developing kidneys have been identified at least partially, the intracellular signalling by which each WNT protein exerts its function remains unclear (Iglesias et al., 2007; Merkel et al., 2007).

1.4.2 GDNF

The GDNF family ligands include GDNF, neurturin, persephin, and artemin. They all signal through the Ret receptor tyrosine kinase and activation is facilitated by the GFRα1 co-receptors (Airaksinen et al., 2006). Genes encoding each of these ligands except artemin are expressed by developing kidneys and are described briefly below.

GDNF is perhaps the best characterized morphogen in kidney development. In the developing kidney, GDNF is secreted by the uninduced metanephric mesenchyme (Hellmich et al., 1996). The Ret receptor is found at the UB at early stages of its outgrowth and later locates only at the tips of the ureteric trees. The *Gfra1* co-receptor is expressed by the UB and also by the surrounding mesenchyme (Sainio et al., 1997). *Gdnf*, *Gfra1* and *Ret* are critical to kidney development. Homozygous knockouts of *Gdnf, Gfra1,* or *Ret* show renal malformations ranging from severe dysgenesis to complete agenesis (Cacalano et al., 1998; Moore et al., 1996; Pichel et al., 1996; Schuchardt et al., 1994). The importance of GDNF in UB induction, branching maintenance, UB cell proliferation and MDCK cell migration have been described in section 1.2.1, 1.3.1 and 1.3.3.

Nrtn (neurturin) is expressed in the UB of the developing kidney (Widenfalk et al., 1997). *Nrtn* knockout mice show grossly and microscopically normal kidneys (Heuckeroth et al., 1999). In kidney organ culture NRTN stimulates UB branching only in the presence of function-blocking anti-GDNF antibodies (Davies et al., 1999). PSPN (persephin) is also expressed by the developing kidney. In kidney organ culture, it can partially rescue the inhibitory effect of sodium chlorate on UB branching (Milbrandt et al., 1998).

1.4.3 TGFβ signalling molecules

The transforming growth factor β superfamily comprises a collection of structurally related ligands, including TGFβs, BMPs, Activins, Nodal and growth differentiation factors (GDFs). They are involved in regulating an array of developmental processes

including those in developing kidneys. These ligands signal through type II and type I receptors, both of which are transmembrane serine-threonine kinases, leading to the phosporylation and activation of Smad family of transcription factors. TGFβs signal via the ALK5 receptor whilst Activins and Nodal signal via the ALK4 receptor (Kitisin et al., 2007; Piscione et al., 1997). A schematic diagram for these signalling pathways is shown in Figure 1-7. Members of the TGFβ superfamily and their receptors are expressed in the developing kidneys and play diverse and essential roles in outgrowth and positioning of the UB (Esquela and Lee, 2003), renewal of the mesenchymal progenitor population (Dudley et al., 1999), recruitment of nephrogenic mesenchyme (Oxburgh et al., 2004), and shaping the branching ureteric buds (Bush et al., 2004; Martinez et al., 2002).

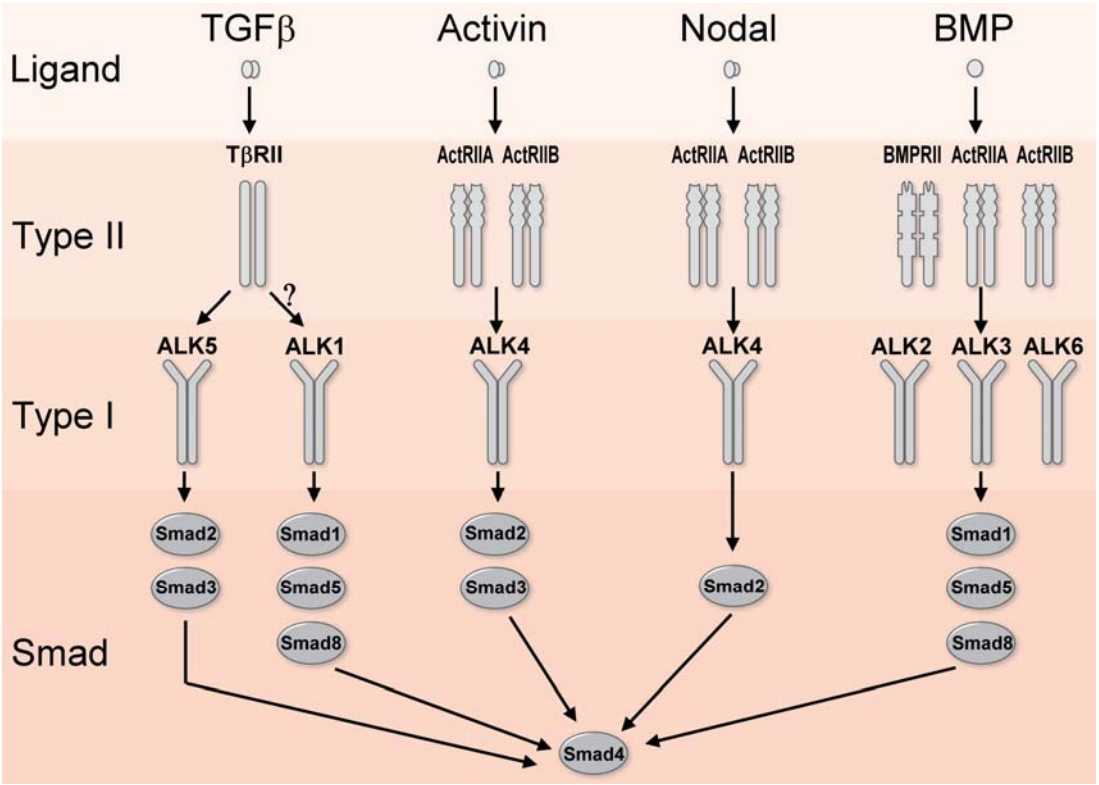

Figure 1-7 A scheme of TGFβ superfamily signalling. Different ligands signal through their type II and type I receptors. Type II receptors are ligand-binding receptors including TβRII, ActRIIA, ActRIIB, and BMPRII. The type I receptor family includes ALK1 through ALK7. Receptor-activated Smads (R-Smads) include Smad1, Smad2, Smad3, Smad5, and Smad8. Smad4 is the common Smad. (Modified from Kitisin, Saha *et al.* 2007)

Tgfb1 is expressed by the stroma in developing kidneys (Partanen, 1990; Vrljicak et al., 2004). *Tgfb1* knockout mice do not have renal defects (Boivin et al., 1995). Exogenous TGFβ1 inhibits UB branching in kidney organ culture (Bush et al., 2004; Ritvos et al., 1995). Results from cell culture based tubulogenesis also support the idea that TGFβ1 inhibits branching (Sakurai and Nigam, 1997).

Activin is expressed by the metanephric mesenchyme. Like TGFβ1, exogenous Activin inhibits UB branching in kidney rudiment culture. This inhibitory effect can be rescued by follistatin, a natural inhibitor of Activin (Bush et al., 2004; Ritvos et al., 1995). In addition to the inhibitory effect on branching, Activin is further characterised as an endogenous inhibitor of UB outgrowth from the Wolffian duct (Maeshima et al., 2006). In the cell culture-based tubulogenesis model, HGF has been established as an inducer of tubulogenesis (Cantley et al., 1994). Further studies have proved that this HGF-mediated tubulogenesis is achieved by blocking the production of Activin within the cells (Maeshima et al., 2000). Transgenic mice expressing the truncated Activin type II receptor, which act as a dominant-negative receptor and block the Activin signalling, present a mild renal phenotype with increased number of glomeruli in the renal cortex. This is possibly due to increase UB branching (Maeshima *et al.* 2001).

Nodal signals through Activin type II receptors, ALK4, Smad2 and Smad4 (Goumans and Mummery, 2000). However, the expression of Nodal in developing kidneys is yet to be confirmed.

1.4.4 Retinoids

Retinoids are important in mammalian kidney development. Vitamin A deficiency during gestation leads to congenital renal abnormalities in rats (Wilson and Warkany, 1948). In humans, the reduced maternal vitamin A level has been shown to be correlated with the reduced newborn renal volume (Goodyer et al., 2007). In agreement with these findings, the addition of retinoids to kidney organ culture stimulates the UB branching and the nephron formation (Vilar et al., 1996).

Developing kidneys express *Rara* and *Rarb2* in the stroma (Mendelsohn et al., 1999). They also express genes encoding enzymes essential for retinoic acid (RA) synthesis such as retinaldehyde dehydrogenases (*Raldh1*, *Raldh2* and *Raldh3*) (Gilbert, 2002; Niederreither et al., 2002) and retinol dehydrogenases (*Rdh10*) (Cammas et al., 2007). Mice carrying mutations in both *Rara* and *Rarb2* present severe kidney malformation (Mendelsohn et al., 1994).

A more interesting finding is that exogenous RA is able to increase the expression of *Ret* by kidney rudiment growing in culture (Moreau et al., 1998). Retinoids cause translocation of the membrane-bound receptors into the nucleus where they act as transcription factors (Duester, 2000). A signal then sends out from the stroma, directly or indirectly, to the UB resulting in upregulation of *Ret*. Batourina *et al.* further showed that enforced expression of *Ret* in mice lacking both *Rara* and *Rarb2* restores UB growth and stromal patterning (Batourina et al., 2001). These results therefore build up a plausible link between retinoid signalling and *Ret*, which modulates branching morphogenesis, nephrogenesis and stromal cell patterning.

1.5 *Dact* genes and kidney development

1.5.1 Dact as a novel gene family

DACT was initially named Dapper. It was identified in a screen for proteins directly binding to DVL, a cytoplasmic protein central to the WNT signalling (Figure 1-6). Cheyette *et al.* performed a yeast two-hybrid screen of a *Xenopus* maternal cDNA library using as bait the PDZ domain and adjacent sequences of *Xenopus* Dishevelled (XDSH). The novel protein thus isolated was further verified by immunoprecipitation and an *in vitro* binding assay. Cheyette *et al.* subsequently proved it to be an antagonist of Dishevelled and named it Dapper (Dpr), the antonym of Dishevelled (Cheyette et al., 2002). Dpr orthologues have been found in vertebrates examined so far but they have not yet identified in invertebrates. Dact is now the official name for all members of this gene family annotated by the Human

Genome Organization Nomenclature Committee and the Mouse Genome Informatics website.

The open reading frame of *Xenopus Dpr* (XDpr) cDNA encodes a protein of 824 amino acids. As predicted from the genomic sequences, the open reading frames of the mouse and human orthologues (*Dpr1* and *DPR1*) encode proteins of 778 and 836 amino acids, respectively. These three proteins are highly conserved and featured with a leucine zipper domain at the amino terminus and a PDZ binding domain at the carboxyl terminus. The two mammalian proteins are more than 75% identical to each other (Figure 1-8). More strikingly, the carboxyl terminal 28 amino acids are completely conserved among all the three proteins, including the final four amino acids that form a consensus PDZ binding (PDZ-B) motif (Cheyette et al., 2002).

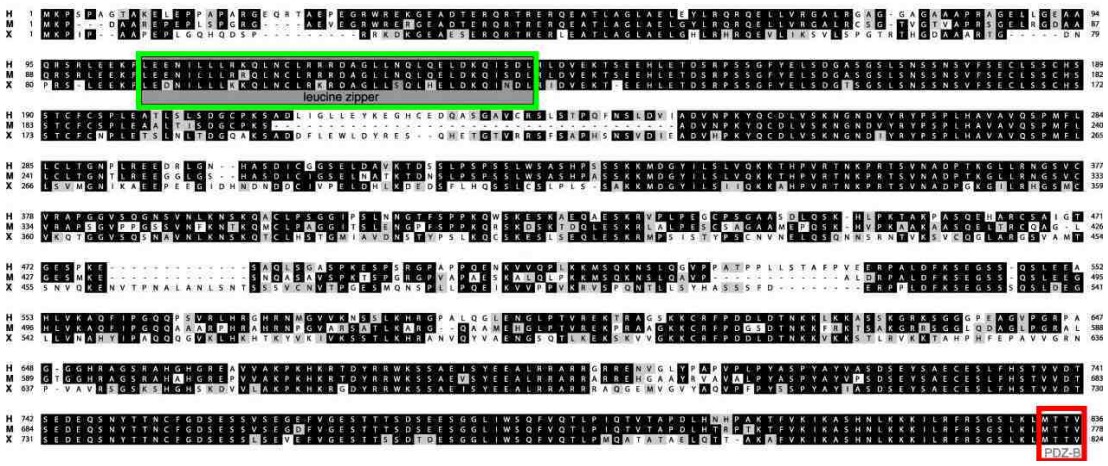

Figure 1-8 Alignment of mouse DACT1 with orthologues from *Xenopus* and human. Amino acid residues shown in black are identical and grey are similar. Green outline shows the leucine zipper domain and red outline indicates PDZ binding motif (M: mouse; X: *Xenopus*; H: Human) (Modified from Cheyette *et al*., 2002).

By using the Dapper sequences from frogs and fish, Fisher *et al.* scanned the mouse genome and expressed sequence tag (EST) databases for similar sequences, and carried out reverse transcriptase-polymerase chain reaction (RT-PCR) to clone full-length cDNAs. Three paralogues in the *Dact* family were thus identified: *Dact1* mapping to chromosome 12D1, *Dact2* to chromosome 17A2 and *Dact3* to chromosome 7A2 (Fisher et al., 2006). The intron-exon structure is conserved among

these three paralogues, comprising three small 5'coding exons, which encode a short 5'-utranslated region (UTR) and the amino terminus of the polypeptide, and a larger fourth exon encoding about two thirds of the translated sequences plus a longer 3'-UTR. The amino acid sequences for DACT1, DACT2 and DACT3 proteins are 778, 757 and 610 residues respectively (Fisher et al., 2006). The orthologues of *Dact1* and *Dact2* have also been identified in zebrafish, *Xenopus* and humans (Fisher et al., 2006; Waxman et al., 2004; Yau et al., 2005). However, *Dact3* is not yet reported in other species. Because it was identified just a few months ago, I was not able to investigate it as part of this thesis.

1.5.2 Biological functions of *Dact* genes

Because DACT proteins were discovered as DVL-associated proteins, most research to date have focused on their roles in developmental events or disease processes controlling by WNT signalling. The first report described the functional role of *Dact1* in *Xenopus* notochord formation. Depletion of maternal *Dact1* RNA from embryos leads to acephalic or microcephalic embryos whilst overexpression of *Dact1* results in embryos with enlarged head and spinal curvature. Cheyette *et al.* further showed that DACT1 and DVL colocalised intracellularly and formed a complex with Axin, GSK3, CKI, and β-catenin, which are all key components of the WNT/β-catenin pathway. *Dact1* has been also shown to inhibit activation by Dishevelled of c-Jun N-terminal kinase (JNK) pathway. Cheyette *et al.* therefore concluded that *Dact1* is a common antagonist of Dishevelled (Cheyette et al., 2002).

In zebrafish, however, *Dact* genes were reported as pathway-specific modulators of WNT signalling. Endogenous *Dact1* is able to augment WNT/β-catenin activity in embryos hypomorphic for *Wnt8* whereas *Dact2* is required for normal convergence extension movement in embryos that are hypomorphic for *Stbm* or *Wnt11* (Waxman et al., 2004). In mice, Suriben *et al.* noticed that *Dact1* presomitic mesoderm expression oscillates in time with *Axin2* in the somitogenesis clock (Suriben et al., 2006). This observation also supports the role of *Dact1* in WNT signalling.

In addition to the involvement in the WNT signalling, DACT2 has been implicated as a modulator in TGFβ signalling. In zebrafish, DACT2 binds to the TGFβ receptors ALK4 and ALK5, promoting degradation of these receptors thereby repressing mesoderm induction (Zhang et al., 2004). The ability of DACT2 to antagonise TGFβ signalling is evolutionally conserved. Su *et al.* demonstrated that in mammalian cells, overexpression of mouse *Dact2* inhibited the TGFβ induced expression of the Smad-responsive reporters and accelerated the degradation of TGFβ receptor ALK5. More strikingly, overexpression of mouse *Dact2* in zebrafish embryos results in a phenotype mimicking that generated by overexpression of fish *Dact2* (Su et al., 2007). *Dact1* is also regulated by BMP2, a member of the TGFβ superfamily. BMP2 is a key regulator in the transformation of the uterine stroma during embryo implantation. Ablation of *Bmp2* results in the reduction of *Dact1* in the uterus (Lee et al., 2007).

Also there are emerging papers on *Dact* genes and diseases. Human *DACT1* has been reported to be downregulated in hepatocellular carcinoma wherein oncogenic activation of WNT/β-catenin is a common mechanism (Yau et al., 2005). Increased *DACT1* expression is noted in invasive ductal carcinoma of breast (Schuetz et al., 2006). In a mouse model for systemic sclerosis, the mRNA levels of several genes of WNT signalling components including both *Dact1* and *Dact2* are found to be increased (Bayle et al., 2007). *DACT2* is also implicated in genitourinary tract tumours and endometrial adenocarcinoma (Katoh and Katoh, 2003). Notably *Dact* genes seem to play roles in these currently non-curable diseases of various organs. It is therefore important to understand their functional roles in basic cellular mechanisms such as proliferation, survival, differentiation and migration, which may contribute to the identification of novel pharmaceutical targets and the development of new therapeutic strategies.

1.5.3 *Dact* genes in mammalian kidneys

To date, the literature describing the biological functions of *Dact* genes have focused on somitogenesis and nervous system development. Little is known about their

functions in kidney development. Fisher *et al.* characterised the expression patterns of the three *Dact* genes in E14 mouse embryos. Although their whole work put more emphasis on central nervous system, they also showed that *Dact2* was expressed by the ureteric buds of the kidneys at E14 (Fisher et al., 2006). This has been so far the only evidence providing a link between *Dact* genes and developing mammalian kidneys.

1.6 Aims of this thesis

WNT signalling is required for normal kidney development but the details of the pathways used remain a challenging question to most developmental biologists in this field. One strategy is to work out the intracellular pathways by which WNT exerts its function. DVL-associated proteins seem to be the ideal candidates for this strategy as they regulate the cytoplasmic scaffold protein, DVL, which acts as a hinge of diverse WNT signalling pathways. My initial drive to use DACT as a tool to dissect WNT pathways in developing kidneys arose from two encouraging papers in which *Dact* was found to be expressed in E14 kidneys and, more importantly, *Dact1* and *Dact2* were shown to be pathway-specific modulators of WNT signalling (Fisher et al., 2006; Waxman et al., 2004). However, as information on *Dact* genes in developing kidneys is so limited in the literature, there are many interesting areas worth exploring. Based on the reviews in previous sections, several interesting questions on *Dact* genes in kidney development can be addressed. Examples of these questions are as follows.

1. When, where and how are *Dact* genes expressed in developing kidneys?
2. In what developmental events of kidney development are *Dact* genes involved? Possibilities include;
   (a) UB induction
   (b) UB branching
   (c) Nephron induction
   (d) Nephron differentiation
   (e) Stromal development
3. What cellular events are modulated by *Dact* genes? Possibilities include;

(a) proliferation
(b) apoptosis
(c) migration
(d) differentiation

4. What are the possible signalling pathways that *Dact* genes are involved in regulating kidney development?

It is not possible for this thesis to answer all the questions listed above but this question list serves as a theme for the present and future projects on *Dact* genes in kidney development. In this study, I started with establishing the expression patterns of both *Dact1* and *Dact2* in embryonic and postnatal kidneys. Based on these expression patterns, I designed experiments on a hypothesis-driven basis to explore the functions of both *Dact* genes. The specific aims of this thesis were as follows.

1. To characterise the temporospatial expression patterns of *Dact1* and *Dact2* in embryonic and postnatal mouse kidneys.
2. To explore *Dact1* function by siRNA-mediated RNAi in 2D cell culture.
3. To examine *Dact1* function in kidneys growing in organ culture.
4. To make stable renal epithelial cell lines expressing *Dact2* shRNA.
5. To investigate *Dact2* functions in both 2D cell culture and a 3D cell culture-based tubulogenesis model.

The functions of these two genes found in this study shed light on their functional roles in mammalian kidney development.

Chapter 2

Materials and Methods

2.1 Cell and organ culture

Culture media, salts and supplements were purchased from Sigma unless otherwise stated. They were all stored at 4°C.

2.1.1 Cell culture

The NIH3T3 cell line was purchased from ATCC-LGC Promochem (ATCC number: CRL-1658). The culture medium was composed of 1:1 mixture of Nutrient Mixture F-12 Ham and Dulbecco's modified Eagle's medium (DMEM) and was supplemented with 10% (v/v) foetal calf serum (Biosera), 2mM L-glutamine, 100units/ml penicillin and 100µg/ml streptomycin. Cells were maintained at 37°C with 5% CO_2.

The mIMCD-3 (murine inner medullary collecting duct) cell line was purchased from ATCC-LGC Promochem (ATCC number: CRL-2123) and was cultured in the same way as NIH3T3 cells except that L-glutamine was not added to the culture media.

2.1.2 Kidney dissections and culture

CD1 outbred mice were raised and mated liberally. The morning when the vaginal plug was detected was defined as E0.5. Metanephric kidneys were dissected from E11.5 embryos. Dissections were performed in 35mm petri dishes in Eagle's minimum essential medium (MEM) using 0.5x16m needles (BD Microlance 3). The dissection procedures are depicted in Figure 2-1. Dissections were started with the removal of the unnecessary tissues including the rostral end of the embryo and its tail. Longitudinal bisection was then done on the caudal part rudiment. At this stage, kidney was located close to the hindlimb and was ready to be dissected out. Kidneys were cultured on 5µm pore size polycarbonate filters (Millipore) at a gas-medium interface on metal grids in petri dishes. The culture medium was composed of MEM

with 10% (v/v) foetal calf serum, 100units/ml penicillin and 100µg/ml streptomycin. All cultures were maintained in a humidified incubator with 5% CO_2 at 37°C.

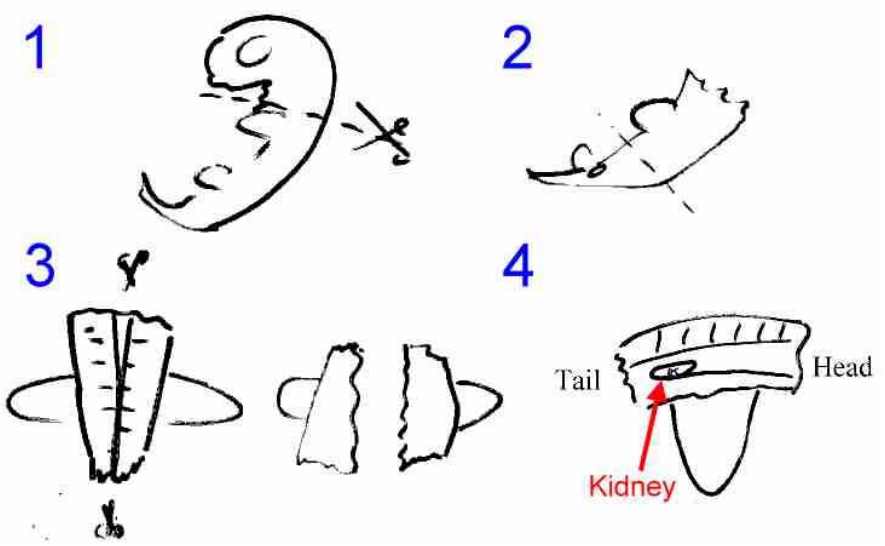

Figure 2-1 Stepwise procedures of kidney dissections in an E11.5 embryo. The first two steps were to remove the unnecessary tissues including head and forelimbs. Step 3 was to longitudinally bisect the caudal part of the embryo. At step 4, kidney was identified close to the hindlimb.

2.2 Nucleic acid manipulation

2.2.1 Solutions for nucleic acid manipulation

All chemicals were purchased from Sigma, BDH and Invitrogen unless otherwise stated. Solutions were prepared in deionised water and were stored at room temperature. Autoclaving procedures were carried out at 121°C, 15lbs/square inch for 30 min.

EDTA

EDTA (ethyldiaminetetraacetic acid di-sodium salt) was dissolved in water and was titrated to pH 8.0 by NaOH.

Tris.HCl

Tris base (tris[hydroxymethyl]aminomethane) was dissolved in water and was titrated to required pH value by HCl.

TE buffer

TE buffer was made up of 10mM Tris.HCl (pH 7.5) and 1mM EDTA.

TBE buffer

TBE (Tris-Borate-EDTA) was purchased as 5X concentrate powder and was diluted in water to 1X buffer containing 89mM Tris-borate and 2mM EDTA, pH 8.3.

Gel loading dye, 6X

Blue/Orange Loading Dye, 6X (Promega) contained 0.4% orange G, 0.03% bromophenol blue, 0.03% xylene cyanol FF, 15% Ficoll® 400, 10mM Tris-HCl (pH 7.5) and 50mM EDTA (pH 8.0).

Ethidium bromide

Ethidium bromide was purchased as a 10mg/ml solution and was added directly to the agarose gel to obtain the final concentration of 0.3µg/ml.

PCR Primers

Primers were designed from published sequences and by Primer3 online software (http://frodo.wi.mit.edu/cgi-bin/primer3/primer3_www.cgi). They were carefully checked by BLAST (National Centre for Biotechnology Information, website: http://www.ncbi.nlm.nih.gov/blast/Blast.cgi) to confirm the specificity of these primers. Primers were purchased as lyophilised, desalted compounds (MWG Biotech). Stocks were made up to 100µM using TE buffer and stored at -20°C. Working stocks were diluted to 5µM with nuclease-free water and stored at –20°C.

dNTPs

dNTPs (deoxyribonucleotide triphosphate) were purchased as individual stocks (dATP, dCTP, dGTP, dTTP) of 100mM (Promega). Working stocks were made by

mixing each of the dNTPs with distilled water to a final concentration of 10mM. Stocks were kept at –20°C.

2.2.2 Total RNA isolation

Total RNA was extracted from mouse metanephroi or cultured cells with the SV Total RNA Isolation System (Promega) according to the manufacturer's instructions and quantified by a Cecil 2000 spectrophotometer (Cecil Instruments). RNA samples were diluted by nuclease-free water into 125ng/µl aliquots and stored at -70°C.

2.2.3 RT-PCR

The mixture of 250ng total RNA, 500ng of random primers and nuclease-free water together in a final volume of 12.5µl was heated to 70°C for 5 min to melt secondary structure within the template. 5X reverse transcription buffer, 10mM dNTPs, 20units of RNase inhibitor, and 200units of reverse transcriptase were added in order to produce a final volume of 20µl. One reaction mixture was prepared without adding the reverse transcriptase and was used as a negative control in the downstream PCR. After incubation at 37°C for 1 hour, the reverse transcription reaction was terminated by heating at 75°C for 8 min. The newly synthesized cDNA was amplified by PCR. The reaction mixture contained 2µl of cDNA template, 25mM $MgCl_2$, 1unit of Taq polymerase, and 50ng of primers. β-actin primers were used as an internal control. The reactions were carried out in a TC-312 thermal cycler (Techne). Amplification thermal cycles were: 94°C for 5 min, then 35 cycles of 94°C for 1 min, 55°C for 1 min, 72°C for 1 min, followed by a final extension at the end for 10 min at 72°C.

2.2.4 Agarose gel electrophoresis

Agarose gels were used to determine the presence or size of nucleic acid molecules. A 1.5% (w/v) agarose gel was made by dissolving 0.75g agarose in 50ml 1X TBE in a microwave oven (900w) for 1 min. Ethidium bromide was then added to a final concentration of 0.3µg/ml agarose. The molten agarose was poured into a tape-sealed

rectangular mould and allowed to set. A 100bp DNA Ladder (Promega) was run alongside experimental samples to estimate the size and amount of DNA in the samples. 10µl of each DNA sample was mixed with 2µl of 6X loading dye. When electrophoresis finished, gels were visualised by UV trans-illumination and photographed.

2.2.5 Quantitative real time PCR

QuantiTect SYBR Green PCR Kit (Qiagen) was used according to manufacturer's instructions. Each reaction contained 25µl of 2X QuantiTect SYBR Green PCR Master Mix, primer pairs 0.3µM and 2µl of template DNA. Nuclease-free water was added to a final volume of 50µl.

Amplification was carried out in a 96-well plate on the DNA Engine Opticon® system (MJ Research). Thermal cycles were: 95°C for 15 min to activate HotStarTaq DNA polymerase (Qiagen), then 40 cycles of 15 sec of denaturation at 94°C, 30 sec of annealing at 55°C and 30 sec extension at 72°C, followed by a plate reading with a final extension at the end for 10 min at 72°C. All reactions were performed in triplicate unless otherwise stated. Each run included at least two non-template controls for the PCR amplification step. Data were analysed by the Opticon Monitor software (MJ Research) using a standard curve method. Standard curves were generated by using serial two-fold dilutions of a reverse-transcribed RNA containing the sequence of interest for every primer pair. The resulting standard curve plots were then used to convert the threshold cycle number into arbitrary quantities of initial template of a given sample.

2.2.6 PCR products purification

PCR products were purified by QIAquick PCR purification kit or Gel extraction kit (Qiagen) according to the manufacturer's protocols. The choice of kit depended on the purity of the PCR products shown on agarose gel. Purified products were used directly for ligations or stored at -20°C.

2.2.7 Ligations

Specific PCR products were cloned into pGEM®-T Easy vector system (Promega). In this project, the subsequent use of these ligations included riboprobe synthesis and DNA sequencing. Each reaction contained 50ng of pGEM®-T Easy vector, 5µl of 2X ligation buffer, 3units of T4 DNA ligase and 2µl of insert DNA. Distilled water was added to produce a final volume of 10µl. Positive control of the ligation reaction was carried out by setting up a ligation reaction using the positive control insert DNA provided. A ligation reaction set up without adding any insert DNA served as the negative control. Both the positive and negative control ligations were used for subsequent transformations. Ligations were incubated at 4°C overnight and were used on the next day.

2.2.8 Plasmid linearisation

Plasmids were linearised by restriction enzymes to facilitate riboprobe synthesis by *in vitro* transcription. Restriction enzyme digestion was carried out using Promega enzymes and buffers. The restriction enzyme digest was performed in a volume of 50µl containing 1µg of substrate DNA, 5µl of appropriate buffer, 5µg of BSA and deionised water and was incubated in a 37°C water bath for 2 hours. Linearised plasmids were analysed on a gel at once or stored at 4°C. The choice of restriction enzyme and its appropriate buffer was made according to the manufacturer's recommendation.

2.2.9 DNA sequencing

Plasmid DNA containing the insert sequences was purified by QIAprep Spin Miniprep Kit (Qiagen) according to the manufacturer's instructions and was sent to DBS Genomics at the University of Durham for sequencing. The instrument used for sequencing was the 3730 DNA Analyser (Applied Biosystems).

2.3 Microbiology

2.3.1 Solutions

All chemicals were purchased from Sigma, BDH and Invitrogen unless otherwise stated. Solutions were stored at room temperature.

Luria-Bertani (LB) Broth

LB broth was made up of tryptone 5.0g, yeast extract 2.5g, NaCl 5.0g and glucose 0.5g. Distilled water was added to a final volume of 500ml and the solution was then autoclaved.

LB Agar

LB agar was made up of tryptone 5.0g, yeast extract 2.5g, NaCl 5.0g and agar 7.5g. Distilled water was added to a final volume of 500ml. The solution was then autoclaved.

X-Gal, 500X

40mg of X-Gal (5-bromo-4-chloro-3-indolyl-β-D-galactoside) was diluted in 2ml of N,N-dimethylformamide (DMF) and stored at -20°C.

Ampicillin, 1000X

100mg of ampicillin (D-[-]-α-aminobenzylpenicillin sodium salt) was diluted in 2ml of ethanol and stored at -20°C.

Glycerol, 80%

80ml of glycerol was added to 20ml of distilled water, autoclaved and stored at room temperature.

2.3.2 Heat shock transformation

Transformants were made by adding 2µl of the DNA ligation reaction (described in section 2.2.7) to 50µl of thawed competent *E. coli* cells (JM109, Promega) in a sterile 1.5ml microcentrifuge tube. The ligation/cell suspension was incubated on ice for 30 min. Cells were then heat shocked in a 42°C water bath for 20 sec followed by incubation on ice for additional 2 min. The transformed bacteria were suspended in 1ml of LB broth and incubated at 37 °C for 1 hour in an orbital shaker. By using a sterile inoculation loop, 50µl of bacterial suspension were spread onto a LB agar plate containing 1X X-Gal and 1X ampicillin. The agar plates were left upside down and incubated at 37°C overnight.

2.3.3 Screening transformants for inserts

The vector used contained a lacZ gene coding for β-galactosidase. When β-galactosidase was produced by the *E. coli*, it converted the colourless X-Gal, which was supplied in the agar plate, into a bright blue product. Successful cloning of an insert into the pGEM®-T Easy vectors interrupted the coding sequence of β-galactosidase and therefore recombinant clones were shown as white colonies on the agar plates. After the overnight incubation, a single white colony was picked, spotted onto a new agar plate and incubated at 37°C overnight.

2.3.4 Isolation of recombinant plasmid DNA

To isolate recombinant plasmid DNA from the bacteria, a single white colony was picked and inoculated in 10ml of LB broth containing 1X ampicillin. This culture was incubated at 37°C in an orbital shaker overnight (16-24 hours). Recombinant plasmid DNA was extracted by using the QIAprep Spin Miniprep Kit (Qiagen) according to the manufacturer's instructions. The concentration of the purified plasmid DNA was determined by a spectrophotometer (Cecil Instruments). Using the purified plasmid DNA as templates, RT-PCR was performed to confirm to correct

DNA inserts and/or to determine the direction of the cloned PCR products in the plasmids.

2.3.5 Preparation of bacterial stocks

Once a plasmid harbouring the correct insert was verified, a single colony of the host bacteria was picked from the agar plate and inoculated in 10ml of LB broth containing 1X ampicillin. This culture was left at 37°C in an orbital shaker overnight. Cells were pelleted by centrifugation. The bacterial pellet was harvested and resuspended in 1ml of LB broth. The glycerol bacterial stock was made by adding 800µl of this suspension to 200µl of 80% glycerol in a sterile 1.5ml cryotube. The bacterial stock was stored at -70°C.

2.4 RNA *in situ* hybridisation

2.4.1 Whole kidney mount *in situ* hybridisation

2.4.1.1 Solutions

DEPC-treated water

1ml of DEPC was added to 1000ml of deionised water and agitated overnight at 37°C. The solution was then autoclaved and kept at room temperature.

PBS

One PBS tablet was dissolved in 200ml of DEPC-treated water to yield 0.01M phosphate buffer, 0.0027M potassium chloride and 0.137M sodium chloride, pH 7.4, at 25°C. The solution was then autoclaved and kept at 4°C.

PBST

PBST consisted of 0.1% Tween-20 in PBS.

4% PFA in PBS

2g of PFA was added to 50ml of DEPC-treated PBS and was heated to 60°C until the PFA fully dissolved. The solution was aliquoted and stored at -20°C.

SSC, 20X, pH 7.0

20X SSC stock solution was made by dissolving 8.82g of sodium citrate and 17.5g of NaCl in DEPC-treated water. The final volume was 100ml and the pH was adjusted to 7 with 1M HCl. The solution was stored at room temperature.

SSC, 20X, pH 5.0

This solution was made by adding 1ml of 1M citric acid to 40ml of 20X SSC (pH 7.0).

Torula yeast tRNA

Torula yeast tRNA solution was made by adding 3g of torula yeast tRNA powder to 45ml of boiling DEPC-treated water. The solution was allowed to cool and was centrifuged. Any undissolved powder was discarded. The concentration of RNA was measured by a spectrophotometer (Cecil Instruments) and was adjusted accordingly to achieve 50mg/ml. The solution was then aliquoted and stored at -20°C

Hybridisation solution

To make hybridisation solution, 1.0g of blocking powder (Roche) was added to 25ml of deionised formamide (Ambion) and 12.5ml of SSC (20X, pH5.0). This solution was heated at 65°C until completely dissolved. Once dissolved, 1ml of yeast torula RNA (50mg/ml), 0.25ml of heparin (10mg/ml), 0.25ml of Tween-20 (20%), 0.5ml of CHAPS (10%) and 1.25ml of EDTA (0.2M) were added. DEPC-treated water was added to a final volume of 50ml. The solution and was then filtered through a 0.20µm filter. The solution was aliquoted and stored at -20°C.

Solution I

Solution I consisted of 50% formamide, 5X SSC, pH 4.5, and 1% SDS.

Solution II

Solution II consisted of 50% formamide, 2X SSC, pH 4.5.

MAB

MAB consisted of 5.8g of maleic acid and 4.38g of NaCl. DEPC-treated water was added to a final volume of 500ml and the pH was titrated to 7.5 with 1M NaOH. The solution was autoclaved and stored at room temperature.

MABT

MABT consisted of 0.1% Tween-20 in MAB and was stored at room temperature.

NTMT

NTMT solution was made immediately prior to use from concentrated stocks including 1ml of 5M NaCl, 5ml of 1M Tris.HCl (pH 9.5), 2.5ml of 1M $MgCl_2$, 0.25ml of Tween-20 (20%) and 41.25ml of DEPC-treated water.

Staining solution

18µl of 18.75 mg/ml NBT/ 9.4 mg/ml BCIP (Roche) was added to 1ml of NTMT buffer.

2.4.1.2 Riboprobe synthesis

Riboprobes for *in situ* hybridisation histochemistry were made by *in vitro* transcription using digoxigenin (DIG)-labelled dNTP mix. The DIG labelling mix, polymerases, and transcription buffers were from Roche. Measures taken to prevent RNA degradation included wearing gloves all the time, keeping RNA products on ice as much as possible and soaking the electrophoresis equipment in 0.1% SDS overnight.

Plasmids containing the riboprobe sequence were linearised by restriction enzymes following the procedures described in the section 2.2.8. 1µg of linearised plasmid was precipitated in $1/10^{th}$ volume of 3M sodium acetate and 2 volumes of pure

ethanol. After centrifugation at 13000rpm for 15 min, the supernatant was discarded and the pellet was resuspended in 5µl of DEPC-treated water. The choices of restriction enzyme and of RNA polymerase were determined by the direction of the DNA cloned into the pGEM®-T Easy vector (Table2-1). The reaction was carried out in a 500µl microcentrifuge tube containing 1µg of linearised plasmid, 2µl of 10X transcription buffer, 2µl of 10X DIG RNA labelling mix, 40units of T7 or Sp6 RNA polymerase and 40units of RNase inhibitor. DEPC-treated water was added to a final volume of 20µl.

Table 2-1 Restriction enzymes and RNA polymerases used to generate riboprobes.

Gene	Antisense Probe		Sense Probe	
	Polymerase	Enzyme	Polymerase	Enzyme
Dact1	T7	*Spe*I	Sp6	*Nco*I
Dact2	T7	*Spe*I	Sp6	*Nco*I

The reaction was incubated at 37°C for 2 hours using a heating block. The template DNA was then digested by incubating with RNase-free DNase1 (Promega) at 37°C for additional 15 min. 2µl of 0.2M EDTA (pH8.0) was added to stop the digestion. The DIG-labelled RNA probes were precipitated by adding 2.5µl of 4M LiCl and 75µl of prechilled pure ethanol followed by incubation at -20°C overnight. The following day, the RNA probes were centrifuged for 15 min at 13000rpm. The supernatant was carefully removed and the pellet was washed with 50µl of prechilled 70% ethanol. After centrifugation for further 15 min, the supernatant was removed and the pellet was resuspended in 50µl of DEPC-treated water. 1µl of RNase inhibitor was added. RNase-free gel electrophoresis was performed using 1µl of the RNA solution to check the integrity of the RNA and to estimate its concentration. The RNA solution was diluted in the hybridisation solution, aliquoted and stored at -70°C until use.

2.4.1.3 Tissue preparation

At the end of the kidney culture, the culture medium was aspirated off and replaced by 100% ice cold methanol. This was left for 10 min so that kidneys could fix to the filters. The filters with attached kidneys were transferred to a labelled bijou and fixed in 4% PFA at 4°C overnight. For long term storage, these samples were kept in 100% methanol at –20°C.

2.4.1.4 Hybridisation protocol

Kidneys on the filters were processed for *in situ* hybridisation based on Wilkinson's protocol (Wilkinson, 1992) with slight modifications. Unless otherwise stated, washes were for 5 min with gentle rocking. Kidneys were rehydrated through a series of graded methanol in PBST on ice. After washing in PBST twice on ice, kidneys were digested with 10µg/ml proteinase K (Sigma) in PBST for 30 min at room temperature. Digestions were stopped by washing in freshly prepared 2mg/ml glycine in PBST for 5 min. Kidneys were washed twice in PBST and were then fixed in 4% PFA for 40 min on ice. After two washes in PBST, most of the liquid was removed and replaced by the mixture of PBST and hybridisation solution (1:1) followed by incubation in pure hybridisation solution. Kidneys were prehybridised in this solution for 3 hours at 70°C before the probe was added. The probe at a final concentration of 200ng/ml was heated to 80°C for 5 min before adding it to the kidneys. Hybridisation with the probe was carried out at 70°C overnight. Protect RNA (Sigma), at the concentration of 2µl/ml, was used in all solutions after digestion with proteinase K until the end of hybridisation. The following day, kidneys were washed in preheated solution I (30 min x 3) at 70°C followed by washing in preheated solution II (30 min x 3) at 65°C. Kidneys were then washed with MABT before being blocked for 3 hours at 4°C in MABT with 10% sheep serum (Sigma) and 2% (w/v) blocking powder (Roche). Samples were incubated in alkaline phosphatase-conjugated anti-DIG antibody (Roche) at 1:2000 dilution in fresh blocking solution at 4°C overnight. Excess antibody was removed by washing the kidneys in MABT (5 min x 3 followed by 1 hour x 5). Final wash was carried out

in NTMT (10 min x 3). Kidneys were then subjected to colour development in staining solution. After colour development in the dark, the kidneys were fixed in 100% methanol before mounting on slides.

2.4.2 RNA *in situ* hybridisation on sections

2.4.2.1 Solutions

Most solutions were the same as those used in whole mount *in situ* hybridisations except some modifications. These modifications are listed in Table 2-2.

Table 2-2 Solutions for *in situ* hybridisation on kidney sections

Solution	Composition
TEA (triethanolamine) buffer, 0.1M TEA pH 8.0	295ml DEPC-treated water, 4ml triethanolamine, 0.525ml 10N HCl
Proteinase K buffer	50mM Tris-HCl pH 7.5, 5mM $CaCl_2$
Prehybridisation buffer pH 8.5	50% formamide (Ambion) 10% dextran sulfate 5X SSC 1X Denhart's 100mM DTT 250µg/ml yeast tRNA 0.1% SDS
20XSSC pH 7.5	NaCl 87.66g, Trisodium Citrate 44.12g in 500ml of DEPC-treated water
Post-hybridisation wash buffer I	1X SSC, 10mM DTT
Post-hybridisation wash buffer II	0.5XSSC,10mM DTT
TBS (Tris-buffered saline) pH 7.5	100mM Tris.HCl, 150mM NaCl
Blocking solution	0.1% Triton X-100, 1% normal sheep serum in TBS
B2 buffer	0.1M Tris pH 9.5, 0.1M NaCl, 50mM $MgCl_2$
Developing buffer	0.1M Tris pH 9.5, 0.1M NaCl, 1mM levamisole

2.4.2.2 Tissue preparation

Immediately after dissection, kidneys were fixed by 4% PFA at 4°C overnight and stored in 70% ethanol at 4°C. Kidneys were then embedded in paraffin, sectioned by

microtome (10μm in thickness), mounted onto slides and dried at room temperature overnight. Dried sections can be directly subjected to *in situ* hybridisation procedures or kept at 4°C for future use.

2.4.2.3 Hybridisation protocol

Kidney sections mounted onto slides were washed twice in Histoclear (Brunel Microscopes Ltd) to remove wax and were rehydrated through a series of graded ethanol followed by washing twice in PBS. Samples were fixed again in 4% PFA at room temperature for 15 min. After two washes in PBS, slides were incubated in TEA buffer for 5 min including freshly added acetic anhydride to a concentration of 0.25% (v/v). Additional acetic anhydride was added to a final concentration of 0.5% (v/v) to acetylate samples for another 5 min. Samples were washed in 2X SSC for 3 min and were subjected to proteinase K digestion at 37°C for 30 min. Digestions were stopped by washing in freshly prepared 2mg/ml glycine in PBS for 5 min. Kidneys were washed twice in PBS and were then incubated in prehybridisation buffer at 37°C in a humidified chamber for 2 hours. After prehybridisation, slides were immersed into 2X SSC for 5 min. The probe at a final concentration of 200ng/ml was heated at 80°C for 5 min before being added onto the sections. Hybridisation with the probe was carried out at 50°C overnight. Protect RNA (Sigma), at the concentration of 2μl/ml, was used in all solutions after digestion with proteinase K until the end of hybridisation. Post-hybridisational washes were performed as one quick wash in post-hybridisation wash buffer I at room temperature, two 15 minutes' washes in post-hybridisation wash buffer I at 65°C, two 15 minutes' washes in post-hybridisation wash buffer II at 65°C, and a 10 minutes' wash in post-hybridisation wash buffer II at room temperature. After washing in TBS (5 min x 3), kidney sections were covered with blocking solution for 30 min and were incubated overnight at 4^{o}C in alkaline phosphatase-conjugated anti-DIG antibody (Roche) at 1:2000 dilution in fresh blocking solution. The next day, sections were washed in TBS (5 min x 3) followed by B2 buffer for 10 min. Samples were developed in developing buffer containing NBT/BCIP (18μl/ml). When satisfactory staining was

obtained, the colour reaction was stopped by rinsing the slides several times in tap water and the samples were mounted in 50% glycerol in PBS.

2.5 Immunofluorescence

2.5.1 Tissue preparation

At the end of kidney culture, the culture medium was aspirated off and replaced by 100% ice cold methanol. This was left for 10 min so that kidneys could fix to the filters. The filters with attached kidneys were transferred to a labelled bijou and fixed in pure methanol at 4°C overnight. For long term storage, these samples were kept in 100% methanol at –20°C.

2.5.2 Immunofluorescence protocol

Kidneys were washed in PBS for 1 hour at room temperature with gentle rocking. They were then incubated in primary antibodies diluted in PBS at 4°C overnight. Next day, the kidneys were washed in PBS for 1 hour at room temperature and were then incubated in secondary antibodies diluted in PBS at 4°C overnight (see result chapters for the antibodies used and their dilutions). The kidneys were washed again in PBS for 30 min at room temperature. Kidneys with filters were then mounted on a glass slide using the aqueous mountant Mowiol and were imaged by confocal microscopy.

2.6 siRNA-mediated RNA interference

2.6.1 siRNA oligos

siRNA oligos were purchased from Dharmacon. siRNA oligos were resuspended in 1X siRNA buffer to make 20µM stocks. The siRNA stocks were aliquoted and stored at -20°C. The siRNA oligos used in this project included *Dact1* siRNA, non-targeting siRNA (siCONTROL) and fluorescently-labelled siRNA, siGLO. *Dact1*

siRNA was a pool of four rationally designed siRNAs targeting the open reading frame of *Dact1* mRNA (NCBI RefSeq Database, accession number NM_021532). The 5' start positions for each of the four oligos were 381, 656, 1078 and 1653. Table 2-3 listed the target sequences of these four oligos and Tabe 2-4 showed the sequences of these four siRNAs. Non-targeting siRNA was designed to share little or no homology with known mRNA targets. They were used as controls detecting non-specific effects caused by the introduction of any siRNA. siGLO was a Cy3-labelled siRNA targeting mouse lamin A (NCBI RefSeq Database, accession number NM_019390) and was used to establish the conditions for optimal siRNA delivery and to monitor siRNA transfection efficiency during the experimental procedures.

Table 2-3 Target sequences of the *Dact1* siRNA duplexes.

Duplex	5' start positions	Target sequences
1	1078	GGAATAACCTCTTTGGAAAAC
2	381	GCAGATAAGTGACCTGAGACT
3	656	GGAATGACGTATATCGCTACC
4	1653	GAAGTGCCGTTTCCCAGACGA

Table 2-4 Sequences of the *Dact1* siRNA duplexes. All are represented in a 5’ to 3’ orientation.

	Sense siRNA strand	Antisense siRNA strand
Duplex 1	AGAUAAGUGACCUGAGACUUU	AGUCUCAGGUCACUUAUCUUU
Duplex 2	AAUGACGUAUAUCGCUACCUU	GGUAGCGAUAUACGUCAUUUU
Duplex 3	AAUAACCUCUUUGGAAAACUU	GUUUUCCAAAGAGGUUAUUUU
Duplex 4	AGUGCCGUUUCCCAGACGAUU	UCGUCUGGGAAACGGCACUUU

2.6.2 siRNA transfections

siRNA transfections were carried out in a 24-well plate. Each treatment was performed in triplicate. One day prior to transfection, cells were plated at a density of $5x10^4$cells/well in plating medium. The medium was replaced by fresh plating

medium 0.4ml/well 30 min before transfection. For each well, proper amount of siRNA and 1.2µl of siLentFect (Bio-rad) were diluted in 50µl of Opti-MEM (Gibco) in two separate tubes and incubated at room temperature for 5 min. Transfection mix was made by mixing the solutions of these two tubes and incubated at room temperature for 20 min. 100µl of transfection mix was then added to each well, yielding 10nM siRNA. After gently rocking, the plate was then moved into the cell culture incubator with 5% CO_2 at 37°C.

2.7 BrdU incorporation assay

2.7.1 BrdU incorporation

Cells were grown on a coverslip in a well of a 24-well plate. The cell culture medium was replaced by BrdU (Sigma) 20µM in DMEM 45 min prior to immunocytochemistry. The cells were cultured at 37°C with 5% CO_2.

2.7.2 BrdU immunocytochemistry

All the procedures were carried out at room temperature unless otherwise stated. Cells were washed in PBS (5 min x 3) and were fixed by 4% PFA at 4ºC for 30 min. Following fixation, cells were washed in wash buffer, which was 1% Triton X-100 in PBS (5 min x 3). 2N HCl was then used to denature the DNA in cells at 37ºC for 30 min. After one wash in wash buffer, cells were neutralised by 0.1M sodium tetraborate (pH 8.5) for 2 min followed by washing in wash buffer (5 min x 3). 1% BSA in wash buffer was used as blocking buffer and primary antibody diluent. Cells were blocked in blocking buffer at 37ºC for 30 min and were then incubated with rat anti-BrdU antibody (Oxford biotechnology) at 1:100 dilution in the blocking buffer at 4ºC overnight. The next day, cells were washed in wash buffer (5 min x 3) and were then incubated in TRITC-conjugated anti-rat IgG (Sigma) at 1:100 dilution in PBS at 37ºC for 2 hours. After washing for three times, cells were counterstained by 2µl of TO-PRO-3 (Invitrogen) in 500µl of PBS for 5 min followed by PBS wash for 5 min. Cells were then subjected to mounting and imaging.

2.8 Generation of *Dact2* shRNA stable cell lines

2.8.1 Vector information

The SureSilencing *Dact2* shRNA plasmids (Superarray) were designed and validated to knockdown the expression of *Dact2* specifically by RNAi. This kit contained four *Dact2* short-hairpin RNA (shRNA) plasmids and one control plasmid. Each plasmid was constructed based on the same parent vector, pGeneClip^{TM} Neomycin vector (Figure 2-2, Promega), and was able to express a shRNA under the control of the U1 promoter. It also expressed a neomycin resistance gene, which enabled selection of stably transfected cells. The only difference between control and *Dact2* shRNA plasmids was the shRNA sequences, as the former contained a scrambled artificial sequence which does not match any mouse, rat or human gene.

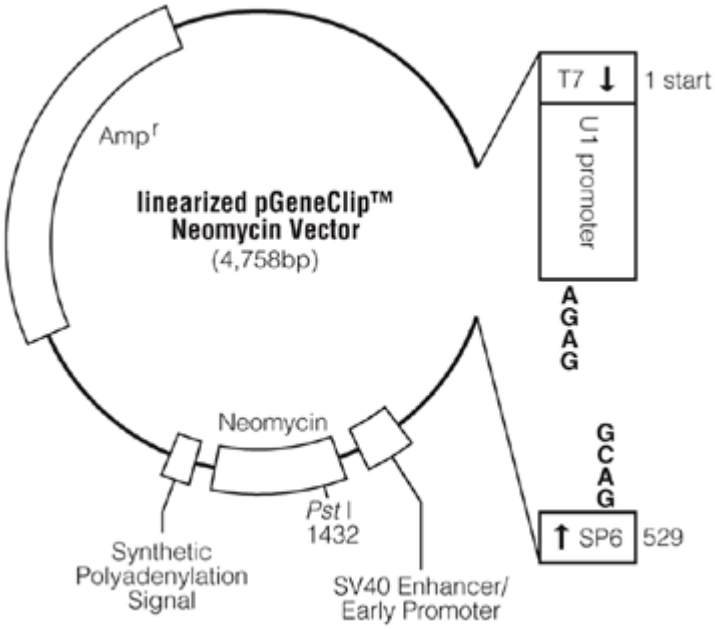

Figure 2-2 pGeneClip™ Neomycin Vector.

2.8.2 *E. coli* transformation

2µl of each stock plasmid was added to 50µl of thawed competent *E. coli* cells (JM109, Promega) in a 1.5ml microcentrifuge tube on ice. The following procedures were the same as those described in section 2.3.2.

2.8.3 Plasmid purification

Plasmid DNA was isolated using a commercially available kit (EndoFree Plasmid Maxi Kits, Qiagen). For the extraction of plasmid DNA, a single colony was picked with a sterile loop to inoculate 2.5ml of LB broth containing 50µg/ml ampicillin. This starter culture was incubated with vigorous shaking at 37°C until just a hint of turbidity observed. 250µl of the starter culture was then inoculated into 250ml of LB broth containing 50µg/ml ampicillin. This culture was incubated with vigorous shaking at the speed of 225rpm in an orbital shaker at 37°C overnight. After incubation of 12-16 hours, plasmid DNA was extracted according to the manufacturer's instructions. The concentration of the isolated DNA was determined by spectrophotometry.

2.8.4 Diagnostic restriction digest

To verify the purified plasmids containing the shRNA inserts, a *Pst*1 restriction enzyme (Roche) digestion was performed on each plasmid. The restriction digestion procedures were the same as those described in the section 2.2.8. A diagnostic pair of bands, with the sizes of 3827bp and 991bp respectively, shown on agarose gel confirmed the correct insert in each plasmid.

2.8.5 Plasmid transfection

In a 6-well cell culture plate, mIMCD-3 cells were plated at a density of $5.0x10^5$cells/well in fresh plating media and were cultured at 37°C in a humidified incubator. Transfection mix was prepared when cells have reached 90-100% visual

confluency. For each well, 2µg of plasmid and 6µl of Metafectene Pro (Biontex) were diluted in 100µl of serum- and antibiotic-free medium in separate tubes and incubated at room temperature for 5 min. The DNA solution was then added into the Metafectene Pro solution and the mixtures were incubated at room temperature for 20 min. After incubation, the DNA-lipid complexes were added dropwise into each well and cells were cultured at 37°C in a humidified incubator with 5% CO_2.

2.8.6 Selection for neomycin resistance

Before plasmid transfection, a G418 (Calbiochem) killing curve was performed to determine the effective concentration, that is the minimal concentration needed to kill all the untransfected cells. In this project, the minimal G418 concentration required to kill untransfected cells was 400µg/ml. After transfection, cells were plated at 10% confluency in a 6-well plate growing in culture media containing 400µg/ml G418. Control plates, including untransfected cells growing in G418 media and transfected cells growing in media without G418, were also carried out in parallel to ensure the selection conditions were working. Media were replaced every three days for two weeks when the drug resistant clones appeared. Cells were then passed onto separate sterile 10cm petri dishes. In each dish, several individual cells were selected and marked. Once the colonies developed to an appropriate size, they were picked by sterile pipette tips and seeded to separate wells in a 24-well plate. Eight clones were selected for each transfectant. Cells were cultured in media with reduced G418 concentration (100µg/ml). A stock of stably transfected cells was frozen down and kept in liquid nitrogen.

2.9 Imaging

2.9.1 Mountants

Mountants used in this project were 50% glycerol in PBS for *in situ* hybridisation samples and Mowiol mounting medium for immunofluorescence samples.

To prepare Mowiol mounting medium, 2.4g of Mowiol (Calbiochem) was added to 4.76ml of glycerol in a 50ml conical flask and stirred to mix. 12ml of distilled water was added and the mixture was left overnight at room temperature. The following day, 12ml of 0.2M Tris (pH8.5) was added and the solution was heated to 50°C for 2 hours with occasional vortexing. When the Mowiol had dissolved, the solution was clarified by centrifugation at 2000rpm for 15 min. 0.72g of 1,4-diazobicyclooctane was then added. The solution was aliquoted and stored at -20°C. This mountant was warmed to room temperature before use.

2.9.2 Confocal microscopy

Samples stained by immunofluorescence were imaged using the TCS NT Leica confocal laser scanning microscope (Leica Microsystems). Samples were imaged on the FITC and TRITC channels separately to avoid cross talk between the two channels. For kidney samples, optical sections were set to 5μm in thickness and serial optical sections were obtained. Sections were scanned four times and averaged. Maximum projection images of a series were presented. For cell samples, images were captured on the FITC and TRITC channels individually and the maximum projection images were presented.

2.9.3 *In situ* hybridisation imaging

In situ hybridisation images were captured by using a Zeiss Axioplan II microscope (Carl Zeiss) equipped with a Photometrics CoolSnap HQ CCD camera (Roper Scientific). Images were captured using scripts written by Dr. Paul Perry for IPLab Spectrum v3.6 (Scanalytics) which controlled camera capture, scale bar generation and filter selection via motorised filter wheels (Ludl Electronic Products).

Chapter 3

Expression patterns of *Dact1* and *Dact2* in kidneys

3.1 Introduction

More and more genes are being shown to be involved in kidney development. To learn more about these genes, one important question to address is when, where and how they are normally expressed. From the viewpoints of developmental biologists, temporal and spatial expression profiles can shed light on particular events (cell proliferation, cell differentiation, tissue patterning, etc) in the developmental process. This information may also reveal valuable clinical significance when compared to those in pathological state such as cancer and degenerative diseases. This will, at least, contribute to early and accurate diagnosis and precise prognosis and may render new therapeutic strategies.

Expression of *Dact* genes in mouse embryos has been described before (Cheyette et al., 2002; Fisher et al., 2006) but little is known about expression in developing kidneys. The first goal of this study was to fill this research gap. In this chapter, I will demonstrate the expression of both *Dact* genes in embryonic kidneys and describe their temporal and spatial expression patterns in kidneys at a series of developmental stages. These results were expected not only to offer biological significance of both genes in kidney development but to serve as a foundation for subsequent gene knockdown and regulation experiments.

The importance of transcript diversity in organ development has been published in various organ systems including kidneys (Hammes et al., 2001; Igarashi et al., 1995; Natoli et al., 2002), testes (Elliott and Grellscheid, 2006) and limbs (Narita et al., 2007). The crucial roles of transcript diversity in kidney development can be exemplified by the work on NKCC2, a gene encoding Na-K-Cl cotransporter, and *Wt1* (Wilms' tumour gene). Igarashi *et al.* showed different expression patterns of the three isoforms of NKCC2 in E16.5 metanephroi (Igarashi et al., 1995). By generating mouse strains that specifically lack the *Wt1*(-KTS) or *Wt1*(+KTS) splice variant, Hammes *et al.* demonstrated that homozygous mice lacking the *Wt1*(-KTS) variant showed hypoplastic kidney whilst homozygous mice lacking the *Wt1*(+KTS) variant showed defects in podocyte differentiation (Hammes et al., 2001).

When this project was started, two transcript variants of *Dact1* had been reported in the database ASD (Alternative Splicing Database Project) (Stamm et al., 2006), which has been now combined into a new database ASTD (Alternative Splicing and Transcript Diversity) (http://www.ebi.ac.uk/astd/). In this database, they were designated as splicing pattern 1 (SP1) and splicing pattern 2 (SP2) with the transcript ID TRAN00000167620 and TRAN00000167621, respectively. However, whether these transcripts are expressed in developing kidneys remained unknown. In this chapter, I will demonstrate the expression of these predicted transcripts in developing kidneys. I will also show a novel transcript variant, which was previously undiscovered, in developing kidneys. Besides, verifying the expression of these *Dact1* transcript variants helped to design efficient siRNA duplexes to target all the transcripts simultaneously in my subsequent RNAi experiments (refer to chapter 5 and 6). Therefore, I will examine the expression of these transcript variants in developing kidneys and NIH3T3 cells, both of which were key models used to investigate *Dact1* functions in this project.

3.2 Experimental design

3.2.1 RT-PCR

Conventional end-point RT-PCR was performed to confirm the expression of *Dact1* and *Dact2* expression in embryonic kidneys and, in addition, it was used to show the transcript diversity of *Dact1* in an embryonic cell line and in kidneys. The primer pairs used to confirm the expression of both *Dact* genes were designed to span exon 2 (Figure 3-1). The binding sites of these primers are depicted in Figure 3-1 and the sequences are listed in Table 3-1. To illustrate the transcript diversity of *Dact1*, primers were designed to span the exon 3-exon 4 boundary. The binding sites of these primer pairs are depicted in Figure 3-2 and the sequences are listed in Table 3-2.

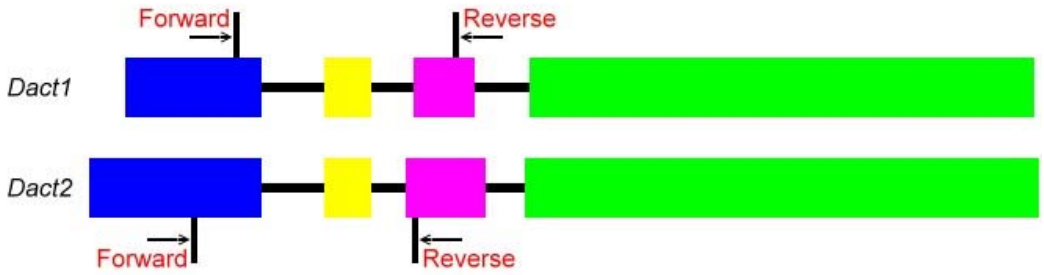

Figure 3-1 Binding sites of PCR primers used to clone mouse *Dact1* and *Dact2* genes. A schematic diagram shows the binding sites of PCR primers on *Dact* genes. Coloured bars refer to different exons i.e. exon 1 (blue), exon 2 (yellow), exon 3 (magenta) and exon 4 (green). The forward primer binds to the antisense strand, the reverse primer to the sense strand. Amplicons generated by *Dact1* primers were 321bp in size whilst those generated by *Dact2* primers were 341bp in size.

Table 3-1 The sequences of the PCR primers used to clone mouse *Dact1* and *Dact2* genes. The forward primer binds to the antisense strand, the reverse primer to the sense strand. All oligos are represented in a 5' to 3'orientation.

Gene	RefSeq accession number	Forward Primer	Reverse Primer
Dact1	NM_021532	GGAGGAGAAGTTCCTGGAAGA	CCGTCTGAGATGGTCAAGG
Dact2	BC058740	GACTACGAGCCGCACTGG	GCAGGAGGTGGACAGAGAAC

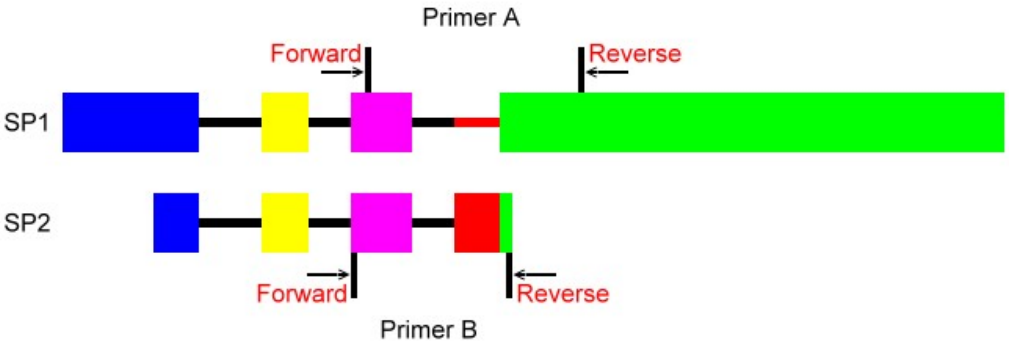

Figure 3-2 PCR primer binding sites on cDNA of the two transcripts of *Dact1*. Primer A was designed to only amplify SP1 while primer B would amplify both SP1 and SP2. Coloured bars refer to different exons. The red segments with 111bp in size indicate the source of the extra band shown on Figure 3-4.

Table 3-2 The sequences of PCR primers used to illustrate transcript diversity of *Dact1*. The forward primer binds to the antisense strand, the reverse primer to the sense strand. All oligos are represented in a 5' to 3' orientation.

Primer names	Forward Primer	Reverse Primer
A	TTCGGGCTCCCTCTCTAACT	CAGATCCAATGCAGATGTCG
B	GGTTTTATGAGCTGAGTGATGG	GACACAAGATCACACTGGTATTTAGG

3.2.2 Quantitative real time PCR

Quantitative real time PCR was used to establish the expression profiles of *Dact1* and *Dact2* on kidneys at various times during embryonic and postnatal development. In order to validate the technique, I performed quantitative real time PCR to measure *Notch1* expression in the microdissected kidneys. *Notch1* is a well-investigated gene in developing kidneys and I found that the *Notch1* expression level was very low at E12.5 and was greatly increased from E15.5 to E17.5. This expression pattern was consistent with the work that has already been published (Chen and Al-Awqati, 2005). Table 3-3 shows the sequences of the primer pairs used. Kidneys at stages with significant developmental importance were chosen. Namely, E11.5 was the time when nephrogenesis started, E14.5 and E15.5 stood for the most intensive renal organogenesis period, and P14 was the time when nephrogenesis ceased (Bard, 2003; Saxen, 1987). Adult kidneys were also included to complete the temporal expression profiles. Expression levels were obtained by normalisation to a housekeeping gene, *Actb*. In *Dact1* expression profile, expression levels were converted to those relative to E11.5 kidneys while in *Dact2* expression profile, expression levels were shown as those relative to E17.5 kidneys. Three independent experiments were carried out and the results are shown in Figure 3-7 and 3-8. Student *t* tests were used to assay the differences in the expression levels between samples. When a *p*-value was less than 0.05, the difference was considered to be statistically significant.

Table 3-3 Quantitative real time PCR primers used to profile *Dact1* and *Dact2* expressions. The forward primer binds to the antisense strand, the reverse primer to the sense strand. All oligos are represented in a 5' to 3'orientation. *Actb* was used as an internal control.

Gene	RefSeq accession number	Forward Primer	Reverse Primer
Dact1	NM_021532	GCCGGTTTGTTGAATCAGTT	CGAAGCTCCATCACTCAGC
Dact2	BC058740	AGCTGGATGTGAGCAGGTCT	GCAGGAGGTGGACAGAGAAC
Actb	NM_007393	GATCTGGCACCACACCTTCT	GTACATGGCTGGGGTGTTG

3.2.3 RNA *in situ* hybridisation

RNA *in situ* hybridisation was performed in whole mounts and on sections to characterise the spatial expression patterns of both *Dact1 and Dact2*. DIG-labelled RNA probes were made by *in vitro* transcription as described in section 2.4.1 and Table 2-1. Sense controls were carried out in parallel to confirm to specificity of the expression patterns.

3.3 Results

3.3.1 Demonstration of *Dact1* and *Dact2* expression in metanephroi

Conventional end-point PCR was used to show the expression of both *Dact* genes in embryonic kidneys (Figure 3-3). On E14.5 kidneys, two single bands of the expected size for *Dact1* (321bp) and *Dact2* (341bp) were apparent. The same reactions, without addition of reverse transcriptase, served as negative controls and yielded no bands.

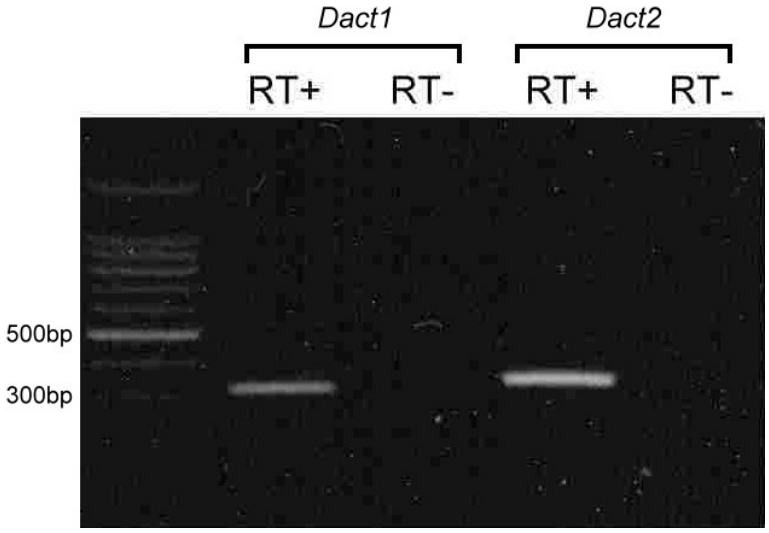

Figure 3-3 E14.5 metanephroi express *Dact1* and *Dact2*. Compared with a 100bp ladder (left lane), PCR ethidium bands of the appropriate size for *Dact1* and *Dact2* cDNA were present in E14.5 metanephros RNA samples with RT added (+) but not in metanephros samples when no RT was added (−).

3.3.2 Identification of three splicing variants of *Dact1*

When this project started, there were only two predicted splicing variants of *Dact1* in the ASTD database. Based on the sequences provided in this database, I designed two primer pairs (Figure 3-2 and Table 3-2) to amplify cDNA fragments derived from these two transcripts in both NIH3T3 cells and E14.5 kidneys. Primer pair A aimed to amplify SP1 transcript whilst primer pair B inevitably amplified both transcripts. Figure 3-2 illustrated the binding sites of these primers.

The transcript diversity of *Dact1* was examined in NIH3T3 cells and E14.5 kidneys. As shown in Figure 3-4, both NIH3T3 cells and E14.5 kidneys expressed the same transcript diversity. Primer pair B amplified the cDNA of the two transcripts and hence yielded two expected bands of appropriate sizes (301 and 190bp). Primer pair A aimed to generate an amplicon at the size of 314bp but also amplified an extra product, which was about 110bp larger in size. This extra band may indicate the presence of another transcript.

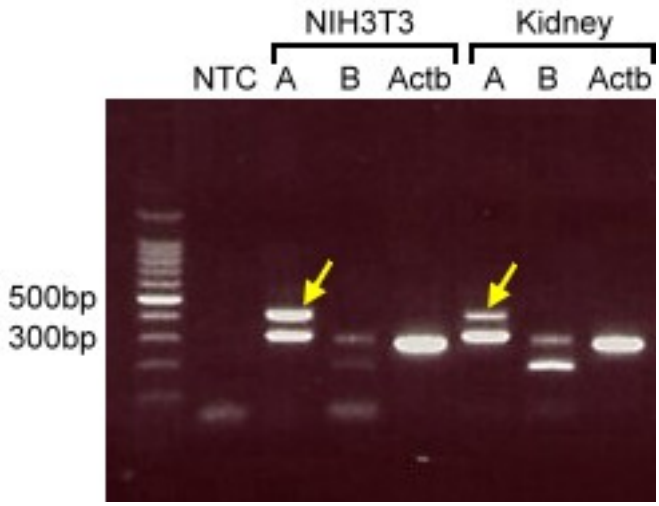

Figure 3-4 Transcript diversity of *Dact1* in both NIH3T3 cells and E14.5 kidneys. Primer pair B amplified cDNA fragments from both transcript variants yielding two bands at the expected sizes (301bp and 190bp). Primer A aimed to obtain an amplicon only from SP1 at the size of 314bp revealed an additional band (425bp) (yellow arrow). *Actb* was used as a positive control. NTC refers to no template control.

By reviewing the sequences of both SP1 and SP2, I noted that the first 111bp of the exon 4 of SP2 was exactly the same as part of the intron sequence immediately upstream to the exon 4 of SP1 (Figure 3-2). Taking into account the size of the extra band, I hypothesized that there may be another transcript, SP3, which shared homology with SP1 but contained an insertion of a short segment of intron sequence with 111bp in size. To confirm this hypothesis, I cloned each PCR product shown in Figure 3-4 into pGEM®-T Easy vectors (Promega) and sent the purified plasmids to DNA sequencing service. The sequencing results, shown in Figure 3-5 and summarised in Figure 3-6, confirmed that SP3 was generated though an alternative 3' site at exon 4.

cDNA fragment amplified by primer A, 425bp

CNNNNCAGCTCCGGCCGCCAGGCGGCCGCGGGAATTCGATTCAGATCCAATGCAGATGT
CGCTGGCATGGCTCCCAAGCCCCTCCTCTTCCCTCAGAGCGTTGCCCGTCAGACAAAGG
AGAAACATTGGGCTCTGCACAGCCACAGCATGAAGTGGACTGGGGTAGCGATATACGT
CATTCCCGTTTTTAGGCACAAGATCACACTGGTATTTAGGATTCACATCTGCAATGACAT
CAAGGGAATTAAATTGTGGTGTGGAGGGGGAACTGCACACTGTCCCTGAGGCCTGGTCT
TCACAGGGGCCGCCTTTACATTCCAACCATCCTATGAGATCTGCAGATTTGGGGCAACC
GTCTGAGATGGTCAAGGCCGCCTCCAAGGGGCTGCAGAAGCAGGTGCTGGAATGGCAA
CTGGACAAACACTCACTGAACACGGAGTTGGAGGAGTTAGAGAGGGAGCCCGAAAATC
ACTAGTGAATTCGCGGCCGCCTGCAGGTCGACCATATGGGAGAGCTCCCAACGCGTTGG
ATGCATAGCTTGAGTATTCTATAGTGTCACCTAAATAGCTTGGCGTAATCATGGTCATAG
CTGTTTC

cDNA fragment amplified by primer A, 314bp

GNNCCGGCGCCAGGCGGCCGCGGGAATTCGATTCAGATCCAATGCAGATGTCGCTGGC
ATGGCTCCCAAGCCCCTCCTCTTCCCTCAGAGTGTTGCCCGTCAGACAAAGGAGAAACA
TTGGGCTCTGCACAGCCACAGCATGAAGTGGACTGGGGTAGCGATATACGTCATTCCCG
TTTTTAGACACAAGATCACACTGGTATTTAGGATTCACATCTGCAGATTTGGGGCAACC
GTCTGAGATGGTCAAGGCCGCCTCCAAGGGGCTGCAGAAGCAGGTGCTGGAATGGCAA
CTGGACAAACACTCACTGAACACGGAGTTGGAGGAGTTAGAGAGGGAGCCCGAAAATC
ACTAGTGAATTCGCGGCCGCCTGCAGGTCGACCATATGGGAGAGCTCCCAACGCGTTGG
ATGCATAGCTTGAGTATTCTATAGTGTCACCTAAATAGCTTGGCGTAATCATGGTCATAG
CTGTTTC

cDNA fragment amplified by primer B, 301bp

GNNCCGGCGCCAGGCGGCCGCGGGATTCGATTGGTTTTATGAGCTGAGTGATGGAGCTT
CGGGCTCCCTCTCTAACTCCTCCAACTCCGTGTTCAGTGAGTGTTTGTCCAGTTGCCATT
CCAGCACCTGCTTCTGCAGCCCCTTGGAGGCGGCCTTGACCATCTCAGACGGTTGCCCC
AAATCTGCAGATCTCATTGGATGGTTGGAATGTAAAGGCGGCCCCTGTGAAGACCAGGC
CTCAGGGACAGTGTGCAGTTCCCCCTCCACACCACAATTTAATTCCCTTGATGTCATTGC
AGATGTGAATCCTAAATACCAGTGTGATCTTGTGTCAATCACTAGTGAATTCGCGGCCG
CCTGCAGGTCGACCATATGGGAGAGCTCCCAACGCGTTGGATGCATAGCTTGAGTATTC
TATAGTGTCACCTAAATAGCTTGGCGTAATCATGGTCATAGCTGTTTCCTGTGTGAAATT
GTTATCC

cDNA fragment amplified by primer B 190bp

GGCGCCAGGCGGCCGCGGGAATTCGATTGGTTTTATGAGCTGAGTGATGGAGCTTCGGG
CTCCCTCTCTAACTCCTCCAACTCCGTGTTCAGTGAGTGTTTGTCCAGTTGCCATTCCAGC
ACCTGCTTCTGCAGCCCCTTGGAGGCGGCCTTGACCATCTCAGACGGTTGCCCCAAATCT
GCAGATGTGAATCCTAAATACCAGTGTGATCTTGTGTCAATCACTAGTGAATTCGCGGC
CGCCTGCAGGTCGACCATATGGGAGAGCTCCCAACGCGTTGGATGCATAGCTTGAGTAT
TCTATAGTGTCACCTAAATAGCTTGGCGTAATCATGGTCATAGCTGTTTCCTGTGTGAAA
TTG

Figure 3-5 DNA sequencing results of cDNA fragments of *Dact1*. PCR products shown in Figure 3-4 were cloned into pGEM®-T Easy vectors and sent to the sequencing service. Green colour refers to sequences of exon 4. Magenta colour refers to sequences of exon 3 and red to the inserted intron sequences immediately upstream to exon 4. The exon organisation of the three transcript variants is depicted in Figure 3-6.

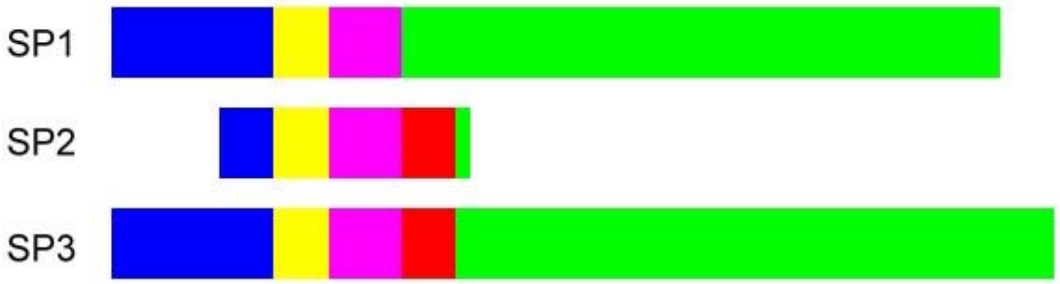

Figure 3-6 The exon organisation of the three *Dact1* splice variants. A schematic diagram illustrates the exon organisation of the three *Dact1* splice variants. Each transcript has four exons. Coloured bars depict different exons, namely exon 1 (blue), exon 2 (yellow), exon 3 (magenta) and exon 4 (green in SP1, red and green together in SP2 and SP3). The red bar in SP2 and SP3 were from intron sequences immediately upstream to exon 4 (green) of SP1.

3.3.3 Temporal expression patterns of *Dact1* and *Dact2* in mouse kidneys

Having confirmed the expression of both *Dact* genes in embryonic kidneys (Figure 3-3), quantitative real time PCR and RNA *in situ* hybridisation were performed to delineate the temporal and spatial expression profiles of both *Dact* genes in kidneys. Quantitative real time PCR showed that the *Dact1* expression levels in embryonic kidneys were higher than those in adult kidneys. In adults, the expression level of *Dact1* was about 20% of that at E11.5 (Figure 3-7). However, the level of *Dact2* expression increased from E11.5, peaked at E17.5, and decreased at P14 and in adult. In adult kidney, *Dact2* was still expressed at a level similar to that at E14.5 (Figure 3-8).

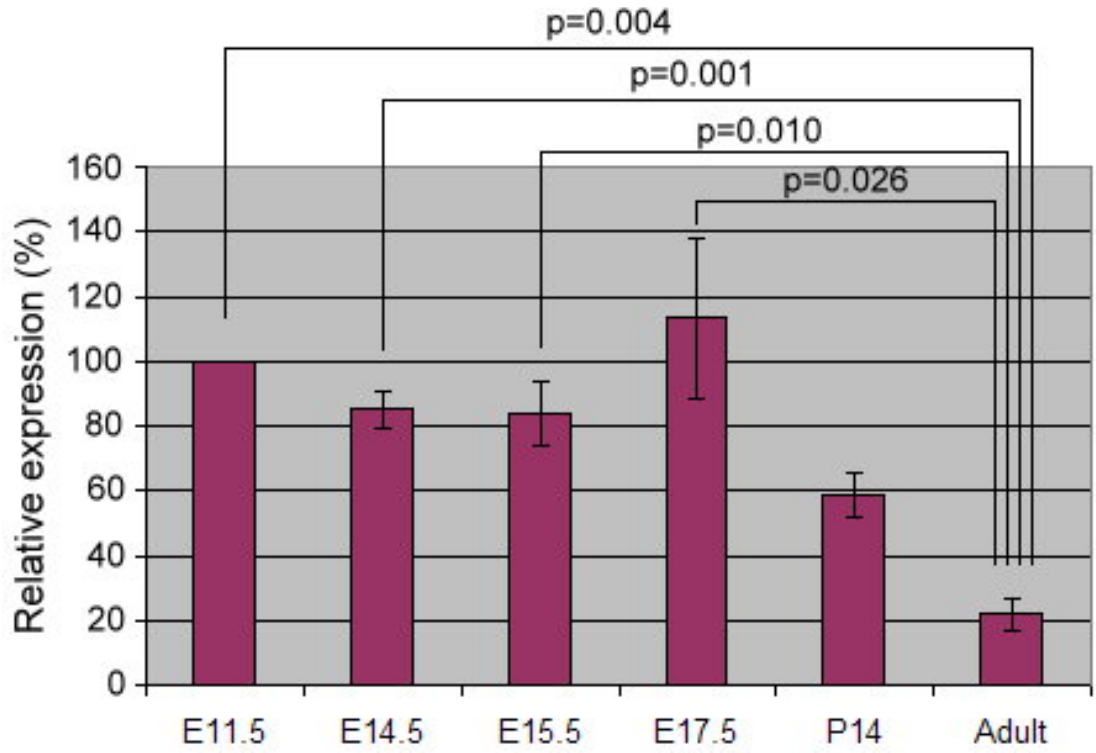

Figure 3-7 The temporal expression pattern of *Dact1* in mouse kidneys. Quantitative real time PCR showed that *Dact1* was downregulated in adult kidneys. *Actb* was used as an internal control. Data were collected from three independent experiments and are represented as Mean ± SEM. Paired comparisons were made by Student *t* tests. The difference was considered to be statistically significant when a *p*-value was less than 0.05.

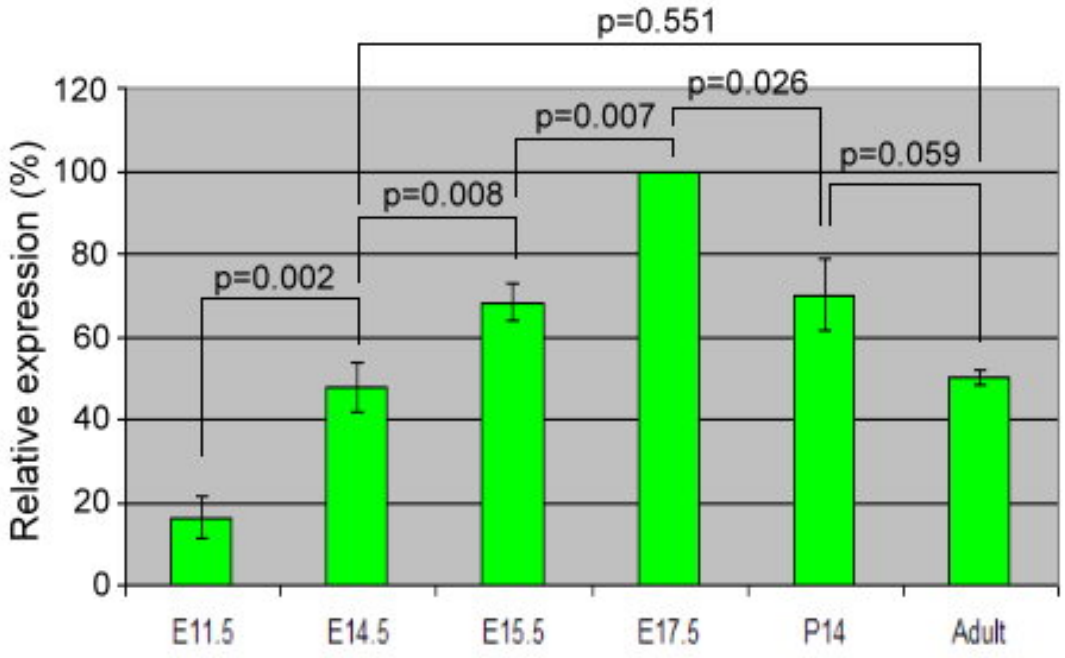

Figure 3-8 The temporal expression pattern of *Dact2* in mouse kidneys. Quantitative real time PCR showed that *Dact2* level increased from E11.5, peaked at E17.5 and then decreased at P14 and in adult. In adult kidneys, the expression of *Dact2* maintained at a level similar to that at E14.5. *Actb* was used as an internal control. Data were collected from three independent experiments and are represented as Mean ± SEM. Paired comparisons were made by Student *t* tests. The difference was considered statistically significant when a *p*-value was less than 0.05.

3.3.4 *Dact1* is expressed in metanephric mesenchyme followed by renal stroma

Spatial expression patterns of both *Dact* genes in E11.5, E12.5 and E14.5 kidneys were illustrated by RNA *in situ* hybridisation. The transcripts, detected by DIG-labelled complementary RNA probes, were shown as purple precipitates in the tissue. Both sense and anti-sense probes for each *Dact* gene were used in parallel to confirm the specificity of the detected signal. As shown in Figure 3-9, at E11.5 and E12.5, *Dact1* was expressed by the metanephric mesenchymal cells. At E14.5, *Dact1* expression showed a honeycomb appearance in the whole kidneys. This pattern was a characteristic pattern of renal stroma (Levinson and Mendelsohn, 2003b; Quaggin et al., 1999). Notably, at E14.5, the differentiated medullary zone showed stronger *Dact1* expression than the nephrogenic zone.

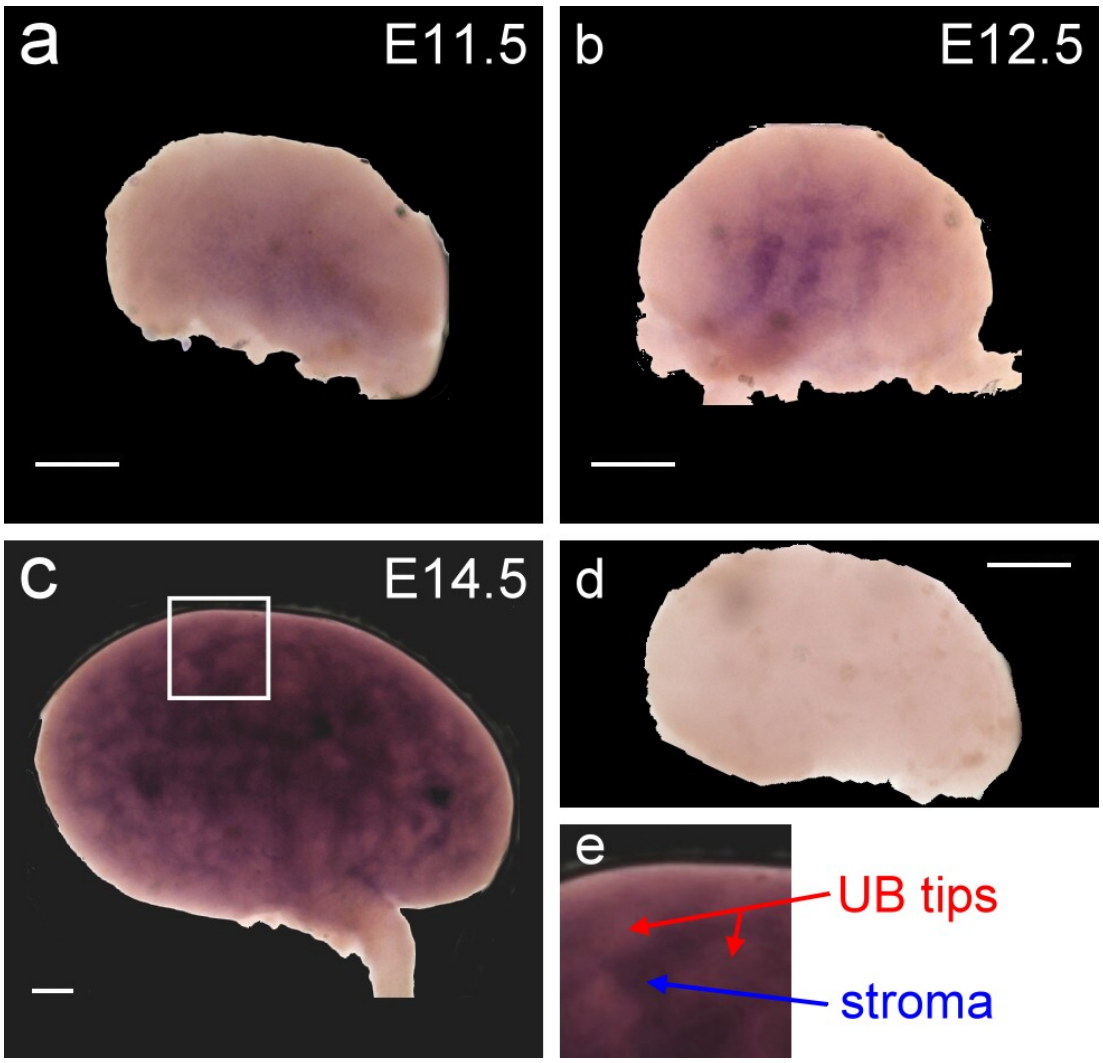

Figure 3-9 Spatiotemporal expression patterns of *Dact1* in kidneys at early developmental stages. RNA *in situ* hybridisation showed that *Dact1* was expressed by metanephric mesenchyme at E11.5 (a) and E12.5 (b). At E14.5 (c), *Dact1* expression exhibited a characteristic honeycomb appearance. Representative sense control (d) revealed no staining. The area encompassed by the white box (c) is shown at higher magnification in panel (e) to illustrate the UB tips (red arrow) and the stroma (blue arrow). Scale bar =100μm.

Expression patterns of both *Dact* genes in kidneys from later stages were also examined. I initially tried to do whole mount *in situ* hybridisation on E17.5 and P14 kidneys but obtained no staining at all. This could be due to the penetration problem resulted from the gradually-formed renal capsule in late stage kidneys. To overcome the penetration problem, the experiments were carried out on kidney sections. These experiments aimed not only to reveal expression patterns but to investigate the reasons of downregulation of both *Dact* genes in adult kidney. As quantitative real

time PCR revealed decreased levels of both *Dact* genes in P14 and adult kidneys (Figure 3-7 and 3-8), RNA *in situ* hybridisation would help to answer whether this down-regulation was caused by reduced numbers of *Dact*-expressing cells or by the less expressed mRNA in P14 and adult kidneys. Figure 3-10 showed that *Dact1* was still highly expressed in kidneys at E17.5 and P14 but weakly expressed in adult kidneys. In adult kidneys, the *Dact1* expression seemed to be restricted only to the central medullary zone. By Figure 3-10, the low level of *Dact1* expression in adult kidneys, as judged by quantitative real time PCR (Figure 3-7), was probably due to the reduction of *Dact1*-expressing cell number.

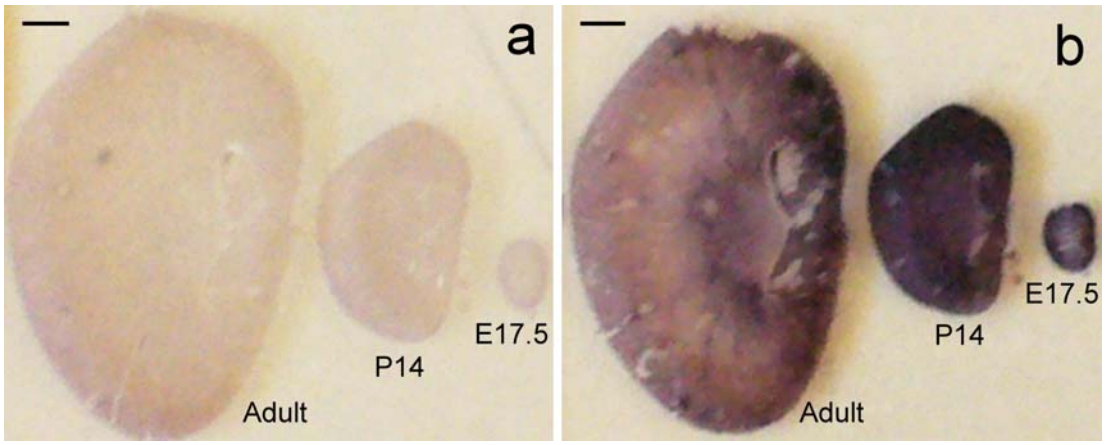

Figure 3-10 RNA *in situ* hybridisation of *Dact1* on kidney sections at E17.5, P14 and adult. Sense controls (a) showed no staining. Antisense (b) showed *Dact1* expression on E17.5 and P14 kidneys while it was weakly expressed in adult kidney. Scale bar =1mm.

In addition to the expression in medullary stroma, *Dact1* was detected in tubular epithelia on E17.5 kidney sections (Figure 3-11). This finding suggested that *Dact1*-expressing mesenchymal cells adopt the fates to be both epithelia and stroma.

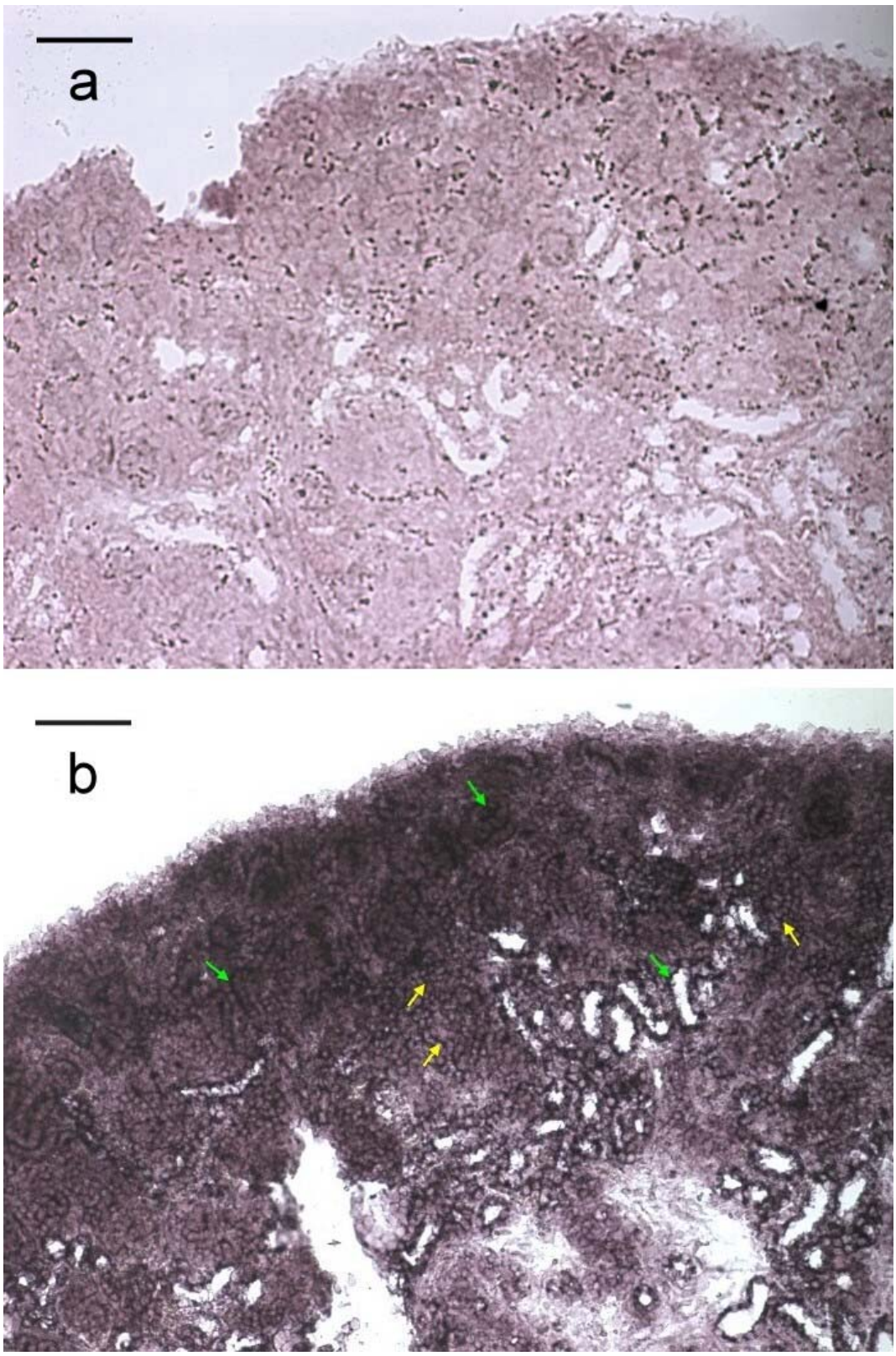

Figure 3-11 *Dact1* expression on E17.5 kidneys. Sense controls (a) showed no staining. Antisense (b) showed *Dact1* expression was detected at tubular epithelia (green arrows) and stromal cells (yellow arrows). Scale bar =100μm.

3.3.5 *Dact2* is expressed exclusively in ureteric buds

Distinct from *Dact1*, *Dact2* was expressed in the ureteric buds throughout the developmental stages (Figure 3-12 and 3-14). It was expressed in both tip and stalk region of the ureteric buds. *Dact2* was easily detected by RNA *in situ* hybridisation on E17.5, P14 and adult kidney sections (Figure 3-13). This finding was compatible with the temporal expression profile of *Dact2* (Figure 3-8).

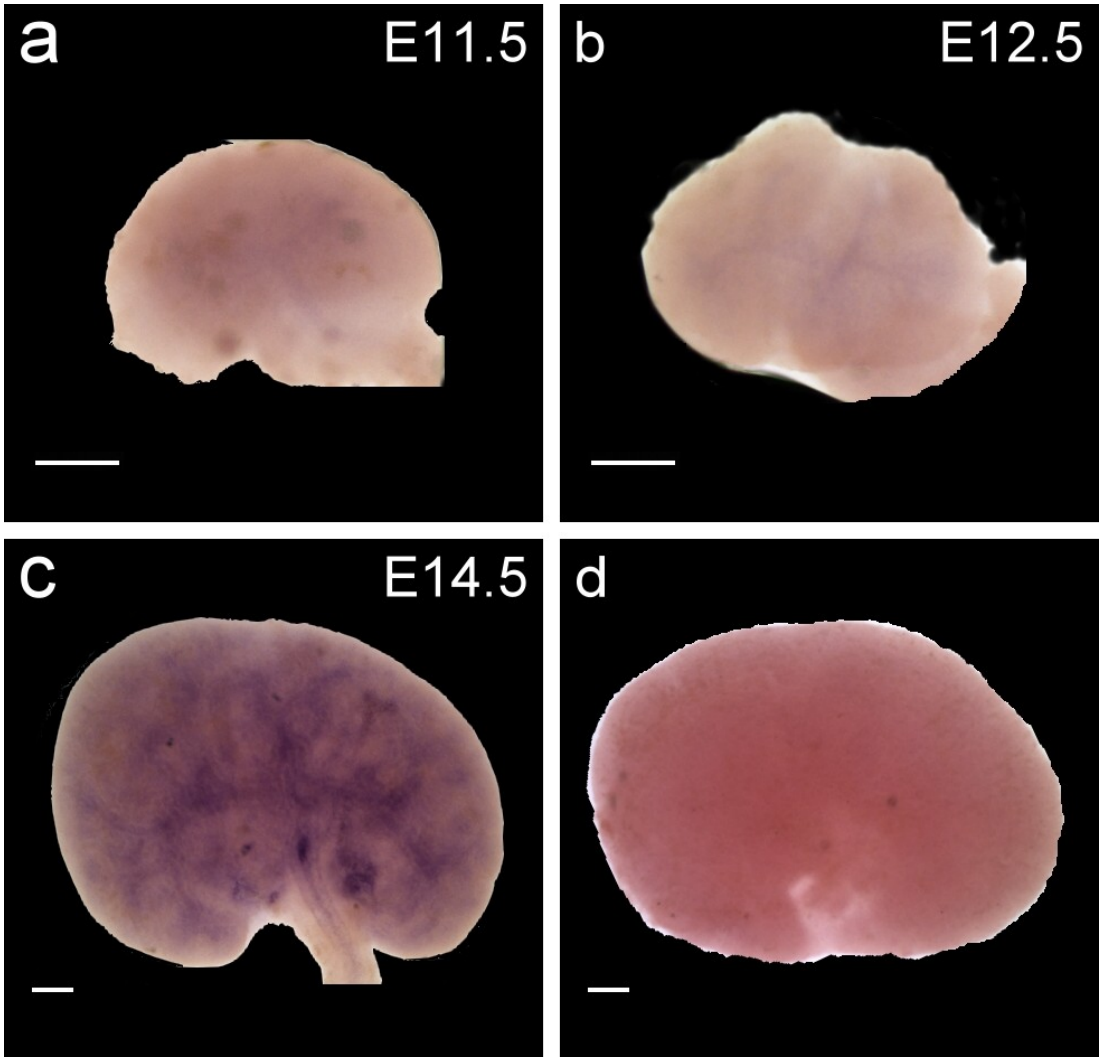

Figure 3-12 Spatiotemporal expression patterns of *Dact2* in kidneys at early developmental stages. RNA *in situ* hybridisation showed that *Dact2* was expressed exclusively by the collecting duct system. *Dact2* transcripts were shown as purple staining at the T-bud stage, E11.5 (a) and more advanced branching at E12.5 (b) and E14.5 (c). Sense controls, represented as (d), were performed in parallel and showed no signal. Scale bar =100μm.

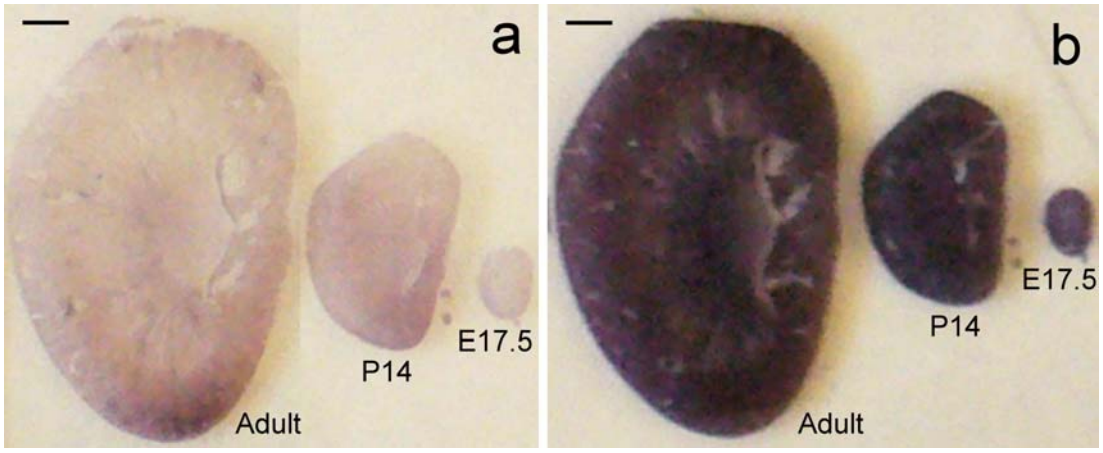

Figure 3-13 RNA *in situ* hybridisation of *Dact2* on kidney sections at E17.5, P14 and adult. Sense controls (a) showed no staining. Antisense (b) showed strong *Dact2* expression on E17.5, P14 and adult kidneys. Scale bar =1mm.

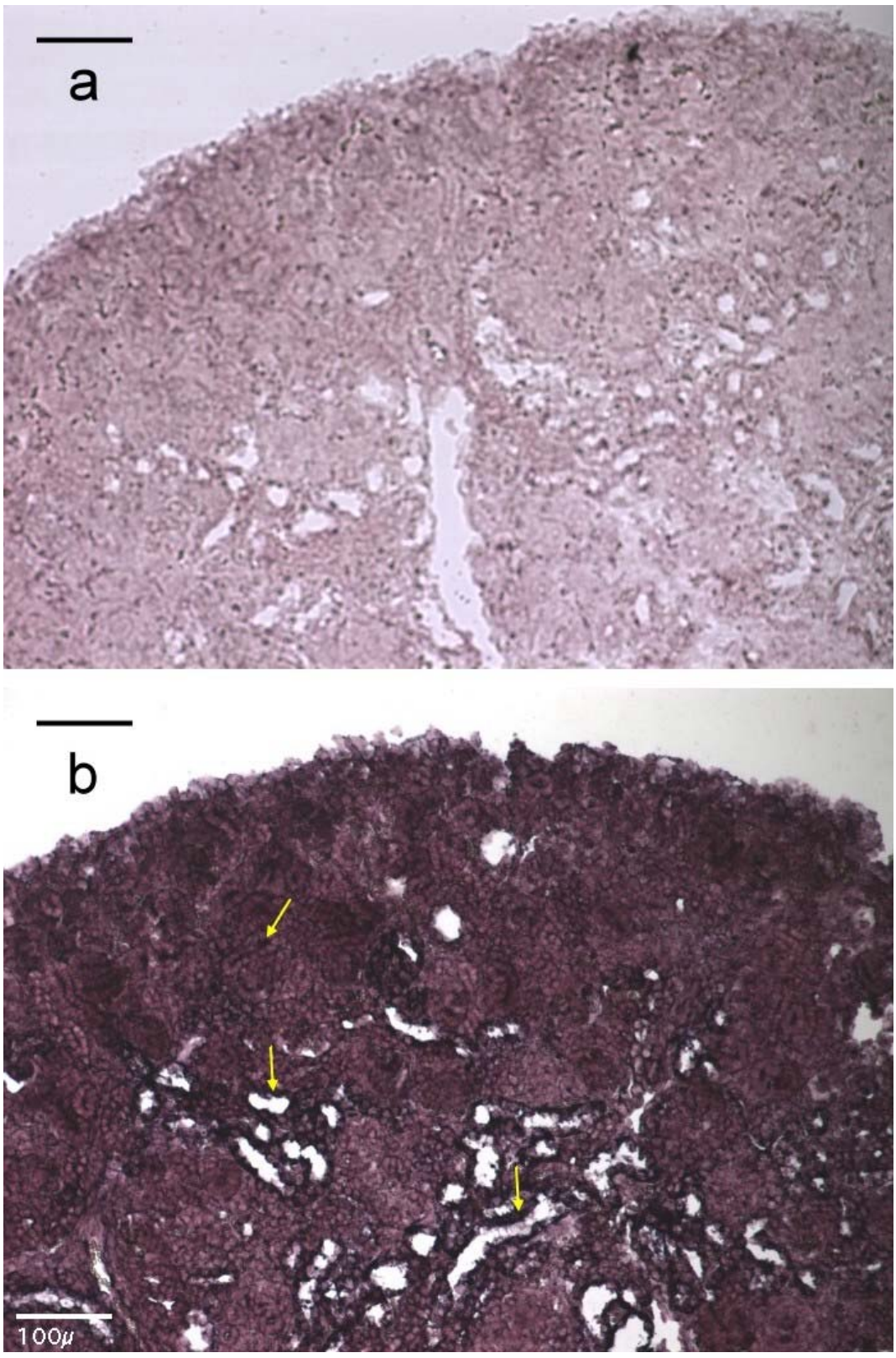

Figure 3-14 *Dact2* expression on E17.5 kidneys. Sense controls (a) showed no staining. Antisense (b) showed *Dact2* expression was found at tubular epithelia (arrows). Scale bar =100μm.

3.3.6 *In vitro* kidney culture retains *Dact1* and *Dact2* expression patterns

Kidney *in vitro* culture is a powerful system where developing kidneys are accessible to exogenous growth factors, drugs, siRNA and to imaging. In this project, I took advantage of this system and aimed to investigate impacts of siRNA and some regulators on the *Dact* expression patterns. It was therefore crucial to obtain evidence to confirm that cultured kidneys developed the same expression patterns as seen *in vivo*. Kidneys were dissected at E11.5 and subjected to *ex vivo* culture for 72 hours. Whole mount RNA *in situ* hybridisation on these cultured kidneys (Figure 3-15) illustrated a characteristic honeycomb appearance for *Dact1* and a tree-like appearance for *Dact2*. Both resembled their characteristic expression patterns at corresponding developmental stages. This confirmed the feasibility of subsequent drugs and RNAi experiments and showed the applicability of RNA *in situ* hybridisation to the kidney *ex vivo* culture system.

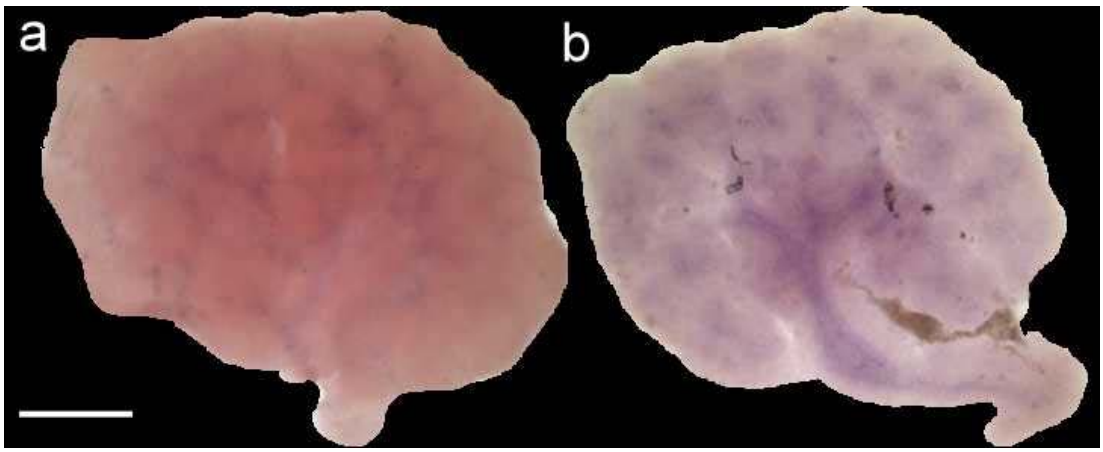

Figure 3-15 *Dact1* and *Dact2* expression patterns in E11.5 kidneys cultured *in vitro* for 72 hours. *Dact1* (a) showed a honeycomb appearance while *Dact2* (b) revealed a tree-like appearance. Both resembled their specific patterns at the corresponding developmental stages shown in Figure 3-9 (c) and Figure 3-12 (c). Scale bar =200μm.

3.3.7 Attempts to localise DACT1 protein in mouse kidneys

In addition to detecting transcripts of both *Dact* genes, I also tried to localise DACT proteins in kidneys. However, I have not obtained encouraging results so far. The

DACT1 antibody (Orbigen) did not work either in whole mounts or sections with 5μm in thickness, although I have tried different fixatives, various methods of antigen retrieval, a range of incubation time and temperature of the antibody and serial dilutions of either primary or secondary antibodies. No DACT2 antibody is commercially available or has ever been described in the literature. The DACT1 antibody used was originally designed to react with human DACT1 and its ability to identify DACT1 has been shown only in human tissues (Schuetz et al., 2006). As described in the data sheet from the supplier, the immunogen used to develop the antibody is KLH-conjugated synthetic peptide consisted of amino acids 152-168 (ETDSRPSSGFYELSDGT) of the human DACT1 protein. This peptide matches the amino acids 145-161 (ETDSRPSSGFYELSDGA) of mouse DACT1 protein except the last amino acid changing from T to A. Therefore, this species-specific factor may account for the failure of this DACT1 antibody to localise DACT1 protein in mouse tissues.

3.4 Discussion

3.4.1 Mapping *Dact1* expression pattern to known mesenchymal genes

Mouse metanephric mesenchyme consists of a few thousand cells at E11.5 when they have similar morphology but will eventually adopt various fates to become nephrons, endothelial cells, vascular smooth muscle cells, neuronal cells and embryonic renal stroma (Sariola et al., 2003b). From E12-13, mesenchymal cells that follow the fate to form renal stroma surround the epithelial components of the developing kidney (refer to section 1.2.3). This arrangement gives rise to a honeycomb expression pattern in whole mounts *in situ* hybridisation. Although those reported genes expressed by the renal stroma show a honeycomb appearance, they may express different intensity in the different zones throughout the whole kidney. For example, the well-researched stromal marker *Foxd1* is highly expressed by subcapsular stromal cells (Hatini et al., 1996) whilst *Smad2* shows a complementary pattern to *Foxd1* (Vrljicak et al., 2004).

Dact1 showed an expression pattern resembled *Smad2*. It was expressed by cells other than ureteric buds at E11.5 and E12.5. By E14.5, these cells formed a characteristic stromal pattern with stronger expression found in the medullary stroma where cells were more differentiated. To better understand how *Dact1* was expressed and regulated by known genes expressed in stroma, an important step was perhaps to characterise the mRNA expression patterns of the stromal genes. Figure 3-16 illustrates four expression patterns. These patterns are based on the relative intensity of expression for a given gene among different zones of kidneys and do not reflect differences in expression levels between genes. *Dact1*, *Smad2*, *Smad7*, *Pod1* and *Snep* were expressed predominantly in medullary stroma (Lee and Davies, 2006; Leimeister et al., 2004; Quaggin et al., 1999; Vrljicak et al., 2004). *Foxd1*, *Smad4* and *Smad6* are strongly expressed in the nephrogenic zone, which is a pattern complementary to *Dact1*. *Tgfb1*, *Smad8*, *Rarb2* and *Pbx1* are expressed equally in both cortical and medullary stroma. *Bmp4*, *Smad1*, *Smad3* and *Smad5* are expressed by both cortical and medullary stroma but have stronger expression in cortical stroma (Hatini et al., 1996; Mendelsohn et al., 1999; Schnabel et al., 2003; Vrljicak et al., 2004). This classification might imply that *Dact1* is regulated in a way resembling *Samd2*, *Smad7*, *Pod1* and *Snep*. Alternatively, it might suggest that *Dact1* is negatively regulated by *Foxd1*, *Smad4* or *Smad6*.

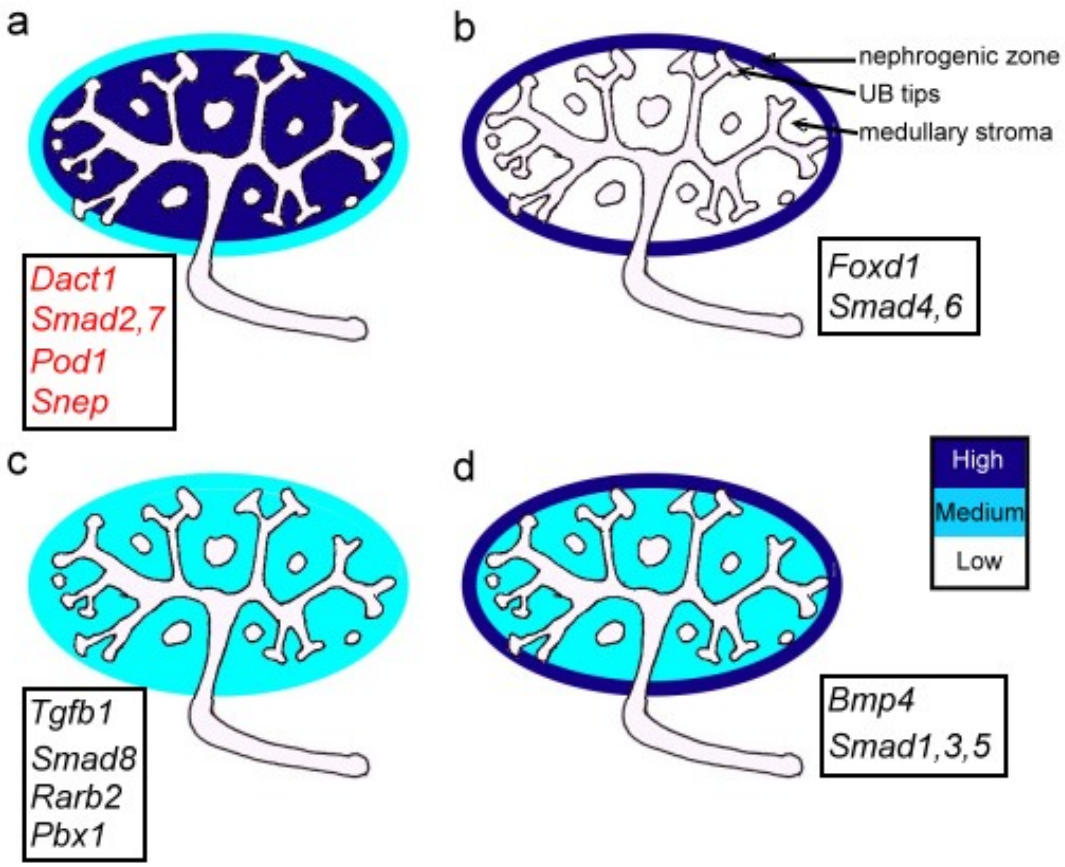

Figure 3-16 Four expression patterns of stromal genes. Schematic diagram shows four different expression patterns of stromal genes based on the relative expression intensity of a given gene among different zones of kidneys. *Dact1*, *Smad2*, *Smad7*, *Pod1* and *Snep* are expressed predominantly by medullary stroma.

3.4.2 Impacts of the discovery of a novel *Dact1* transcript variant

As transcript diversity generated by alternative splicing and associated mechanisms contributes heavily to the functional complexity of various biological systems (Elliott and Grellscheid, 2006; Hoppler and Kavanagh, 2007; Igarashi et al., 1995; Narita et al., 2007; Natoli et al., 2002), it is crucial to examine the expression of these splicing variants of *Dact1* in developing kidneys. In addition, for the benefit of the subsequent RNAi experiments, identification of all potential transcript variants offers useful information not only on the design of effective siRNA duplexes but the design of primers for efficient real time PCR detection of the gene silencing effect. Although the reasons of transcript diversity and the mechanisms of splicing

regulation are beyond the scope of this project, confirmation of predicted transcript variants and the discovery of new variants of *Dact1* gene, render a new direction of research into its function and regulation.

3.4.3 *Dact2* as a new marker of ureteric buds

Unlike *Dact1*, *Dact2* is expressed exclusively in ureteric buds throughout developmental stages and in adult. As development proceeds, ureteric bud cells differentiated into at least two distinct types of cells, tip and non-tip cells. Tip cells express high levels of *c-ros* (Kanwar et al., 1995), *Ret* (Pachnis et al., 1993), and *Wnt11* (Kispert et al., 1996) and show a round stratified morphology whilst non-tips cells do not express these genes and are simple columnar in morphology (Qiao et al., 1995). *Dact2* was expressed in both types of the ureteric bud cells. This pattern resembled those of known ureteric bud markers including calbindin-D28K (Liu et al., 1993), $P_{CD}9$ (Kloth et al., 1998) and cytokeratin (Brophy et al., 2001).

3.4.4 Implications from the temporal expression profiles of both *Dact* genes

The level of *Dact1* expression was markedly decreased in adult kidneys. This was supported by another group (Fisher et al., 2006). By using northern blot, Fisher *et al.* showed that *Dact1* was barely detected in normal adult kidneys. As shown in Figure 3-9, *Dact1* was expressed in renal stroma at E14.5. However, during late kidney development, many stromal cells are lost through massive apoptosis (Koseki et al., 1992). This may, at least in part, explain why *Dact1* expression was greatly decreased in adult kidneys. The temporal expression profile of *Dact1* may also suggest that *Dact1* is likely to exert important functions on embryonic kidney development but needs to be turned off in normal adult kidneys. This may be of clinical significance. Upregulation of *Dact1* in adult kidneys, or any other organs if temporal expression profiles available, may thus indicate some pathological process. Scheutz *et al.* incidentally found upregulation of *Dact1* in invasive ductal carcinoma of breast by using microarray (Schuetz et al., 2006). Although the biological functions of *Dact1* has not been extensively researched, taking into account its

mesenchymal nature and temporal expression profiles, it will not be a great surprise to notice its upregulation in invasive cancer where epithelial to mesenchymal transition is one of the likely mechanisms of its invasiveness (Hugo et al., 2007; Nieman et al., 1999).

The level of *Dact2* expression increased as ureteric bud branching advanced and was still maintained at a comparable level in adult kidneys. This may imply it was a critical component of ureteric buds. Furthermore, as mIMCD-3 cells, a well-characterised kidney epithelial cell line derived from terminally-differentiated adult mouse collecting duct cells, have been used in a well-established tubulogenesis model system (Cantley et al., 1994), the expression of *Dact2* in adult kidneys inspired me the use of this cell line to investigate its functions in branching morphogenesis (chapter 7).

Chapter 4

Expression dependencies of *Dact1* and *Dact2* on known regulators of kidney development

4.1 Introduction

Chapter 3 answered questions on the expression of both *Dact* genes in developing kidneys. The next question I would like to address was: can their expression be modulated by known molecules in developing kidneys? Undoubtedly, there are plenty of molecules to be investigated as kidney development is well coordinated by a delicate molecular network. In this study, I chose a simple and well known molecule, chlorate, to treat the cultured kidneys and assayed the changes in expression of both *Dact* genes.

Sodium chlorate inhibits proteoglycan synthesis and hence stops UB branching, but nephrogenesis still occurs in the mesenchyme near the UB tips. Exogenous sodium chlorate is known to arrest branching morphogenesis of kidneys growing in culture (Davies et al., 1995) and to downregulate mesenchymal gene *Gdnf* (Sainio et al., 1997) and UB tip gene *Wnt11* (Kispert et al., 1996). Based on the expression patterns described in the chapter 3, *Dact1* was expressed by stromal mesenchyme and *Dact2* was expressed by the ureteric buds. Therefore, in addition to the well characterised morphological change caused by chlorate, chlorate was chosen to assay the expression dependencies of both *Dact* genes because it is able to affect the expression of either a mesenchymal gene or a UB gene.

Following the question addressed above, if the expression of *Dact* genes is regulated by known molecules, I would like to investigate if the expression of *Dact1* responds to any signals that affect stroma. All-*trans* retinoic acid (ATRA) is known to signal through renal stroma and in turn stimulate UB branching, nephrogenesis and stroma pattering (Levinson and Mendelsohn, 2003a). I therefore tested the effects of ATRA on *Dact1* expression by using kidney organ culture, quantitative real time PCR and RNA *in situ* hybridisation.

4.2 Methods

4.2.1 Kidney culture with sodium chlorate or ATRA

To set up chlorate-treated culture, E11.5 kidneys were dissected out and cultured in the presence of 30mM sodium chlorate. A control group was set up in parallel and cultured in the same way without adding sodium chlorate. The culture time was 24 hours for quantification of expression levels and 72 hours for kidney morphology.

To investigate the effects of ATRA on *Dact1* expression, E11.5 kidneys were dissected out and subjected to organ culture (detailed in section 2.1.2) in the absence or presence of ATRA at various concentrations ranging from 10^{-8} to 10^{-5}M. The concentrations tested were in the wide range of physiological tissue levels and far below the teratogenic dose (Horton and Maden, 1995). ATRA stock solution was made in absolute ethanol to the concentration of 10mM and was stored at -20°C for up to one week. Serial dilutions of ATRA were made by kidney culture media immediately before use. Kidneys were cultured for 72 hours during which culture media were changed daily.

4.2.2 Quantitative real time PCR

At the end of culturing, eight kidneys in each dish were collected, homogenised and subjected to RNA isolation followed by cDNA synthesis. Quantitative real time PCR reactions were carried out in duplicate. The expression levels were normalised to a housekeeping gene, *Actb*, and were then converted to levels relative to controls. Data collected from three independent experiments were analysed and shown as Mean ± SEM. The differences in expression levels between samples were examined by Student *t* tests. When a *p*-value was less then 0.05, the difference was considered to be statistically significant.

4.2.3 Immunohistochemistry

Immunofluorescence was done to confirm the typical effects of chlorate on kidney morphology. Rabbit anti-laminin antibody (Sigma) was used to outline the epithelial structures of cultured kidneys. The tissue preparation and the staining procedures are described in section 2.5. The secondary antibody used was TRITC-conjugated anti-rabbit IgG (Sigma). Both antibodies were used at 1:100 dilution in PBS.

In addition, I attempted to illustrate the effects of ATRA on *Dact1* expression in the whole developing kidneys rather than in homogenised kidneys. As I have shown the applicability of RNA *in situ* hybridisation to the kidney *in vitro* culture system (Figure 3-15) and there was no suitable DACT1 antibody available (detailed in chapter 3.3.7), RNA *in situ* hybridisation was performed to achieve this goal.

4.3 Results

4.3.1 *Dact1* and *Dact2* are upregulated in kidneys cultured with chlorate

The characteristic effect of chlorate on kidney morphology was confirmed and shown in Figure 4-1. Kidney morphology was evaluated by anti-laminin staining. In Figure 4-1, panel (a) shows that normal kidney morphology was found in kidneys cultured without sodium chlorate whilst panel (b) shows that UB branching was arrested at the T-bud stage when an E11.5 kidney cultured in the presence of 30mM sodium chlorate. Nephrons were found at the tip of the ureteric buds (arrows). Quantitative real time PCR revealed that the expression levels of both *Dact1* and *Dact2* genes were increased in chlorate-treated kidneys. The differences in expression levels between control and chlorate-treated kidneys were statistically significant, as examined by a Student *t* test (Figure 4-1).

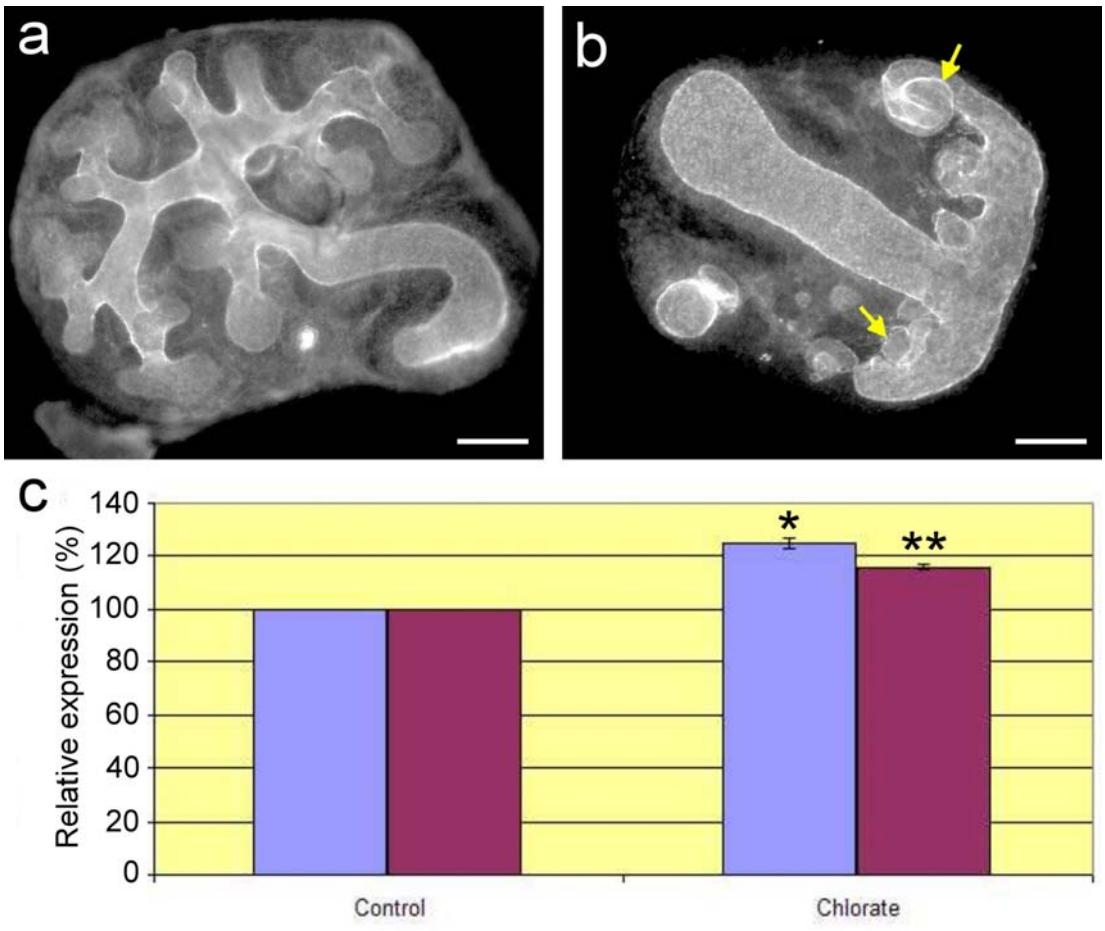

Figure 4-1 Upregulation of *Dact1* and *Dact2* in chlorate treated cultured kidneys. Compared with controls (a), arrested UB branching at the T-bud stage and the nephrons at the tip area (arrow) found in kidneys cultured with 30mM sodium chlorate (b), confirmed its drug effect. Quantitative real time PCR showed upregulation of *Dact1* (blue) and *Dact2* (magenta) genes in chlorate treated cultured kidneys (c). Data collected from three independent experiments are represented as Mean ± SEM and were analyzed by student t test. * p=0.0072; **p=0.0053.

4.3.2 ATRA upregulates *Dact1* expression of kidneys growing in culture

By using quantitative real time PCR, I found that ATRA was able to increase the expression level of *Dact1* in a dose-dependent manner (Figure 4-2). At the concentration of 10^{-8}M, ATRA did not have significant effects on *Dact1* expression. At the concentration of 10^{-5}M, however, ATRA can increase *Dact1* expression level to about 150% of control kidneys.

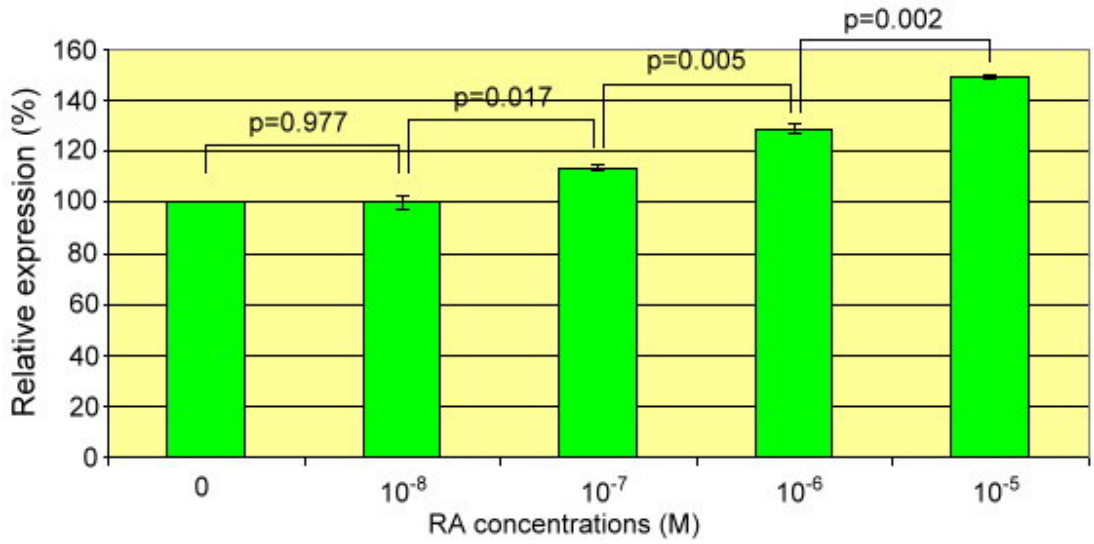

Figure 4-2 ATRA upregulates *Dact1* expression in kidneys. Quantitative real time PCR showed upregulation of *Dact1* in kidneys in a does-dependent manner. *Actb* was used as an internal control. Data were collected from three independent experiments and were represented as Mean ± SEM. Comparisons were made by Student *t* tests. The difference was considered to be statistically significant when a *p*-value was less than 0.05.

Because PCR is based on using homogenised tissues, the increased *Dact1* expression seen in ATRA-treated kidneys may not properly reflect the actual *Dact1* upregulation within renal stroma. In addition to better illustrating the effect of ATRA on *Dact1* expression in developing kidneys, RNA *in situ* hybridisation in ATRA-treated kidneys was able to answer whether ATRA enhanced the stromal pattern of *Dact1* expression or ATRA can even turn on *Dact1* expression in cells of epithelial components. As shown in Figure 4-3, kidneys cultured in the presence of ATRA at the concentration of 10^{-5}M (panel b) exhibited its normal honeycomb expression pattern. Compared to the control kidneys (panel a), ATRA seemed to enhance *Dact1* expression especially in the medullary renal stroma.

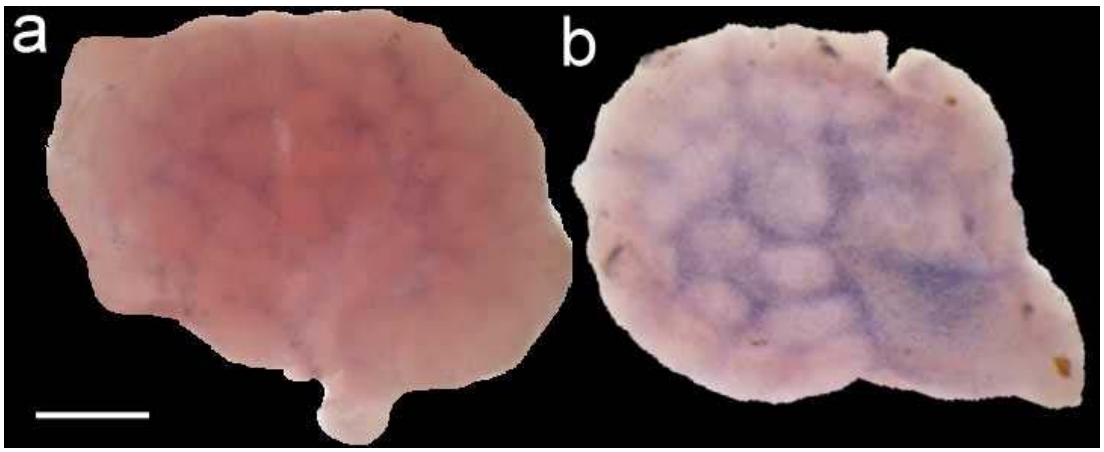

Figure 4-3 ATRA enhances *Dact1* expression in kidneys. RNA *in situ* hybridisation on E11.5 kidneys cultured *in vitro* for 72 hours showed that kidneys cultured in the presence of 10^{-5}M ATRA (b) seemed to exhibite higher *Dact1* expression level than those cultured without ATRA (a). This expression enhancement was prominent in medullary stroma. Scale bar= 200μm.

4.4 Discussion

4.4.1 Sodium chlorate modulates *Dact* gene expression in developing kidneys

In this study, I showed that both *Dact* genes were upregulated in kidneys cultured in the presence of 30mM sodium chlorate. This result confirmed that both *Dact* genes were modulated by known molecules in developing kidneys but the reason for this needs to be further analysed.

By using the same concentration (*i.e.* 30mM) of sodium chlorate in kidney culture, Sainio *et al.* showed that sodium chlorate arrests UB branching leading to diminished mesenchymal factor GDNF (Sainio et al., 1997). However, I found that the mesenchymal gene *Dact1* was upregulated by about 25% in response to chlorate. This finding at least suggested that *Dact1* was not a downstream target of GDNF signalling. It might also be possible that ureteric buds normally sent out signals which negatively regulated *Dact1* expression in the mesenchyme. Exogenous sodium chlorate would abolish this signal and resulted in upregulation of *Dact1* in the mesenchyme.

I also found that the UB gene, *Dact2,* was upregulated by about 15% in kidneys cultured with chlorate. Although the reason for this upregulation remains unclear, it is not uncommon to see that gene expression in the ureteric buds remains in chlorate-treated kidneys. Examples for these genes include *Ret*, *Pax2* and *Bmp7* (Godin et al., 1998; Kispert et al., 1996; Sainio et al., 1997)

A potential pitfall in the interpretation of my PCR results came from the nature of PCR. PCR is based on using homogenised tissues, but I was not sure if there is any difference in chlorate sensitivity among various cell populations in developing kidneys. An interesting example comes from the expression of *Bmp7*. In the developing kidney, *Bmp7* is expressed initially in the UB followed by metanephric mesenchyme and the early tubules derived from the mesenchyme (Dudley et al., 1995; Dudley and Robertson, 1997; Luo et al., 1995; Lyons et al., 1995; Vukicevic et al., 1996). However, when kidneys cultured with chlorate, *Bmp7* expression in mesenchyme was abolished whilst its expression in ureteric buds was unaffected (Godin et al., 1998). This difference was discovered by histology analysis on *Bmp7*/*lacZ* transgenic mice. Errors may thus be introduced if *Bmp7* expression is assayed in homogenised whole kidneys.

In brief, I have shown that the expression of both *Dact* genes was modulated by the well known regulator, chlorate, in developing kidneys. I would not emphasise the extent of upregulation in these two genes because of the potential pitfall in using homogenised tissues. This potential pitfall does not detract quantitative real time PCR from being a powerful tool to quantify gene expression levels, but histology assays (e.g. RNA *in situ* hybridisation, immunofluorescence, etc) may serve as complementary tools especially when analysing gene expression in tissues or organs containing mixed cell populations.

4.4.2 *Dact1* is involved in retinoid-mediated kidney development

The retinoid-mediated kidney development is briefly reviewed in section 1.4.4, but nothing is known about the regulation between the stromal mesenchymal gene, *Dact1,* and retinoids. The first report describing the link between *Dact1* and retinoids was based on the work described above (Lee and Davies, 2007). I have shown that exogenous ATRA increased *Dact1* gene expression in renal stromal cells (Figure 4-3). The concentrations of ATRA being tested ranged from 10^{-8} to 10^{-5}M. I even tried to grow kidneys in the presence of higher concentrations of ATRA, but found that kidneys were not able to survive. This finding was consistent with those described in a rat model where researchers found markedly decreased nephron number, UB branching and *Ret* expression level at high concentrations of retinoids (Moreau et al., 1998; Vilar et al., 1996).

The mechanism by which ATRA upregulates *Dact1* remains unclear. In addition to those stromal genes encoding for receptors and metabolic enzymes for RA, one stromal mesenchymal gene, *Lgl1*, has recently been reported to be upregulated by RA. The upregulation of *Lgl1* by RA is then supported by the identification of a retinoic acid response element (RARE) in the promoter region of this gene (Quinlan et al., 2007). However, no RARE on the *Dact1* gene has been published so far. I attempted to localise consensus RARE in the *Dact1* promoter regions by using an online promoter analysis tool, *Tfsitescan* (http://www.ifti.org/cgi-bin/ifti/Tfsitescan.pl) (Ghosh, 2000). None was identified.

Despite the fact that the causes of *Dact1* upregulation by ATRA are yet to be determined, the quantitative real time PCR performed in this study offered evidence that ATRA upregulated *Dact1*. The complementary histology assay, RNA *in situ* hybridisation, further demonstrated that this upregulation occurred in the renal stroma. Based on the *Dact1* expression pattern described in chapter 3, it may be interesting to ask a question whether ATRA signals through *Dact1* to facilitate stromal differentiation. One critical step before answering this question is to discover

the functions of *Dact1* in developing kidneys. This will be described in chapter 5 and 6.

4.4.3 Implications from regulation of *Dact1* and *Dact2*

In this chapter, I have described the regulation of *Dact1* and *Dact2* expression by known regulators including chlorate and ATRA. Both *Dact* genes were upregulated by sodium chlorate. The expression of the stromal mesenchymal gene, *Dact1*, was also tested by ATRA which is known to signal through renal stroma. By using quantitative real time PCR and RNA *in situ* hybridisation, I showed that *Dact1* was upregulated by retinoids in renal stroma. In addition to offering evidence that both *Dact* genes were regulated by known regulators in developing kidneys, the results presented in this chapter provided insights into potential functions of *Dact* genes. *Dact1* may play a role in retinoid-mediated stromal differentiation, nephrogenesis, and UB branching. *Dact2* may have a role in branching morphogenesis. The functions of both *Dact* genes are described in the following chapters.

Chapter 5

Elucidating *Dact1* functions in mesenchymal cells by RNAi

5.1 Introduction

Having characterised the expression patterns of both *Dact* genes in developing kidneys, an important question to address is what their functions in kidney development are. So far in the literature, however, reports on the biological functions of *Dact1* and its orthologs have been very limited. Zebrafish *Dpr1* is involved in somitogenesis. Loss-of-function studies, carried out by the injection of *Dpr1* morpholinos, show that brain anterior to the midbrain-hindbrain boundary is smaller. Gain-of-function assays are unable to offer useful information because of early embryonic lethality and non-specific toxicity caused by injection of *Dpr* RNAs (Waxman et al., 2004). In *Xenopus*, *Dpr* is required for notochord formation. By using antisense oligonucleotides to deplete *Dpr*, Cheyette *et al.* showed that the *Xenopus* embryos become acephalic or microcephalic. Overexpression of *Dpr* by injection of synthetic *Dpr* RNA into oocytes results in embryos with enlarged heads and curvature of the spine (Cheyette et al., 2002). Studies on the functional roles of *Dact1* in mammals or in kidneys of any species have not yet been described. In this project, I aimed to explore the functions of *Dact1* in mouse kidney development. Different approaches to this are described in this chapter and in chapter 6.

A key strategy to answer the questions about the functions of gene of interest is to remove the gene from the system and look at its consequent phenotype. Following this strategy, one of the most promising methods to investigate the functions of a gene or protein in kidney development is to apply siRNA to *in vitro* kidney organ culture (Davies et al., 2004). This method is more cost effective and less time consuming than generation of knockout mice. It is also technically simple because kidney organ culture renders the kidney rudiment accessible to siRNA duplexes. In addition, researchers can use it to knockdown the gene of interest specifically at any time of their choosing.

Before using this relatively new method, however, it is crucial to validate the siRNA duplexes in conventional 2D cell culture, which is now an established system for RNAi. siRNA-mediated RNAi is a sequence-specific, post-transcriptional gene

silencing mechanism and has been extensively reviewed elsewhere (Hannon, 2002; McManus and Sharp, 2002). Briefly, siRNAs consist of a duplex of 21-nt RNAs. Upon introduction into the cytoplasm of a cell, a siRNA recruits proteins that assemble into a RNA-induced silencing complex (RISC) (Paroo et al., 2007). The bound siRNA then unwinds and the RISC turns into an active form, carrying one strand of the siRNA. The siRNA strand subsequently guides the RISC to a complementary RNA molecule, where they cleave and destroy the cognate RNA (Figure 5-1). The original siRNA strand bound in the RISC remains intact, so the complex can go on to destroy other complementary mRNAs.

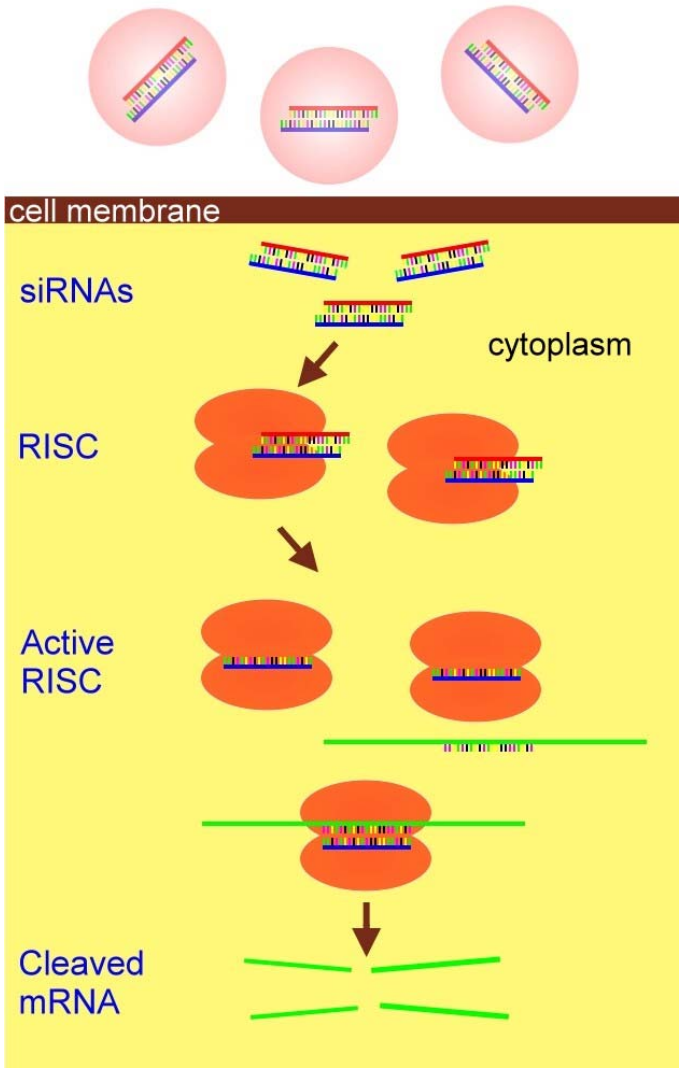

Figure 5-1 The mechanism of siRNA-mediated RNAi (Lee et al., 2008)**.**

NIH3T3 is a well-characterised mouse embryonic cell line and is one of the most commonly used cell lines for RNAi experiments (McManus and Sharp, 2002). More importantly, in Figure 3-4, I have already shown its expression of endogenous *Dact1*. Therefore, it was suitable for the purpose of verifying the silencing efficiency of *Dact1* siRNA duplexes. In this chapter, I demonstrate the successful *Dact1* silencing mediated by *Dact1* siRNA and explore its putative functions in cell culture. The *Dact1* depletion cellular phenotype identified in this study may offer insights into potential functions of *Dact1* in developing kidneys.

5.2 Experimental design

5.2.1 Determination of siRNA transfection efficiency

siGLO (Dharmacon) was a Cy3-labelled (therefore red-fluorescing) siRNA targeting a mouse housekeeping gene, lamin A. I used this powerful tool to optimize siRNA transfection conditions. The conditions of culturing NIH3T3 cells and the siRNA transfection procedures are described in chapter 2. Sixteen hours after transfection, cells were fixed by 4% PFA and counterstained with SYTOX Green nucleic acid stain (Invitrogen). Successfully transfected cells were shown as a green nucleus with perinuclear red dots whilst unlabelled cells were only marked by the green nuclear dye (Figure 5-5). Images were taken by confocal microscopy and the transfection efficiency was calculated as the ratio of transfected cells to all the counted cells.

5.2.2 Transfection of siRNAs

A pool of four siRNA duplexes targeting *Dact1* was transfected into NIH3T3 cells. The sequences of these four duplexes and their target sites are shown in Table 2-3, Table 2-4, Figure 5-2 and Figure 5-3. Appropriate controls, including untreated cells, mock transfection without siRNA, and transfection with non-targeting siRNA, were carried out in parallel to detect any cellular effects caused by transfection process and to detect any off-target effects that might have resulted from the introduction of any

siRNA. Each treatment was performed in triplicate and the experiment layout is depicted in Figure 5-4.

Figure 5-2 Mapping *Dact1* siRNA duplexes on the mouse *Dact1* transcript. Target sequences of the four siRNA duplexes are shown in red. Exons of mouse *Dact1* are distinguished by alternative black and blue colour text.

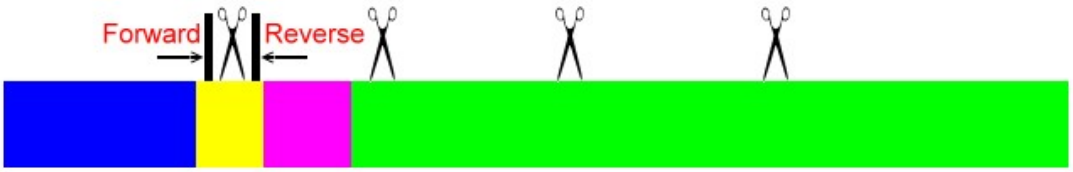

Figure 5-3 *Dact1* siRNA target sites and primer binding sites on the mouse *Dact1* transcript. Schematic diagram depicts the target sites of *Dact1* siRNA on mouse *Dact1* transcript (scissor). Black bars and arrows indicate the binding sites of *Dact1* primers used to detect the silencing efficiency.

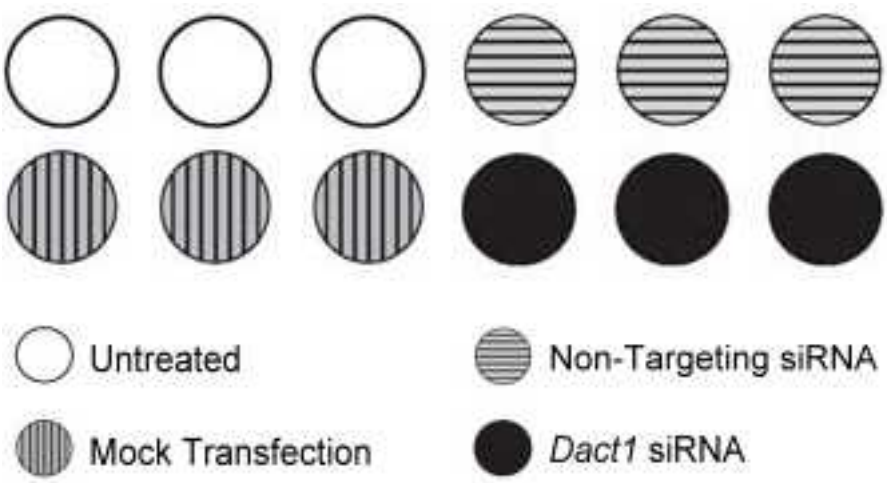

Figure 5-4 Plate layout of the siRNA-mediated *Dact1* knockdown experiment.

5.2.3 Detection of *Dact1* silencing by quantitative real time PCR

A time course experiment was done to determine the kinetics of knockdown. I found that the most significant knockdown, by quantitative real time PCR assay, was 48 hours after transfection. In subsequent RNAi experiments, cells were harvested 48 hours after transfection and then subjected to RNA extraction followed by cDNA synthesis. *Actb* was used as an internal control gene. Quantitative real time PCR was done as detailed in section 2.2.5. Primers were designed to flank the target site of *Dact1* siRNA duplex 2 (refer to Table 2-3 and Figure 5-3) and also to amplify cDNAs made from all the potential *Dact1* transcripts. Their sequences were listed in Table 5-1. *Dact1* expression in each treatment group was normalised to *Actb* and

showed as the percentage of that in the untreated group. Data were obtained from three independent experiments and were represented as Mean ± SEM.

Table 5-1 Real time PCR primers used to detect *Dact1* silencing. The forward primer binds to the antisense strand, the reverse primer to the sense strand. All oligos are represented in a 5' to 3'orientation. *Actb* was used as an internal control.

Gene	RefSeq accession number	Frward Primer	Reverse Primer
Dact1	NM_021532	GCCGGTTTGTTGAATCAGTT	CGAAGCTCCATCACTCAGC
Actb	NM_007393	GATCTGGCACCACACCTTCT	GTACATGGCTGGGGTGTTG

5.2.4 Cell counting

Cells were plated at the density of $2x10^5$cells/well in 6-well plates. Each treatment was carried out in triplicate and the experiment layout is depicted in Figure 5-4. Seventy-two hours after siRNA transfection, cells were harvested and counted by using a haemocytometer. The counting of cells was done blind by masking the labelling of treatments on glass slides.

5.2.5 BrdU incorporation assay

A BrdU incorporation assay was employed to evaluate the effect of *Dact1* silencing on the proliferation of NIH3T3 cells. For this assay, cells were grown on coverslips in a 24-well plate and were plated at the density of $4x10^4$cells/well. Seventy-two hours after siRNA transfection, cells were fixed and subjected to immunocytochemistry. The procedures of BrdU labelling and immunocytochemistry are detailed in section 2.7. Images were taken by confocal microscopy. When taking images, the labelling of treatments on glass slides was masked so that the subsequent cell counting on the images would be done blind. One thousand cells were counted per coverslip and the proliferation index was defined by BrdU labelling rate, which was calculated as the ratio of BrdU labelled cells to the total cell number counted. Data from three independent experiments were collected and subjected to statistical analysis.

5.2.6 Statistical analysis

When analyzing data from cell counting and BrdU proliferation experiments, a one way analysis of variance (ANOVA) was first used to compare the mean of each group. This was done by using the Microsoft Office Excel 2003 software program. The exact *p*-values were shown in the legends of Figure 5-7 and 5-8. When the *p*-value was less than 0.05, the ANOVA test was considered to be statistically significant and Tukey's post hoc tests were then introduced to evaluate whether differences between any two pairs of means were significant. This test was done by an online calculator which can be found at the URL http://web.umr.edu/~psyworld/tukeyscalculator.htm.

5.3 Results

5.3.1 Effective knockdown of *Dact1* in NIH3T3 cell cultures

5.3.1.1 Satisfactory transfection efficiency

To determine transfection efficiency, six independent experiments were performed and 500 cells were counted from each experiment. A successfully transfected cell showed a green nucleus with perinuclear red dots whilst untransfected cells only showed their green nuclei (Figure 5-5). The transfection efficiency was 96.33±0.87% (Mean ± SEM). Negative controls were done by mock transfection without siRNA and yielded no red dots at all.

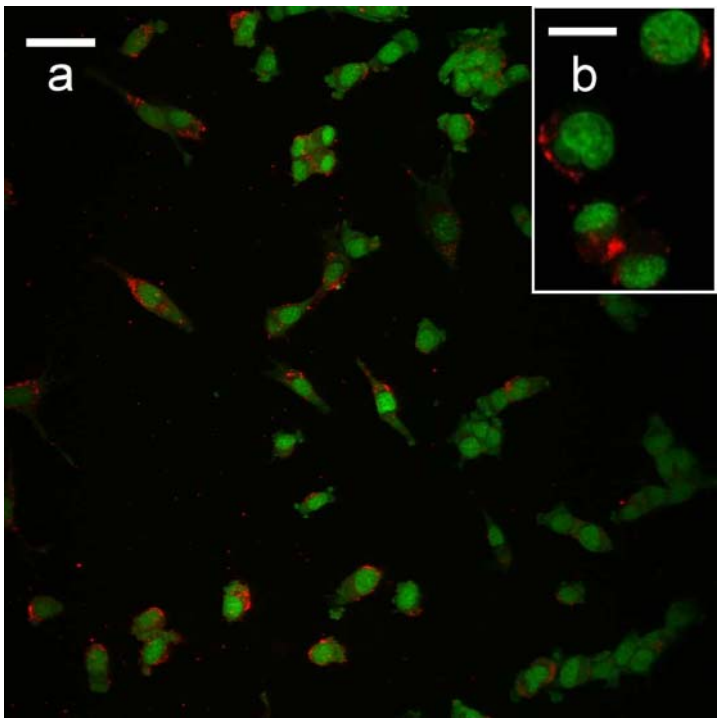

Figure 5-5 siGLO in NIH3T3 cells. siRNA transfection efficiency was determined by the percentage of siGLO labelled cells. Inset depicts the characteristic perinuclear distribution of red dots (siGLO). Cells were counterstained by SYTOX Green nucleic acid stain (green). Scale bar =50µm (a), 25µm (b).

5.3.1.2 Effective *Dact1* knockdown at mRNA level

By quantitative real time PCR, I found that the pool of four *Dact1* siRNA duplexes effectively knocked down *Dact1* expression to 25% of control values. *Dact1* expression was maintained at a high level among control groups (Figure 5-6), indicating the absence of unwanted effects caused by the transfection reagent, by transfection procedures or by the introduction of non-relevant siRNA. Taking together the results of transfection efficiency and knockdown efficiency, I concluded that it was sensible to use this optimised siRNA transfection method to further explore the phenotypes of *Dact1* knockdown cells.

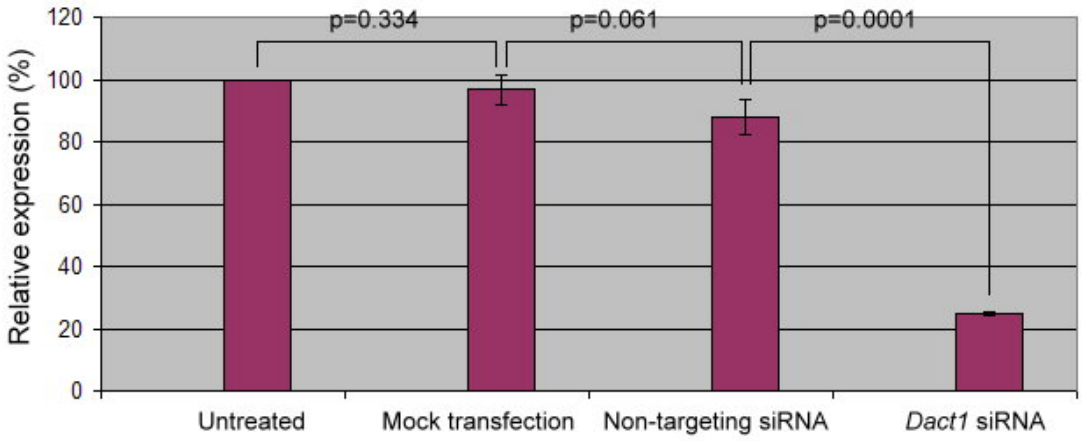

Figure 5-6 *Dact1* knockdown efficiency in NIH3T3 cells. Cells treated with *Dact1* siRNA showed only 25% expression of *Dact1*, whilst controls expressed *Dact1* at a comparable level. Data were collected from three independent experiments and are expressed as Mean ± SEM. Comparisons were made by Student *t* tests. The difference was considered to be statistically significant when a *p*-value was less than 0.05.

5.3.1.3 Attempts to detect *Dact1* silencing by Western blot

Although I have shown the effective knockdown of *Dact1* gene at mRNA level, it is desirable to demonstrate its knockdown effect at protein level (Anonymous, 2003; Duxbury and Whang, 2004; Hannon and Rossi, 2004; Huppi et al., 2005), provided that a specific primary antibody is available. For this purpose, 72 hours after transfection, cells were harvested to isolate protein lysates and then subjected to Western blot. The primary antibody used to detect DACT1 protein has been described in section 3.3.7, where I showed that it was not able to recognise mouse DACT1 protein in immunofluorescence assays. Despite my numerous attempts of trying different dilutions of primary and secondary antibodies, varying the type, strength, and washing time of the washing buffer, it always showed a laddering pattern on the Western blot. The same protein lysates run through the protocol in parallel but targeting by primary anti-GAPDH antibody yielded a single clear band of correct size. Because the primary antibody against DACT1 protein did not work, the attempt to show *Dact1* silencing by Western blot had to be abandoned.

5.3.2 *Dact1* silencing facilitates proliferation of NIH3T3 cells

5.3.2.1 Cell number increases in *Dact1* siRNA-treated NIH3T3 cells

The idea of studying cell number came from the preliminary observation that cells transfected with *Dact1* siRNA seemed more crowded then controls. Figure 5-7 shows that, 72 hours after transfection, the cell number was greatly increased in *Dact1* siRNA-treated cells while the cell number in the controls was unchanged. Data were derived from three independent experiments and were shown as Mean ± SEM. The differences of the means among groups were examined by one way ANOVA followed by Tukey's post hoc comparisons. There was no difference in the cell number among three controls. The increase in cell number in *Dact1* siRNA-treated group was statistically significant.

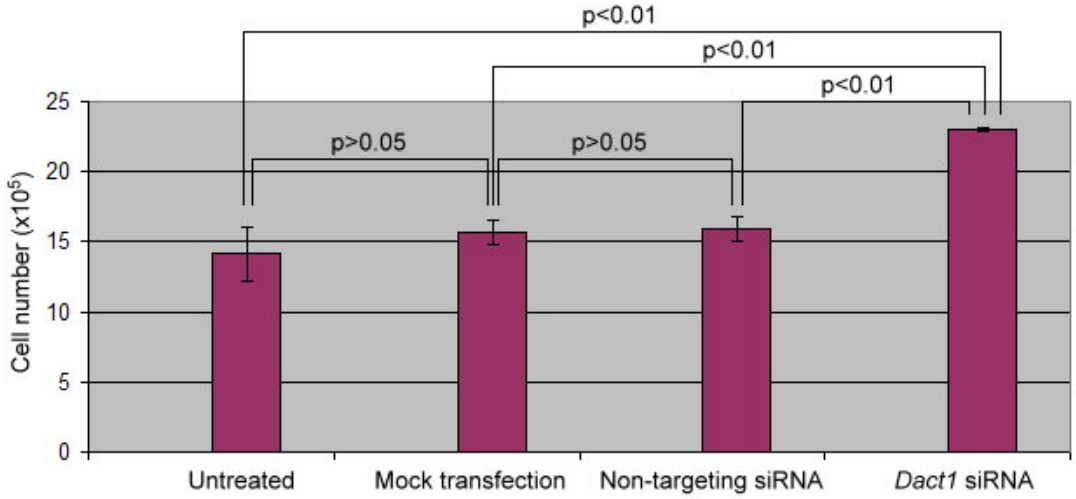

Figure 5-7 Cell number increases in *Dact1* siRNA treated cells. Each group was carried out in triplicate and the experiment layout is depicted in Figure 5-4. Seventy-two hours after transfection, cells were harvested and counted by using a haemocytometer. Counting was done blind by masking the labelling of treatment on glass slides. Data are shown as Mean ± SEM and were subjected to one-way ANOVA, followed by Tukey's post hoc comparisons when main effects were significant. (p=0.017 in one way ANOVA; the *p*-values of paired comparisons in Tukey's post hoc comparisons are shown)

5.3.2.2 Higher proliferation index in *Dact1* siRNA-treated cells

To further explore whether cell proliferation contributed to the increase in cell number found in *Dact1* siRNA-treated cells, BrdU was introduced to label proliferating cells at metaphase and the proliferation index was calculated as the BrdU labelled rate. Panel (a) and (b) in Figure 5-8 showed that cells were more crowded in *Dact1* siRNA transfected cells (b) than in controls (a). The BrdU labelling rate was calculated and plotted in panel (c), showing a higher proliferation index in *Dact1* siRNA transfected cells.

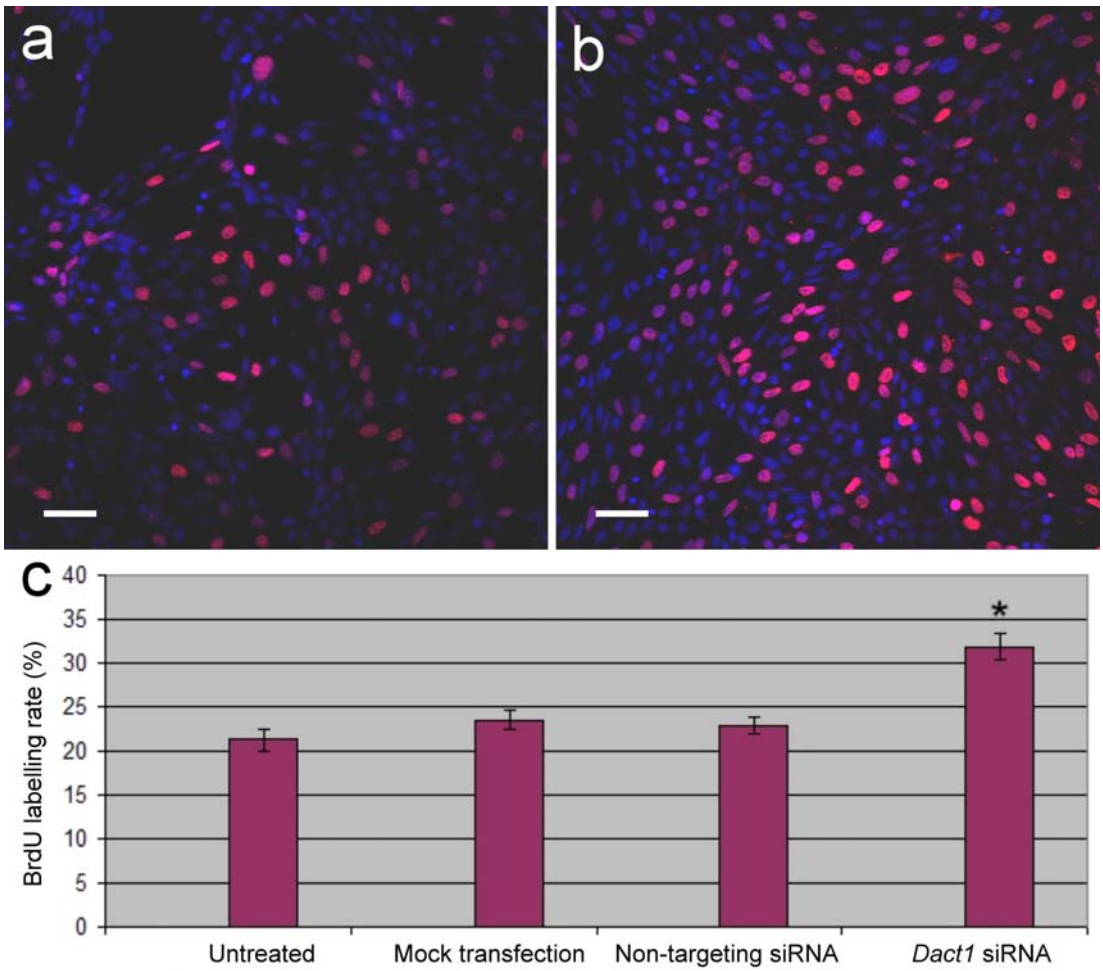

Figure 5-8 Cells treated with *Dact1* siRNA show a higher BrdU labelling rate. BrdU immunocytochemistry is shown in panel (a) and (b). Red (TRITC) nuclei indicated BrdU labelled nuclei while unlabelled nuclei were counterstained by TO-PRO-3 (blue). There were more red nuclei detected in *Dact1* siRNA-treated cells (b) compared to controls (a). The BrdU labelling rates were calculated and plotted in (c). Data are shown as Mean ± SEM and were subjected to one-way ANOVA, followed by Tukey's post hoc comparisons when main effects were significant. ($p=0.001$ in one way ANOVA; *$p<0.05$ vs. untreated in Tukey's post hoc comparisons)

5.4 Discussion

5.4.1 Specificity of this RNAi experiment

Like all other loss-of-function approaches, RNAi has the concerns of specificity. Several mechanisms have been proposed to explain off-target gene silencing in RNAi experiments such as interferon response (Sledz et al., 2003), miRNA-like translation inhibition (Scacheri et al., 2004; Zeng et al., 2003), global stimulation/repression of genes by high concentrations of siRNA (Persengiev et al., 2004), and mRNA degradation mediated by partial sequence complementation (Jackson et al., 2003). To reduce the risk of non-specific effects in RNAi experiments, I based my experimental design on published guidelines for RNAi experiments (Anonymous, 2003; Duxbury and Whang, 2004; Hannon and Rossi, 2004; Huppi et al., 2005) and introduced appropriate controls including untreated cells, mock transfection without siRNA and transfection with non-targeting siRNA. Untreated cells were used as a reference to which all other samples were compared. Mock transfection without siRNA was used to detect effects resulted from the transfection reagent and procedures. Transfection with non-targeting siRNA was to detect cellular effects caused by the introduction of any siRNA.

I also performed a titration experiment to determine the minimal concentration of *Dact1* siRNA at which 75% knockdown efficiency was achieved, as assayed by quantitative real time PCR. The lowest concentration of siRNA determined by my titration experiment was 10nM which was one tenth of the concentrations recommended by the manufacturer and seen in the literature. Semizarov *et al.* showed that non-specific gene activation can be eliminated when the siRNA concentration is reduced from 100nM to 20nM (Semizarov et al., 2003). By using this lowest effective siRNA concentration, I showed the satisfactory knockdown efficiency at mRNA level while all these controls expressed comparable *Dact1* mRNA level (Figure 5-6). Additionally, in cell counting and proliferation assays, these controls revealed differences neither in cell number nor proliferation index. This evidence supports the idea that the increased proliferation seen in *Dact1* siRNA-

treated cells is a specific effect of *Dact1* knockdown. One strategy to further strengthen my results may be the 'multiplicity controls' in which effective *Dact1* siRNAs targeting different regions of *Dact1* would be used in separate experiments and expect them to give the same phenotypes because it is highly unlikely that different siRNAs will cause the same off-target effects (Jackson et al., 2003).

However, the ultimate control for an RNAi experiment is the functional control in which a resultant phenotype is rescued by expression of the target gene in a form refractory to RNAi. Rescue experiments can be done by turning off inducible RNAi or by introducing a plasmid expressing the target mRNA which the RNAi sequence will not affect (Lassus et al., 2002). These methods are time-consuming and may cause inappropriate expression levels of a particular protein, which in turn will not rescue or can cause unexpected effects (Hannon and Rossi, 2004). Kittler *et al.* propose a promising method to do rescue experiment by using bacterial artificial chromosome (BAC) transgenesis. In this study, they make a transgenic human cell line expressing murine BAC harbouring mouse *Snw1* and shows that it is resistant to siRNA probing human *SNW1* (Kittler et al., 2005). The principle of this strategy is engineering a BAC construct carrying an orthologous gene from a closely related species together with its native regulatory sequences. Because of the 'cross-species' difference, this construct is divergent enough to escape from RNAi silencing. Furthermore, in contrast to the conventional cDNA-based constructs, BAC constructs are not driven by viral or model vertebrate promoters and thereby allow physiological gene expression. This strategy also allows the generation of alternatively spliced variants of the transgene. With these advantages, the application of BAC to RNAi rescue experiment is the best control so far for specificity (Sarov and Stewart, 2005).

In summary, I have carefully followed the guidelines yet described (Anonymous, 2003; Duxbury and Whang, 2004; Hannon and Rossi, 2004; Huppi et al., 2005) for RNAi experiments. The increased proliferation rate observed in *Dact1* siRNA transfected NIH3T3 cells was likely to be intrinsic to the depletion of *Dact1*. Further

work, including multiplicity controls and rescue experiments, needs to be done to enhance confidence of these RNAi results.

5.4.2 Potential mechanisms of *Dact1*-mediated growth control of NIH3T3 cells

The mechanisms by which *Dact1* mediates the growth control of NIH3T3 cell are yet to be elucidated. Analysis of the cell cycles of both my control and *Dact1* depleted cells might help to dissect this process. Besides, in the literature so far, *Dact1* has been reported as a crucial modulator in WNT signalling. *Dact1* inhibits WNT-mediated accumulation of soluble endogenous β-catenin and decreases activation of β-catenin responsive genes in *Xenopus* animal caps (Cheyette et al., 2002). Meanwhile, WNT3a has been documented as a stimulator of NIH3T3 cell proliferation (Yun et al., 2005). It can promote G_1 to S phase progression in NIH3T3 cells via activation of WNT/β-catenin, ERK (Yun et al., 2005) and PI3K-Akt (Kim et al., 2007b) pathways. Therefore, it is reasonable to hypothesize that silencing of *Dact1* is able to turn on or enhance WNT/β-catenin signalling and thereby stimulates NIH3T3 cells to proliferate. This hypothesis needs to be tested by further experiments.

5.4.3 Insights into kidney development

Cell proliferation is one of the important mechanisms for renal growth. From E11.5 to E16.5, kidneys double in size every nine to ten hours (Bard, 2002; Davies and Bard, 1998). Proliferation happens in every compartment of a developing kidney and contributes to nephron formation, UB branching and stroma patterning (Bard, 2002). A great number of molecules have been reported to regulate proliferation (Table 1-2) in developing kidneys but relatively few exert non-redundant effect on growth in each compartment. The role of *Dact1* in regulating cell proliferation observed in NIH3T3 cells might add this mesenchymal gene onto the growing list of molecules modulating growth of developing kidneys. In addition, according to the expression pattern, *Dact1* was expressed in mesenchyme at E11.5 and was expressed predominantly in the matured, differentiated medullary stroma by E14.5 (Figure 3-9).

Taken together the expression data and the implications from *Dact1* knockdown phenotypes in NIH3T3 cells, *Dact1* could be a proliferation-to-differentiation switch of a subset of mesenchymal cells in developing kidneys. Its function is further investigated by using RNAi in kidney organ culture and is presented in the following chapter.

Chapter 6

Exploring *Dact1* functions in kidney development by RNAi

6.1 Introduction

Organ culture of isolated kidney rudiments has been a simple but powerful model to investigate kidney development since the 1950s. In this system (Figure 6-1), kidney rudiments can be isolated as early as E10.5 and cultured on a filter at a gas-medium interface. Kidney rudiments growing in this system are able to reproduce the events of first few days of renal development (Grobstein, 1953). Experimenters can further dissect the UB from its surrounding mesenchyme and reassemble them together in this culture system. This tissue recombination technique allows the construction of UB and mesenchyme from donors of different genotypes and thus helps to determine which tissues are affected by the mutation (Kreidberg et al., 1993). Besides, in classical gene targeting strategies, the analysis of the role of a given gene in the kidney development can be confounded by systemic effects of gene inactivation. Organ culture can provide a solution to this problem by isolating the kidney from the rest of the body. An additional limitation of transgenic approaches is that the role of a gene at a specific stage cannot be analysed if the deletion has disrupted earlier stages of development. The organ culture model can be used to circumvent this problem too.

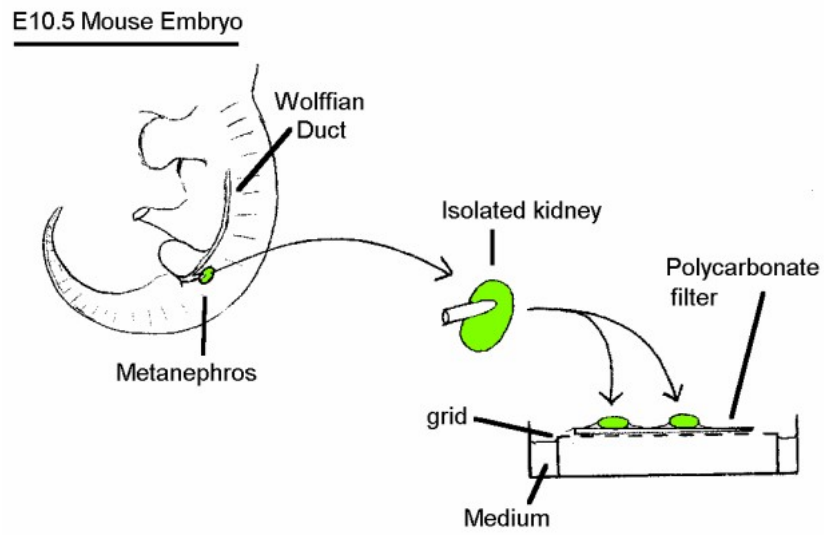

Figure 6-1 Mouse kidney organ culture method (Davies, 2006).

In addition to the advantages of the kidney organ culture model mentioned above, advantage has been taken of high accessibility of the cultured kidneys to exogenous drugs, growth factors and antibodies for a long time. The feature of its high accessibility inspires experimenters to apply RNAi to this powerful model. Sakai *et al.* first described RNAi in organ culture of salivary glands, lungs, and kidneys. By using siRNA targeting fibronectin, an ECM protein, Sakai *et al.* showed that knockdown of fibronectin blocks cleft formation in cultured salivary glands and that this can then be rescued by exogenous fibronectin. More importantly for this thesis, in their supplementary information, they demonstrated that the same siRNA is able to replicate the effect of function-blocking anti-fibronectin antibody in cultured kidneys (Sakai et al., 2003). The second paper on the application of siRNA to kidney organ culture showed the ability of siRNA targeting *Wt1* to generate a phenocopy of *Wt1* knockout mice. Davies *et al.* applied *Wt1* siRNA to cultured E9.5 urogenital ridges, in which kidneys would normally form one day later, and showed renal agenesis. They also used the same techniques to target *Pax2* and *Wnt4* in cultured kidneys and proposed a hierarchy for *Pax2*, *Wt1* and *Wnt4* to control nephron maturation (Davies et al., 2004). These encouraging results make siRNA-mediated RNAi a promising tool to dissect gene functions in developing kidneys.

By using this kidney organ culture model, a great amount of research exploring the interactions between the mesenchyme and UB has been done and has offered much insight into nephrogenesis and branching morphogenesis. One of the simplest and most useful assays to analyse kidney morphogenesis is counting the nephron and UB tip numbers as indicators for nephrogenesis and branching morphogenesis respectively (Davies et al., 2004). In the previous chapter, I have shown the validation of *Dact1* siRNA in NIH3T3 cell culture and the increased cell proliferation as a result of *Dact1* depletion. I therefore hypothesized that knocking down *Dact1* in developing kidneys will stimulate nephron formation and/or UB branching. I put this hypothesis to the test by analysing the change in nephron and UB tip numbers in the kidney culture which have been transfected with *Dact1* siRNA.

6.2 Experimental design

6.2.1 siRNA transfection in kidney culture

Dact1 siRNA duplexes used in this experiment were from Dharmacon and were validated in NIH3T3 cell culture as described in the previous chapter. The procedures of transfecting siRNA into kidney culture were based on that developed by Davies *et al.* (Davies et al., 2004). E11.5 kidneys were dissected and cultured as detailed in section 2.1.2 except using a different culture medium described below. Kidney cultures were set up separately into four dishes and labelled as untreated, mock transfection without siRNA, transfection with non-targeting siRNA and transfection with *Dact1* siRNA. Appropriate amounts of siRNA and 5µl of siLentFect (Bio-rad) were diluted in 250µl of Richter's medium (Gibco) supplemented with 10µg/ml transferrin in two separate tubes and were incubated at room temperature for 10 min. A transfection mix was made by mixing the solutions of these two tubes and incubated at room temperature for 20 min. 500µl of the transfection mix was then added into a clean bijou tube containing 2.5ml of transferrin supplemented Richter's medium yielding 10nM siRNA. Kidneys were cultured in this medium in a humidified incubator at 37°C overnight and the medium was then changed back to normal culture medium (described in section 2.1.2). Kidney cultures were stopped 48 hours after siRNA transfection for RNA extraction and 72 hours after transfection for immunohistochemistry.

6.2.2 Quantitative real time PCR to assay gene knockdown efficiency

To obtain sufficient amount of RNA for the downstream cDNA synthesis and quantitative real time PCR assays, eight kidneys in the same culture dish were pooled together at the end of culturing and were homogenised for RNA extraction. The primers (Table 5-1) to amplify *Dact1* gene were designed to flank the target site of *Dact1* siRNA duplex 2 (refer to Table 2-3 and Figure 5-3) and to amplify cDNAs made from all the potential *Dact1* transcripts. *Dact1* expression in each treatment

group was normalised to *Actb* and was shown as the percentage of that in the untreated group.

6.2.3 Immunohistochemistry to examine kidney morphology

Seventy-two hours after transfection, kidneys were fixed and subjected to immunohistochistry. Nephrons were visualised by anti-WT1 antibody and ureteric buds by anti-Calbindin-D28K antibody staining. The procedures were detailed in section 2.5 and the antibodies used were listed in Table 6-1. Images were taken by confocal microscopy. When taking images, the labelling of treatments on glass slides was masked so that the subsequent counting of nephron and tip number on the images would be done blind. Seven kidneys from each treatment group were counted and averaged. A one way ANOVA was first used to compare the mean of each group. This was done by using the Microsoft Office Excel 2003 software program. When the *p*-value was less than 0.05, the ANOVA test was considered to be statistically significant and Tukey's post hoc tests were then used to evaluate whether differences between any two pairs of means were significant. This test was done by an online calculator which can be found at the URL http://web.umr.edu/~psyworld/tukeyscalculator.htm.

Table 6-1 Antibodies used to examine the kidney morphology.

Name	Manufacturer	Host	Dilutions	Purpose
Monoclonal anti-WT1	Invitrogen	Mouse	1:400	To identify nephrons
Anti-Calbindin-D28K	Abcam	Rabbit	1:200	To show ureteric buds
FITC-anti-mouse IgG	Sigma	Goat	1:100	Secondary antibody
TRITC-anti-rabbit IgG	Sigma	Goat	1:100	Secondary antibody

6.3 Results

6.3.1 Suboptimal knockdown efficiency of *Dact1* siRNA in kidney organ culture

To determine the *Dact1* siRNA concentration to be used in kidney organ culture, 10nM siRNA was used as a starting point based on my results from cell culture (refer to section 2.6.2 and Figure 5-6). Higher concentrations of siRNA were tried but they resulted in substantial reduction of *Dact1* expression in non-targeting siRNA-treated kidneys. Therefore, 10nM of siRNA was used in the experiments described in this chapter. By quantitative real time PCR, the pool of four siRNA duplexes targeting different regions of *Dact1* knocked down *Dact1* mRNA to 60% of control values (Figure 6-2). Although there seemed to be an about 20% knockdown in the kidneys treated with non-targeting siRNA, the difference in the *Dact1* expression was not statistically significant as judged by a Student *t* test (p=0.105).

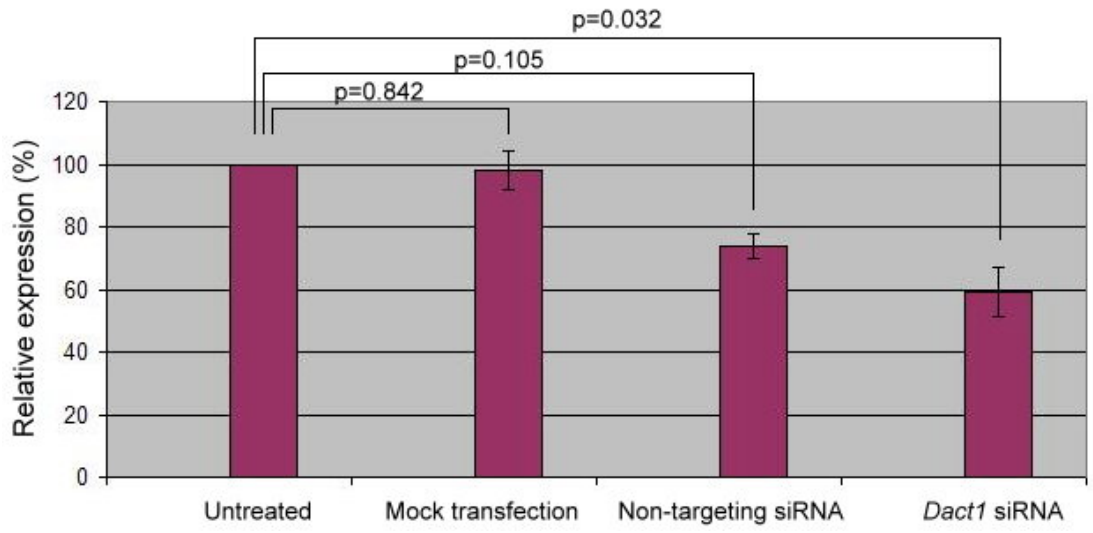

Figure 6-2 *Dact1* knockdown efficiency in E11.5 kidneys cultured *in vitro* for 48 hours. Eight kidneys were used in each treatment group. Quantitative real time PCR was performed to assay *Dact1* expressions. The *Dact1* expression level was normalised to *Actb* and is shown as percentage of the untreated group. *Dact1* expression is knocked down to 60% of the untreated control kidneys by *Dact1* siRNA. This knockdown is statistically significant as judged by a Student *t* test (p=0.032). Although there seems to be an about 20% knockdown in the kidneys treated with non-targeting siRNA, the difference in the *Dact1* expression is not statistically significant (p=0.105).

6.3.2 Possible *Dact1* knockdown phenotypes in kidneys

Although the knockdown efficiency in kidney organ culture was not as good as that in NIH3T3 cell cultures (40% in kidneys and 75% in cells as shown in Figure 6-2 and Figure 5-6), it might still be sufficient to produce a phenotype according to published work (Maeshima et al., 2006; Wang and Roy, 2006). Wang and Roy showed retarded formation of primordial follicles when *Gdf9* siRNA was transfected into ovary organ culture and knocked down *Gdf9* to 70% of controls (Wang and Roy, 2006). I therefore used my optimised siRNA concentration and transfection procedures in cultured kidneys and analysed their morphology by counting the tip and nephron numbers. Cultured kidneys in the four groups seemed to grow and developed normally. Figure 6-3 (a) and (b) are representative images of controls and *Dact1* siRNA-treated kidneys, respectively. No apparent morphological difference between them was detected. However, by carefully counting the tip and nephron numbers in each group, I found that *Dact1* siRNA-treated kidneys seemed to have more branches than controls. The average UB tip number in *Dact1* siRNA transfected kidney was ~75 per kidney compared with ~60 per kidney in the three control groups. The difference in tip number was statistically significant as judged by one way ANOVA ($p=0.038$) followed by Tukey's post hoc comparisons ($p<0.05$ when compared *Dact1* siRNA-treated kidneys to any controls). There was no significant difference in nephron number among the four groups (Figure 6-3 (c)). This result seemed to confirm the hypothesis that *Dact1* silencing leads to increased ureteric bud branching.

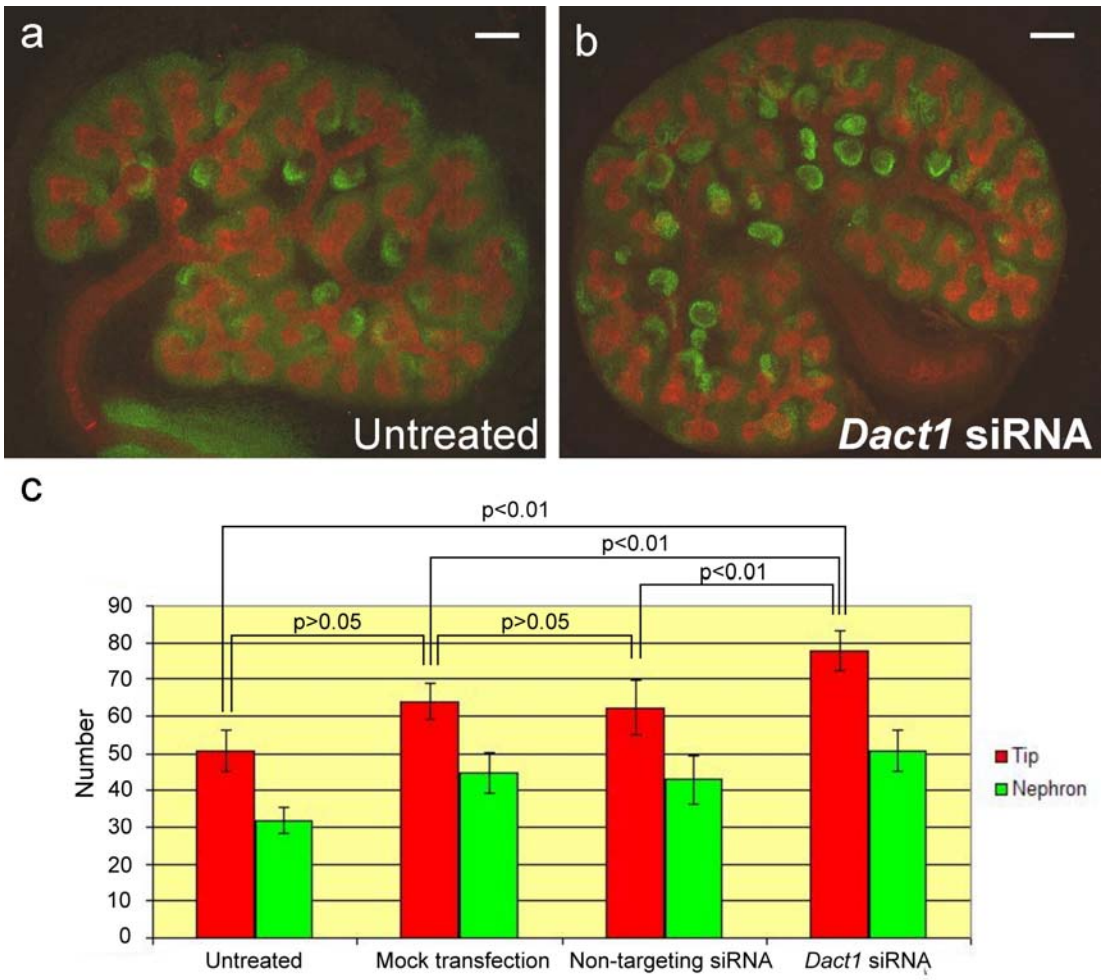

Figure 6-3 *Dact1* knockdown phenotypes in E11.5 kidneys cultured *in vitro* for 72 hours. Kidneys cultured in different treatments were fixed and proceeded to immunohistochemistry. In (a) and (b), ureteric buds were stained with anti-calbindin-D28K antibody (red) while nephrons were stained by anti-WT1 antibody (green). Representative images for renal morphology are shown in (a) and (b) for untreated and *Dact1* siRNA treated cultured kidneys, respectively. The number for both UB tips and nephrons were counted from six kidneys in each treatment. Data are plotted in (c) and are represented as Mean ± SEM. Red bars refer to the number of UB tips while green bars refer to nephron numbers. Kidneys treated with *Dact1* siRNA exhibited more UB tips (p=0.038 in one-way ANOVA; the *p*-values of paired comparisons in Tukey's post hoc comparisons are shown). There were no significant differences in nephron number among the four groups (p=0.124 in one-way ANOVA) Scale bar =100μm.

6.3.3 Transfection efficiency of siRNA in kidney organ culture

The suboptimal *Dact1* mRNA knockdown efficiency and the small increase in the UB tip number observed in the *Dact1* siRNA-treated kidneys cast doubt on the

transfection efficiency in kidney organ culture. Although the transfection procedures had already been optimised by using siGLO in 2D cell culture (refer to chapter 5), it is still necessary to test this transfection indicator in the 3D organ culture. The demonstration of the successful use of siGLO in ovary organ culture suggests it be an efficient transfection indicator in 3D organ culture (Wang and Roy, 2006). I therefore transfected siGLO of several concentrations, ranging from 10 to 500nM, into E11.5 cultured kidneys following the procedures described in section 6.2.1. Twenty-four hours after transfection, kidneys were washed in PBS (5 min x 2) and subjected to imaging. Phase contrast images showed that siGLO seemed to penetrate into the lumen of the UB and the loose mesenchyme. However, it was barely detected in the cap condensates, which are critical precursors of nephrons (Figure 6-4). This uneven distribution of fluorescently-labelled siRNA was seen in all the kidneys with various concentrations of siGLO being tested. It implied that not all the kidney cells were equally affected by the siRNA. It may therefore explain the suboptimal knockdown efficiency detected by quantitative real time PCR and the subtle knockdown phenotype observed.

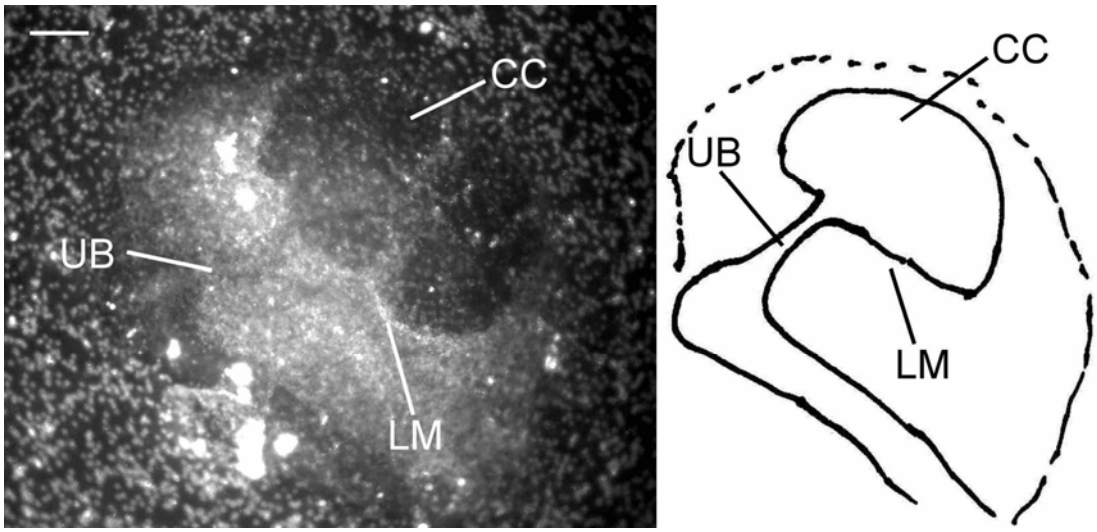

Figure 6-4 Uneven distribution of fluorescently-labelled siRNA in cultured kidneys. On E11.5 kidneys cultured *in vitro* for 24 hours, siGLO was unevenly distributed throughout the kidneys. It seemed to reach the lumen of the UB and the loose mesenchyme (LM) but not the cap condensates (CC). Scale bar =100μm.

6.3.4 Prior enzymatic digestion of kidney does not help siRNA penetration

The fluorescently-labelled siRNA was taken up by most of cells growing in 2D culture (Figure 5-5) but distributed unevenly in the 3D organ culture (Figure 6-4). This preliminary observation implied that in organ culture, cells have unequal chances to access and therefore take up siRNAs. This uneven distribution may result from diffusion pathways packed with ECM and the whole architecture containing fully-formed basement membranes. These elements could act as barriers to diffusion or they can trap siRNAs via multiple low-affinity charge interactions. Pretreatment of the whole organ by enzymatic digestion before being cultured may facilitate the diffusion of the lipid-complexed siRNAs.

Enzymatic techniques in combination with chelating agents have been widely used to dissociate tissues. A common example is trypsin together with EDTA. Trypsin cleaves the peptide bonds on the carbon side of arginine and lysine (Voet et al., 2002) and EDTA chelates the divalent cations that are present at the cell adhesions to the ECM (Gailit and Ruoslahti, 1988). Prolonged exposure of trypsin-EDTA leads to disruption of ECM structure (Teebken et al., 2000), which is a critical component modulating kidney development (Davies et al., 1995). By carefully use of trypsin-EDTA, experimenters can successfully separate the embryonic kidney into its component tissues, the ureteric bud and the mesenchyme. These separated component tissues can be re-combined and grow normally in the organ culture system (Sainio, 2003b). Also, carefully trypsinised kidneys without separation into ureteric buds and mesenchyme still can grow normally in organ culture (Lindström, personal communication). Therefore I decided to treat the kidneys with trypsin-EDTA followed by culturing and siRNA transfection.

Trypsin-EDTA medium was prepared as 500µl of trypsin-EDTA (Sigma) and 5µl of DNase in 2.5ml of MEM. E11.5 kidneys were dissected and the organ cultures were set up by using the trypsin-EDTA medium. After being incubated at 37°C for 10 min, the culture medium was replaced by fresh complete culture medium to inactivate trypsin. siGLO transfections were then followed according to the procedures

described in section 6.2.1. One day after transfection, kidneys were mounted and scanned by confocal microscopy. In addition to using siGLO to assay the transfection efficiency, I set up groups of kidney cultures for mock transfection, transfection with non-targeting siRNA and for normal kidney culture without trypsin-EDTA pretreatment. These kidneys were then assayed by quantitative real time PCR to examine if knockdown efficiency improved. Unfortunately, with the trypsin-EDTA pretreatment, siGLO was still unevenly distributed and the confocal images found it to be trapped in the middle portion of the kidney. The result of quantitative real time PCR did not show any improvement in knockdown efficiency.

6.3.5 Transfection efficiency in alternative culturing methods for kidney rudiments

The preceded enzymatic digestion of kidneys did not much improve the siRNA transfection efficiency. More intensive digestion might break the diffusion barrier more efficiently but caused impaired nephrogenesis and decreased branching (data not shown). Therefore I turned to another established culture system where metanephric mesenchyme was manually dissected out and cultured in a hanging drop. In this way, siRNA might gain more direct access to the cells. More importantly, in early kidneys, mesenchyme is easier for siRNA to penetrate than epithelia (Davies et al., 2004). Hanging drop culture is able to support induced mesenchymal cells to grow and form tubular structures for up to four days (Sainio, 2003b), which is long enough to assay the siRNA transfection efficiency. Metanephric mesenchyme from E11.5 kidneys was dissected out and incubated in a hanging drop at 37°C for 6 hours. The composition of the hanging drop was 100nM of siGLO and 1.2µl of siLentFect (Bio-Rad) in MEM. At the end of culturing, tissues were washed in PBS twice and then were mounted for imaging. In this way, siGLO seemed to diffuse into most of the mesenchymal cells. As shown in Figure 6-5, phase contrast micrograph (a) illustrates the mesenchyme. When scanned through the whole thickness of the mesenchyme by a confocal microscope, siGLO was found to distribute through the whole tissue. Panel (b) showed a representative optical confocal section of the middle part of the mesenchyme. This encouraging result suggested better siRNA

transfection efficiency in metanephric mesenchyme cultured in a hanging drop. However, if carrying out siRNA experiments in this way, it was extremely difficult to assay the gene knockdown efficiency by quantitative real time PCR because of the tiny size of the tissues. It was also difficult to analyze the morphological phenotypes in these fragmented tissues.

The improved siRNA transfection efficiency seen in the mesenchymal hanging drop culture inspired me to culture the whole kidney in a hanging drop. The whole kidney hanging drop culture would also make the subsequent quantitative real time PCR and morphology analysis easier. E11.5 kidneys were dissected and incubated with the transfection mix in a hanging drop for 6 hours. The composition of the hanging drop was as described in the previous paragraph. At the end of culturing, tissues were washed by PBS twice and then were mounted for imaging. Unfortunately, as shown in Figure 6-5 (c), siGLO was only seen at the edge of the kidneys.

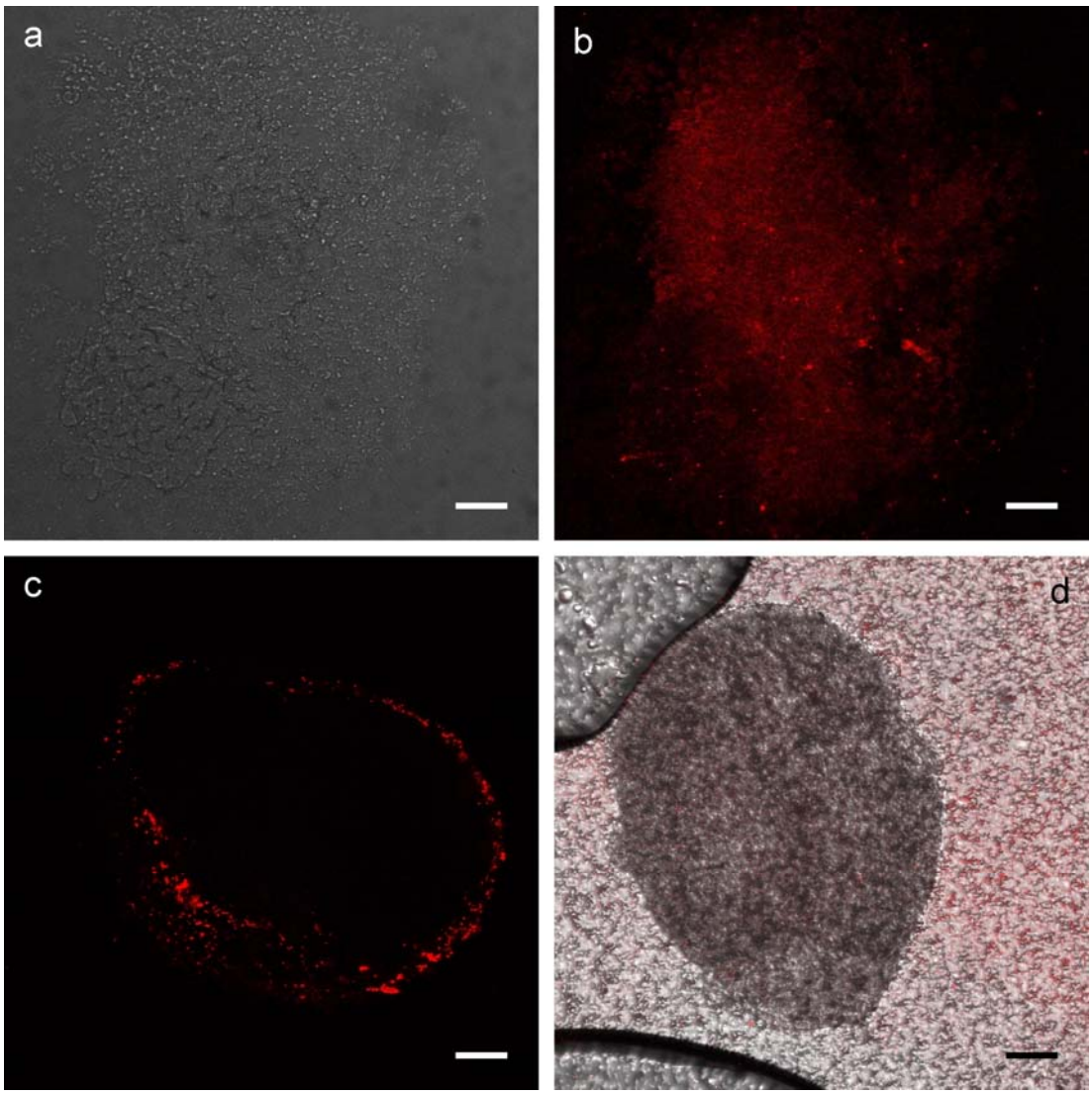

Figure 6-5 Using fluorescently-labelled siRNA as a transfection indicator in various culturing methods for kidney rudiments. Phase contrast micrograph (a) and an optical confocal section at the middle part of the mesenchyme (b) showed that siGLO seemed to enter into most of the mesenchymal cells when cultured in a hanging drop containing siGLO. However, when whole kidneys were cultured in a hanging drop (c), siGLO were not able to diffuse into kidneys. Panel (d) was an overlay of the phase contrast micrograph and TRITC channel confocal image showing that kidneys failed to uptake siGLO when cultured in the same way as described by Wang and Roy (Wang and Roy, 2006). Scale bar =50μm in a,b,c; 200μm in d.

Wang and Roy described a successful siRNA transfection method in ovary organ culture in which siGLO was taken up by more than 90% of the ovarian cells (Wang and Roy, 2006). I adopted their method but using E11.5 kidneys instead of ovaries. Kidneys were cultured on a cell culture insert fitted into a 24-well plate. Appropriate

amount of siRNA and 10µl of Metafectene Pro (Biontex) were diluted in 80µl of OptiMEM in two separate tubes and incubated at room temperature for 10 min. Transfection mix was made by mixing the solutions of these two tubes and incubated at room temperature for 20 min. 160µl of transfection mix was then added into a clean bijou tube containing 640µl of transferrin (10µg/ml) supplemented DMEM yielding 100nM siGLO. Kidneys were cultured in 400µl of this mixture for 6 hours. At the end of culturing, tissues were washed by PBS twice and then were mounted for imaging. However, siGLO did not enter into the kidney, as shown in Figure 6-5 (d). This may indicate that the diffusion barrier to siRNA was present in kidneys but not in ovaries.

6.4 Discussion

6.4.1 How can *Dact1* be a negative regulator of UB branching?

The kidney phenotype of *Dact1* knockdown found in this study answered the question about the functions of *Dact1* in kidney development. This phenotype raised one interesting question: how does *Dact1* silencing result in more UB branching? Two ideas might help to answer this question. One was that the *Dact1* silencing lead to localised proliferation of mesenchymal cells around the UB tips. The localised cell proliferation in turn stimulate UB branching. In this study, *Dact1* siRNA was added into the organ culture when *Dact1* was expressed by mesenchymal cells of the kidney (Figure 3-9). Some of these mesenchymal cells took up *Dact1* siRNA and as development proceeded, they became condensed at the UB tips. As implicated from the results of *Dact1* silencing in the embryonic mesenchymal cell line NIH3T3 (Figure 5-8), mesenchymal cells were encouraged to proliferate once *Dact1* was silenced. These processes generated high cellular proliferation zones around the UB tips. Cells in these zones might send out paracrine signal to stimulate ureteric buds to branch. The temporospatial expression pattern of *Dact1* (as described in section 3.3.4) seemed to support this hypothesis. In normal E14.5 kidneys, *Dact1* expression levels were much higher in the medullary stroma, which was the compartment with less cell proliferation, than the nephrogenic zone (Figure 3-9). This seemed to imply that

Dact1 expression was turned off when cells were about to proliferate in the nephrogenic zone.

The other idea came from known molecules regulating UB branching. As reviewed in section 1.2.1, the GDNF/Ret pathway is perhaps the best-characterised pathway for UB branching. I would hypothesised that silencing of *Dact1* in mesenchymal cells results in increased generation of GDNF and thus stimulates UB branching. These two ideas were not mutually exclusive. Instead, both of them might be present and complementary to each other. Experiments including the detection of proliferation marker such as proliferating cell nuclear antigen (PCNA) (Winyard et al., 1996), and the expression of *Gdnf*, *Ret* and *Wnt11* in *Dact1* siRNA-treated kidney organ culture are required to test these hypotheses.

6.4.2 Pitfalls of application of siRNA to kidney culture

Since the first application of RNAi in organ culture (Sakai et al., 2003), siRNA-mediated RNAi has been successfully applied to several organ culture systems including kidneys (Davies et al., 2004), palatal shelves (Shiomi et al., 2006), lungs (Gill et al., 2006; Sakai et al., 2003), ovaries (Wang and Roy, 2006), urogenital ridges (Zhan et al., 2006), Wolffian ducts (Maeshima et al., 2006), and atrioventricular canals (Mercado-Pimentel et al., 2007) (Table 6-2). By showing impressive phenotypes in various organs, these successful studies encourage the use of siRNA as a tool for investigating organ development in *in vitro* culture system.

However, the expanding use of siRNA in organ culture also urges a need to evaluate the difficulties this field might have. The siRNA-mediated RNAi response depends mainly on the overall transfection efficiency. Fluorescently-labelled siRNA may be a good indicator to illustrate siRNAs delivered to the cells. Among the examples listed in Table 6-2, only one of them use the fluorescently-labelled siRNA to demonstrate a satisfactory transfection efficiency achieved (Wang and Roy, 2006). Using siGLO in my project, I have shown the diffusion problems in the whole kidneys cultured on the classical organ culture system (Figure 6-4), in a hanging drop (Figure 6-5c) and on a

cell culture insert (Figure 6-5d). Satisfactory transfection efficiency seemed to be achieved only when isolated metanephric mesenchyme in a hanging drop culture where cells can have more direct access to siRNAs (Figure 6-5ab). Besides, as seen in Table 6-2, the large amount of siRNA used in the experiments (Sakai et al., 2003; Shiomi et al., 2006) also indicates the poor transfection efficiency in organ culture.

The diffusion barrier may vary from organ to organ because in early salivary gland, Sakai *et al.* found that epithelium is easier for siRNA to be delivered than mesenchyme (Sakai et al., 2003) whilst the opposite results are found in early kidneys (Davies et al., 2004). Also by using the same culture systems, transfection indicator and procedures as that described by Wang and Roy (Wang and Roy, 2006), I have shown that kidneys were harder for siRNA to enter than ovaries. Additionally, the diffusion barrier can vary between developmental stages within the same organ. As shown in Figure 6-4, at the stage of mesenchymal condensation (Davies and Bard, 1998), an intra-mesenchymal barrier seems to form that hinders penetration of siRNA into the cap condensates. New strategies need to be developed to overcome the problems of siRNA delivery in organ culture.

The second problem for applying siRNA-mediated RNAi in organ culture was the methods to detect gene knockdown efficiency. In 2D cell culture, it is desirable to detect gene knockdown efficiency at mRNA and protein levels by using quantitative real time PCR and Western blot respectively (Anonymous, 2003; Duxbury and Whang, 2004; Hannon and Rossi, 2004; Huppi et al., 2005). However, in organ culture, it is often difficult to perform these assays in the limited number of cells within the tissues. For example, in a E11.5 kidney, there is only 200-300 cells in the UB and a few thousand cells in the mesenchyme (Sainio, 2003b). These cell numbers are approximately 1% of those used for an RNAi experiment carried out in 2D cell culture. This may partly explain why about half of the published work did not show the knockdown efficiency (Table 6-2).

Off-target effect is also a crucial concern of an RNAi experiment carried out in organ culture system. In order to overcome the diffusion problem, experimenters might try

to force the system by delivering extremely large amount of siRNA (Sakai et al., 2003). This may lead to numerous undesired effects as a high concentration of siRNA has been shown to cause off-target effects in 2D cell culture (Persengiev et al., 2004; Semizarov et al., 2003). Therefore appropriate controls, including mock transfection, transfection with non-targeting siRNA, and functional rescue experiments should also be done to show that the phenotype is intrinsic to the depletion of the target gene.

Table 6-2 Successful applications of siRNA-mediated RNAi in organ culture

Organ	Targeted genes	Time (hours)	%KD	Verification	siRNA concentration (nM)	Transfection reagent	References
Salivary gland	Fibronectin	NS	NS	IF	500	oligofectamine	(Sakai et al., 2003)
Kidney	Fibronectin	NS	NS	NS	1000		
Kidney	Wt1, Wnt4, Pax2	NS	NS	IF (for Wt1)	200	oligofectamine	(Davies et al., 2004)
Kidney	Gdnf	NS	NS	NS	200	oligofectamine	(Michael et al., 2007)
WD	Activin A	24	75	Real time PCR	NS	lipofectamine 2000	(Maeshima et al., 2006)
		48	40	WB	NS		
Urogenital ridges	Alk2, Alk3, Smad1, Smad5, Smad8	NS	NS	NS	200	oligofectamine	(Zhan et al., 2006)
Ovary	Gdf9	216	33	Real time PCR	100	transfectane	(Wang and Roy, 2006)
			30	IF			
Lung	Fak	NS	NS	IF	16	lipofectamine 2000	(Gill et al., 2006)
Palatal shelves	Smad2	24	60	WB	500	oligofectamine	(Shiomi et al., 2006)
AV canal	Endoglin	24	75	Real time PCR	10*	oligofectamine	(Mercado-Pimentel et al., 2007)
	Alk5	24	95	Real time PCR	10*		

siRNA-mediated RNAi has been successfully applied to salivary glands, kidneys, Wolffian ducts (WD), urogenital ridges, ovaries, lungs, palatal shelves and atrioventricular (AV) canals. Gene knockdown (KD) was verified by immunofluorescence (IF), Western blot (WB) and real time PCR.*two transfections of 10nM siRNA; NS: Not shown.

6.4.3 New directions of application of siRNA to kidney culture

New strategies have been developed to deliver siRNA into cultured organs more reliably. The common feature of these strategies is to dissociate the tissues into cells, deliver siRNA or shRNA into cells and re-aggregate these cells followed by *in vitro* culture. For example, Park *et al.* dissected ovaries and used enzymes to dissociate them into cell suspensions. They then used lipid transfection reagent to deliver siRNA into either oocytes or somatic cells. In this way, they showed transfection efficiencies of 40-50% and 30-40% for each cell type respectively and knockdown of *Wee1* expression to 30-40% of wild type levels. The transfected cells (and untransfected controls) were aggregated with phytohaemagglutinin and coated with sodium alginate. These alginated cells were then encapsulated by calcium alginate and thus formed the reconstructed 'ovaries'. These reconstructed 'ovaries' were cultured for four days. Compared with sham controls, the ones with *Wee1* knockdown showed irregular follicle shape (Park et al., 2006).

This dis-aggregation and re-aggregation strategy and other new methods for culturing organotypic tissues from dispersed cells are being steadily reported in various organs including retinas (Palfi et al., 2006), teeth (Song et al., 2006), skins (Mildner et al., 2006), blood vessels (Perez-Pomares et al., 2006), neurons (Ajioka and Nakajima, 2005), cartilages (Rosowski et al., 2006), and livers (Zhu et al., 2007). Many of these systems seem to offer more direct access to siRNA or shRNA, albeit the transfection methods may vary. In the tooth model, Song *et al.* showed that 92% shRNA delivery efficiency were achieved when E13.5 molar mesenchyme was dispersed into a single cell suspension (Song et al., 2006). To date, there have not been reports on kidney culture using the dis-aggregation and re-aggregation strategy but the dispersed embryonic kidney cells, at least at E11.5, retain their ability to grow organotypically when re-aggregated and cultured (Unbekandt, personal communication). This technique may therefore be promising to sharpen the tool of siRNA-mediated RNAi for investigating kidney development in *in vitro* culture system.

In summary, by using the conventional lipid mediated transfection method in the whole kidney organ culture, I have shown that *Dact1* was knocked down to 60% of controls. This suboptimal knockdown efficiency may partly be explained by the uneven distribution of the siRNA. According to the distribution pattern shown by fluorescently-labelled siRNA, the loose mesenchyme of the cultured kidneys seemed to be able to take up siRNA. Also most mesenchymal cells cultured in a hanging drop seemed to take up siRNA. Although there was diffusion problems in kidney organ culture, these preliminary observations seemed to support that substantial amount of *Dact1* siRNA reached the right place where *Dact1* was expressed (Figure 3-9). The observed subtle increase in UB branching in kidneys treated with *Dact1* siRNA might be intrinsic to the sub-optimally delivered *Dact1* siRNA. In organ culture, sometimes it is not easy to know how much a given gene been depleted will exhibit its phenotype. Wang and Roy showed a *Gdf9* knockdown phenotype in ovaries when 70% of expression remained (Wang and Roy, 2006). The encouraging results from the dis-aggregation and re-aggregation of kidney cells render more direct access to siRNA delivered and may therefore overcome the diffusion problems delineated by fluorescently-labelled siRNA (Figure 6-4). In the future, adopting this new strategy, together with the appropriate controls done in this experiment, will strengthen the confidence of the observed *Dact1* knockdown phenotype.

Chapter 7

The function of *Dact2* in cell line based models of UB development

7.1 Introduction

Branching morphogenesis is a crucial event for permanent kidney development. This process begins with the outgrowth of an unbranched epithelial tube, called ureteric bud, from the Wolffian duct. The UB grows towards and invades the metanephric mesenchyme where it is induced to undergo branching morphogenesis so that the epithelial tube finally turns into a tree-like arrangement of tubules. Meanwhile, the epithelial tree induces some of the surrounding mesenchymal cells to aggregate, condense and epithelialise into vesicle, comma-shaped bodies, S-shaped bodies, developing capillary loop and maturing glomerulus (Abrahamson and Wang, 2003; Davies, 2006; Saxen, 1987). Disruptions in UB branching, for example in *Gdnf* (Moore et al., 1996; Pichel et al., 1996), *Ret* (Schuchardt et al., 1994) and *Gfrα1* (Cacalano et al., 1998) knockout mice, cause severe renal malformation or agenesis.

There are three main models to study metanephric branching morphogenesis: *in vivo*, in organ culture and in cell culture. *In vivo* approaches have the advantage that development is seen in a genuine environment but its disadvantages include poor access and potentially being confounded by systemic effects on the embryos. Organ culture has many advantages described in the previous chapter but seems to have diffusion barrier to siRNA (Figure 6-4). Cell culture models are based on a few kidney-derived epithelial cell types that can be induced to develop branching tubules in 3D collagen matrices. MDCK, mIMCD-3, and UB cells have all been used for this system (Cantley et al., 1994; Montesano et al., 1991; Sakurai et al., 1997a).

MDCK cells derive from an unknown site of the adult dog nephron (Feifel et al., 1997). When embedded in matrices, these cells proliferate and form cysts with the same apico-basal polarity as a normal UB. These cysts form branching tubules when cultured in the presence of HGF (Montesano et al., 1991). mIMCD-3 cells derive from adult mouse inner medullary collecting duct (Rauchman et al., 1993). When suspended in matrices, these cells multiply and form cysts. These cysts are induced to form branching tubules in response to HGF (Cantley et al., 1994) or ligands of epidermal growth factor (EGF) receptor, including EGF and TGFα (Barros et al.,

1995; Sakurai et al., 1997b). An immortalised cell line derived from the UB (Barasch et al., 1996) is capable of generating branching tubules in collagen I matrix in the presence of medium conditioned by BSN mesenchymal cell line (Sakurai et al., 1997a). These culture systems allow experimenters to analyse branching morphogenesis from a single cell type in the absence of the indirect effects from mesenchymal development that would be present in organ culture. Most of all, these cell culture models have a great advantage that the cells can be transfected before use. This advantage allows advanced genetic manipulations (e.g. transfection with mutants and reporter genes) to be performed on them. In this project, I took advantage of this and transfected mIMCD-3 cells with plasmids expressing *Dact2* shRNA before growing them in the 3D collagen I gel.

It has been postulated that tubulogenesis requires cell migration and cell proliferation prior to the formation of lumen-containing tubules (Orellana and Avner, 1998). Cell migration is widely understood as the movement of individual cells that undergo a cyclic 5-step process: protrusion of the leading edge, cell-matrix interaction and formation of focal contacts, localised proteolysis, actomyosin contraction and detachment of the trailing edge (Friedl and Wolf, 2003). However, in tubulogenesis, cells migrate in a fashion called 'collective cell migration' (Friedl and Wolf, 2003; Zegers et al., 2003). In this migration mode, cells are mobile yet simultaneously connected by cell-cell junctions. When in contact with the substrate, collectively moving cells develop multicellular outward ruffling at substrate binding sites and generate traction. This force generation occurs only at the free pole of the cell group. A unipolar leading edge is thus formed. If the moving cells at the leading edge remain connected to other cells by cell-cell junctions, the trailing edge drags the neighbour cells along the emerging migration track (Friedl et al., 2004). The simplest approach to study collective cell migration is the 'wound healing assay' in which an artificial wound is created by a needle scratch across a confluent monolayer of cells and the distance between the two margins or the whole area of the wound was measured (Nobes and Hall, 1999).

The effect of gene silencing caused by siRNA-mediated RNAi is transient and frequently lasts for only 3–5 days in cell culture (Holen et al., 2002). Although this may be sufficient for many applications, the insufficient longevity of the silenced state limits its use in the mIMCD-3 cell-collagen matrix model. Another potential problem is the transfection efficiency because mIMCD-3 is a difficult-to-transfect cell line. The solution to these problems is the stable expression of RNAi effector molecules from plasmids or viral vectors. Vector-based RNAi also permits co-expression of reporter genes such as GFP or luciferase, which facilitates tracking of transfected cells (Amarzguioui et al., 2005).

One of the aims of this project was to investigate the functional roles of *Dact2* in developing kidneys by using siRNA-mediated RNAi in kidney organ culture system. However, as *Dact2* was expressed by the UB epithelium, which is more difficult for siRNA to enter (Davies et al., 2004) and the diffusion problems of the 3D organ culture system are yet to be overcome, an alternative RNAi-based approach was employed to explore potential *Dact2* functions in mammalian kidney development. This alternative strategy was composed of vector-based RNAi, the wound healing assay and the mIMCD-3 cell-collagen matrix model and aimed to discover the potential role of this UB marker, *Dact2*, in renal branching morphogenesis. I made mIMCD-3 cell lines that stably expressed plasmids harbouring *Dact2* shRNA sequences. The negative control cells were mIMCD-3 cells which stably expressed the same vector but harboured scrambled artificial sequences. Gene knockdown efficiency was assayed by quantitative real time PCR. A wound healing assay was used to examine if *Dact2* plays a role in collective cell migration. Based on the significant differences in wound healing assay seen between *Dact2* knockdown and controls cells, these cells were then grown in 3D collagen gel to evaluate the impact of *Dact2* knockdown on branching morphogenesis.

7.2 Experimental design

7.2.1 RT-PCR

To study the *Dact2* functions in mIMCD-3 cells, which were the key materials used in the following experiments, the critical step was to confirm their expression of *Dact2*. Conventional end-point RT-PCR was used for this purpose. The procedures are detailed in section 2.2.3. The sequence of the forward primer is 5'ACGGCTAAGGAGACAGGATG3' and the sequence of the reverse primer is 5'GGACAGTGGTCTCATCAGCA3'. The binding sites of these primers on the *Dact2* transcript are depicted in Figure 7-1. The PCR amplicons were 305bp in size.

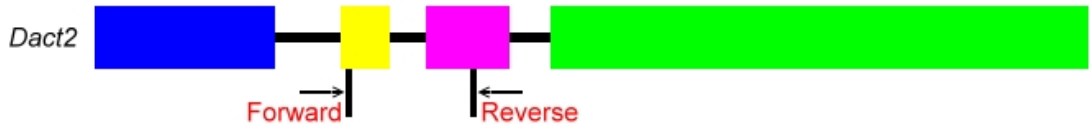

Figure 7-1 Binding sites of PCR primers used to illustrate the expression of *Dact2* in mIMCD-3 cells. Schematic diagram shows the binding sites of PCR primers on *Dact2* gene. Coloured bars refer to different exons i.e. exon 1 (blue), exon 2 (yellow), exon 3 (magenta) and exon 4 (green). The forward primer binds to the antisense strand, the reverse primer to the sense strand.

7.2.2 Generation of *Dact2* shRNA stable cell lines

The procedures for generating *Dact2* shRNA stable cell lines are detailed in section 2.8. There were four clones of plasmids encoding different *Dact2* shRNA sequences and one clone of negative control (NC) plasmid with scrambled artificial sequences to be separately transfected into mIMCD-3 cells. The insert sequences are listed in Table 7-1 and were mapped to the *Dact2* transcript as shown in Figure 7-2 and Figure 7-3. Cells that stably expressed *Dact2* shRNA and NC shRNA were obtained by antibiotic resistant clonal selection and their expressions of *Dact2* mRNA were assayed by quantitative real time PCR. The sequences of primer used are listed in Table 3-3. The *Dact2* primer pair was the one used to profile its expression in

developing kidneys (described in chapter 3) and it happened to flank the target sequences of plasmid clone 3 and clone 4 (Figure 7-3).

Table 7-1 Insert sequences on shRNA plasmids.

Clone ID	Insert sequence
1	AAGGTCAGAAGAAGAGTTAGT
2	AAGGACAGCCTCAAGCAACAT
3	AGACCCAGCTCAGGTTTCTAT
4	TGGATGTGAGCAGGTCTTCTT
NC	GGAATCTCATTCGATGCATAC

Figure 7-2 Mapping *Dact2* shRNA target sequences on the mouse *Dact2* transcript. Target sequences of the four plasmids encoding *Dact2* shRNAs are shown in red (clone 1), brown (clone 2), green (clone 3) and magenta (clone 4). Exons of mouse *Dact2* are distinguished by alternative black and blue colour text.

Figure 7-3 *Dact2* shRNA plasmids target sites and primer binding sites on the mouse *Dact2* transcript. Schematic diagram depicts the target sites of *Dact2* shRNAs on the mouse *Dact2* transcript (scissor). Black bars and arrows indicate the binding sites of *Dact2* primers used to detect the silencing efficiency. P: plasmid.

7.2.3 Wound healing assay

Cells that stably expressed *Dact2* shRNA and NC shRNA were used in a wound healing assay. $1x10^6$cells per well were plated in G418 media in a 6-well plate. The following day, when cells had formed a monolayer, a straight scratch wound was created by a yellow pipette tip. Cells were then washed by G418 media for three times and were subjected to time-lapse microscopy (Zeiss Axiovert 200). The setting parameters of time-lapse imaging system included 10X objectives and 25ms exposure time. Images were taken at the same position of each well at 10-min intervals over 24 hours. Stacks of images of the same well were converted into an AVI movie by the software IPLab (Scanalytics). Wound areas were also measured at two-hour intervals by the same software.

7.2.4 BrdU incorporation assay

To investigate whether cell proliferation affects the wound healing in these cells, a BrdU incorporation assay was performed together with this wound healing assay. Four hours after a scratched wound was made, a short pulse of BrdU (20μM) was introduced for 45 min. Cells were then fixed and subjected to BrdU immunocytochemistry as detailed in section 2.7.2. At the end of the immunocytochemistry, cells were mounted and imaged by confocal microscopy. When taking images, the labelling of clones on glass slides was masked so that the subsequent cell counting on the images was done blind. Two hundred cells were

counted per coverslip and the proliferation index was defined by BrdU labelling rate, which was calculated as the ratio of BrdU labelled cells to the total cell number counted. Data from three independent experiments were collected and subjected to statistical analysis. By using the Microsoft Office Excel 2003 software program, a one way ANOVA was used to compare the means of each group. When the *p*-value was less than 0.05, the ANOVA test was considered to be statistically significant.

7.2.5 3D collagen gel cell culture

To prepare the collagen I gel matrix, appropriate volumes of each component were calculated as 20µl of 10X PBS, 2.3µl of 1N NaOH, 77µl of distilled water and 100µl of rat tail collagen type I (BD Biosciences) for a well in a 24-well plate. These components were mixed together in a sterilised tube on ice. 5000 cells were added to the collagen mixture and seeded in each well. This low cell density was used to avoid cell–cell contact when cells were seeded. 200µl of the cell/collagen I gel mixture was plated onto a coverslip at the bottom of a 24-well plate and incubated in a humidified incubator at 37°C for 20 min. HGF was added into G418 culture medium to yield a final concentration of 25ng/ml. 500µl of HGF medium was carefully added into each well. Cells in collagen gel matrices were cultured at 37°C with 5% CO_2. The HGF medium was changed every three days. After seven days, cells were fixed by 4% PFA followed by mounting and imaging.

7.3 Results

7.3.1 mIMCD-3 cells expressed endogenous *Dact2*

RT-PCR was used to verify the presence of *Dact2* expression in mIMCD-3 cells. In Figure 7-4, in the presence of RT, RNA samples from mIMCD-3 cells showed a single band of correct size (305 bp) on agarose gel whilst negative control, RNA samples from mIMCD-3 cells without adding RT, yielded no bands.

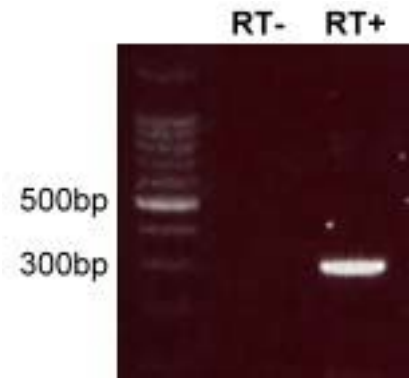

Figure 7-4 mIMCD-3 cells express *Dact2*. Compared with a 100bp ladder (left lane), PCR ethidium bands of the correct size for *Dact2* cDNA are present in mIMCD-3 cell RNA samples with RT added (+) but not samples when no RT was added (−).

7.3.2 Effective *Dact2* knockdown in stably transfected mIMCD-3 cells

Quantitative real time PCR was used to assay *Dact2* knockdown efficiency in mIMCD-3 cells. The *Dact2* expression level was normalised to a housekeeping gene, *Actb*. Data were expressed as percentage of the control clones that harboured plasmid encoding scrambled artificial sequences. Knockdown of *Dact2* in several mIMCD-3 clones was verified by using quantitative real time PCR. Most clones showed satisfactory knockdown efficiency except the ones expressing plasmid clone 3 (Table 7-2). In Table 7-2, the names of cell clones are composed of a number and a letter. The number refers to the shRNA plasmids transfected. Figure 7-5 showed the knockdown efficiencies in the selected clones. In clones 1b and 4c, *Dact2* expression was reduced to 10% of control cells. These two clones of cells were therefore chosen for the subsequent wound healing assay and the 3D collagen gel culture. In the wound healing assay and 3D culture experiments, these clones were designated P1 and P4 respectively.

Table 7-2 Relative expression of *Dact2* in all the clones tested.

Cell clones	Relative expression of *Dact2* (% of control)	Cell clones	Relative expression of *Dact2* (% of control)
1a	16.1	3a	61.3
1b (P1)	9.8	3b	51.3
1c	12.0	3c	49.8
2a	43.0	4a	185.1
2b	28.7	4b	11.2
2c	31.3	4c (P4)	10.6

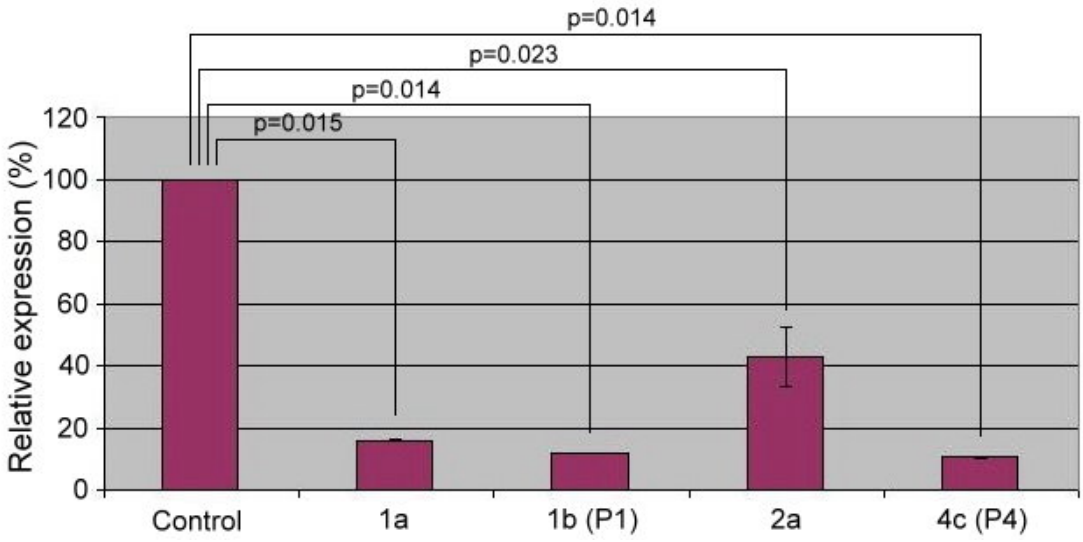

Figure 7-5 *Dact2* silencing efficiencies in selected clones stably expressing *Dact2* shRNA. Quantitative real time PCR showed that the relative *Dact2* expression in selected clones of mIMCD-3 cells. *Dact2* expression was normalised to *Actb* and was expressed as percentage of the control. Control refers to cells transfected with negative control plasmid. In clone 1a, 1b and 4c, *Dact2* expression was knocked down to about 10% of the control. Data are represented as Mean ± SEM. The difference in *Dact2* expression was examined by Student *t* tests and the *p*-values are shown.

7.3.3 *Dact2* is required for the coordinated migration of renal epithelial cells

Having verified the knockdown efficiencies in *Dact2*-depleted mIMCD-3 cells, a wound healing assay was used to examine their phenotypes. After wounding, cells were monitored by time-lapse imaging system for 24 hours. These experiments were carried out independently three times and representative images for control clone, P1 and P4 at time zero, three hours and six hours after wounding are shown in Figure 7-6. Six hours after wounding, control cells closed the wound but the wounds of the *Dact2* knockdown cells, clone P1 and P4, were still open. At the end of the whole 24-hour monitoring by time-lapse imaging system, images taken at two-hour intervals were picked from the stacks of images for each clone. These images were analysed by measuring the wound area at each time point relative to the area at time zero. The calculated percentage of wound area is plotted and shown in Figure7-7. Control cells took six hours to close the wound. Clone P1 and P4 cells took ten and 18 hours to heal the wound, respectively. Compared to control cells, both clone P1 and P4 cells moved more slowly. Although both P1 and P4 expressed comparably low *Dact2* mRNA levels (Figure 7-5), clone P4 cells moved far more slowly than clone P1 cells (Figure 7-6, 7-7 and AVI movies in attached CD). Nevertheless, clone P1 and P4 served as multiplicity controls for each other in an RNAi experiment. The phenotype was a specific result of *Dact2* depletion because it is very unlikely that different shRNAs will lead to the same off-target effects (Jackson et al., 2003). In addition to the rate of wound closure, aberrant motility responses were also noted in *Dact2* knockdown P1 and P4 cells. Unlike control cells, which showed a coordinated sweeping of a joined-up epithelial sheet, cells lacking *Dact2* exhibited a much amoeboid movement (Figure 7-8 and AVI movies in the attached CD).

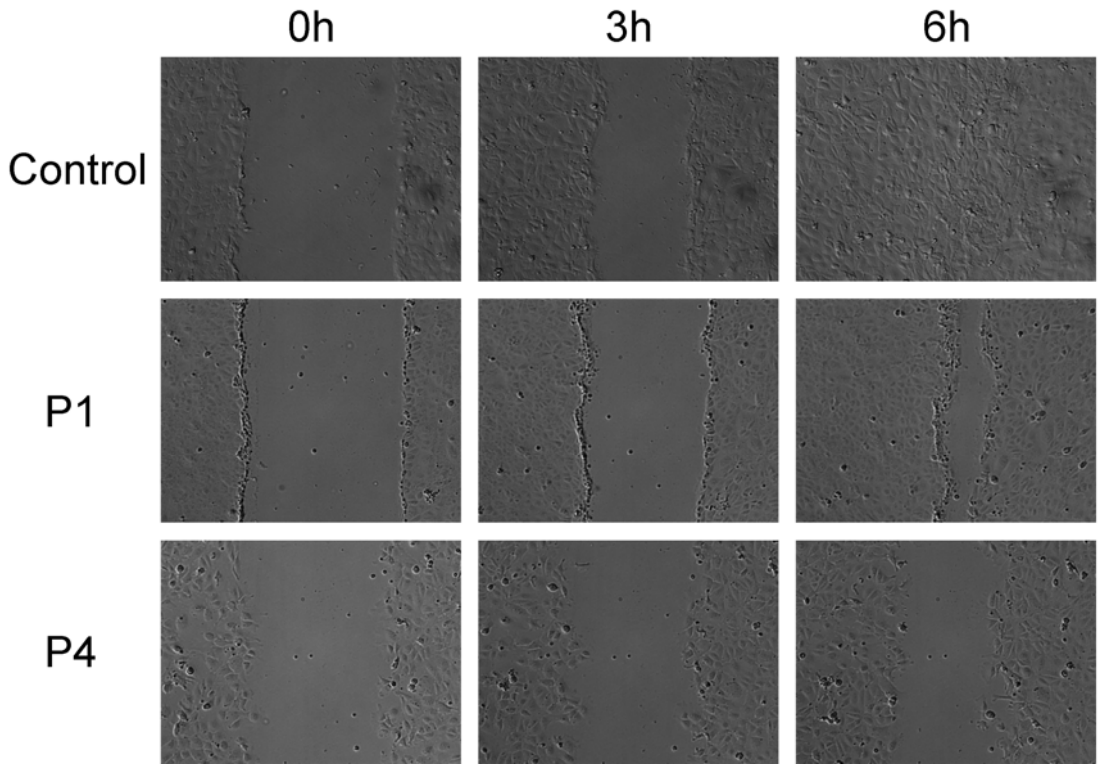

Figure 7-6 Collective migration of mIMCD-3 cells in response to wounding. Cells for wound healing assay were monitored by time-lapse imaging system for 24 hours. Images taken at time zero, three and six hours after wounding were shown. Cells lacking *Dact2* (clone P1 and P4) moved more aberrantly and slowly than control cells. By six hours, control cells already closed the wound whilst the wounds were still present in clone P1 and P4. Clone P4 cells moved more slowly than clone P1. The complete time course of wound closure is plotted in Figure 7-7.

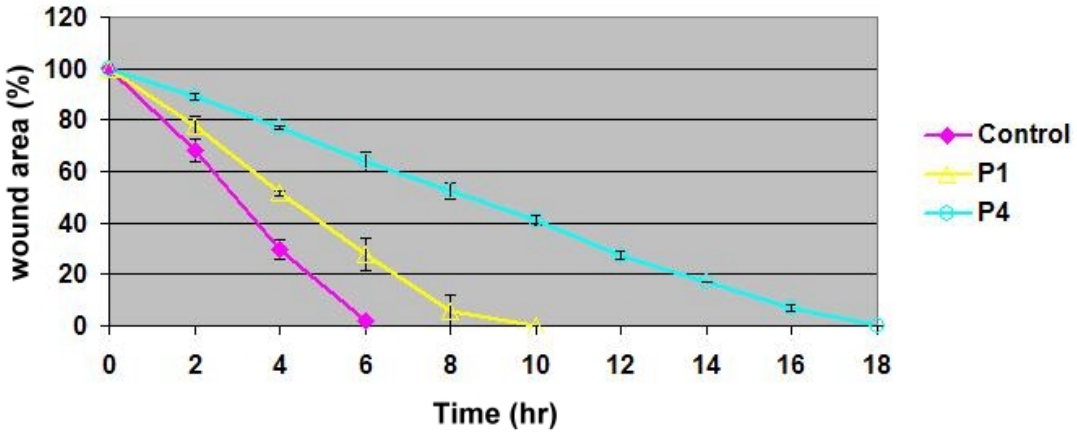

Figure 7-7 Time course of the wound healing assay. In wound healing assays, images taken at two-hour intervals were chosen to measure the area of the wound. The area at each time point was measured as the percentage of the area at time zero. Data were collected from three independent experiments and are represented as Mean ± SEM. Control cells (pink) took six hours to close the wound. Both clones of cells lacking *Dact2* moved more slowly than control cells. Clone P4 cells (blue) took 18 hours to heal the wound.

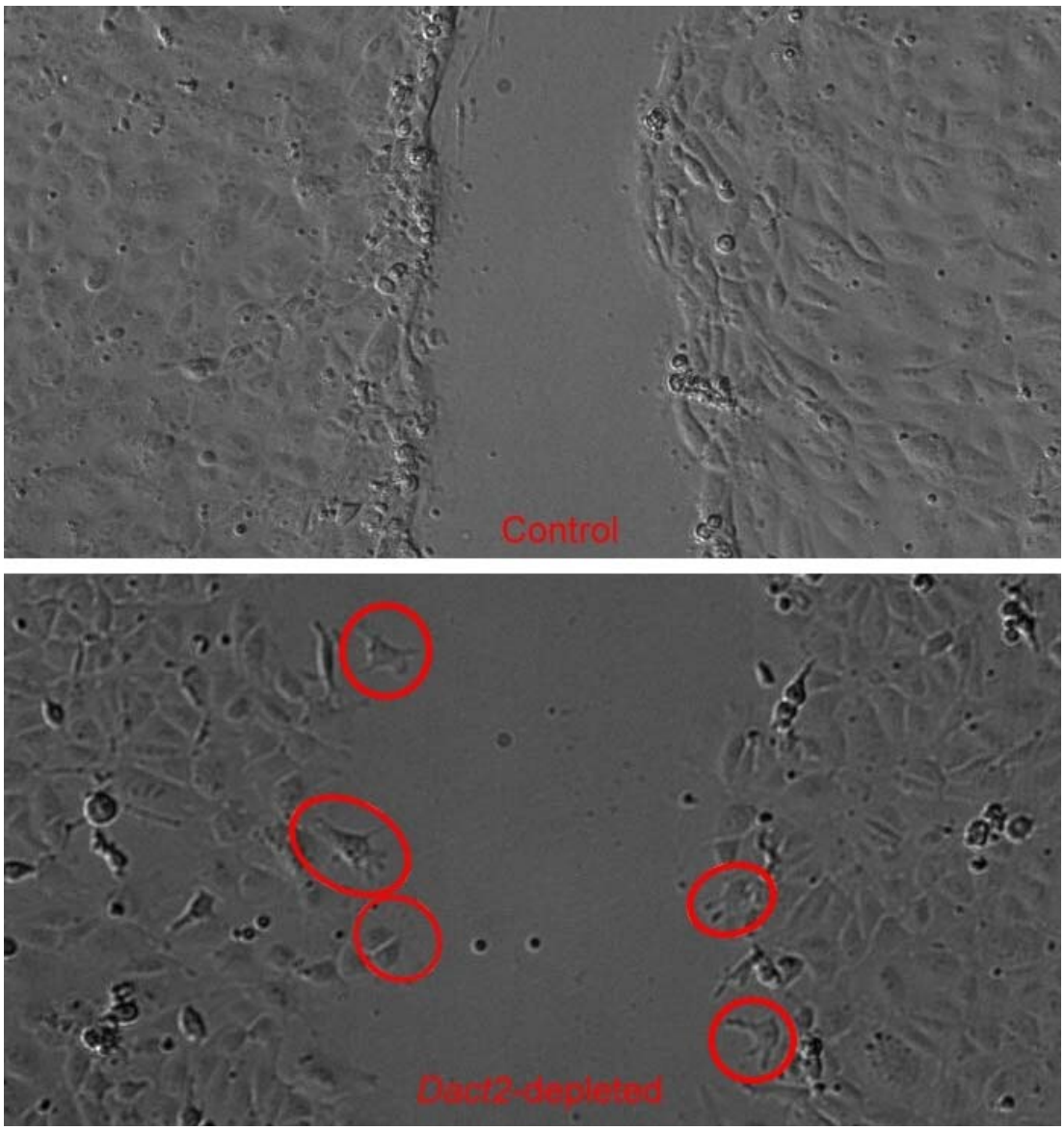

Figure 7-8 Amoeboid movements in *Dact2*-depleted cells. In wound healing assays, amoeboid migration movements were noted in both clones of *Dact2*-depleted cells but not in control cells (upper panel). Red circles in lower panel (clone P4 cells) highlight some individual cells showing amoeboid movements. This amoeboid migration movement is better demonstrated in the AVI movies in the attached CD.

In some epithelial cells, for example human corneal epithelial cells, scratching a wound induces cell proliferation and migration of the surrounding intact cells, which finally closes the wound (Yin et al., 2007). However, in the well-researched MDCK wound healing model, cell proliferation does not contribute to the healing of the wound (Fenteany et al., 2000; Sponsel et al., 1994). To examine whether disruption in cell proliferation contributes to the delayed closure of the wound in *Dact2*-

depleted mIMCD-3 cells, I performed a BrdU incorporation assay in both control and *Dact2*-depleted cells four hours after scratching the wound. Low power images (Figure 7-9 a,b,c) were to illustrate the distribution of BrdU-labelled cells across the wound. High power images, clearly showing the BrdU-labelled pink nuclei and the unlabelled blue nuclei, were taken for cell counting. The calculated proliferation rate was plotted in panel (d). Figure 7-9 showed that both control and clone P4 cells had similar proliferation rate but clone P1 cells seemed to show an increased proliferation rate. However, this difference in proliferation rate was not statistically significant as examined by one-way ANOVA ($p=0.149$). Therefore, in response to wounding, *Dact2* knockdown impeded mIMCD-3 cells migration, probably by changing the migration mode, without affecting cell proliferation.

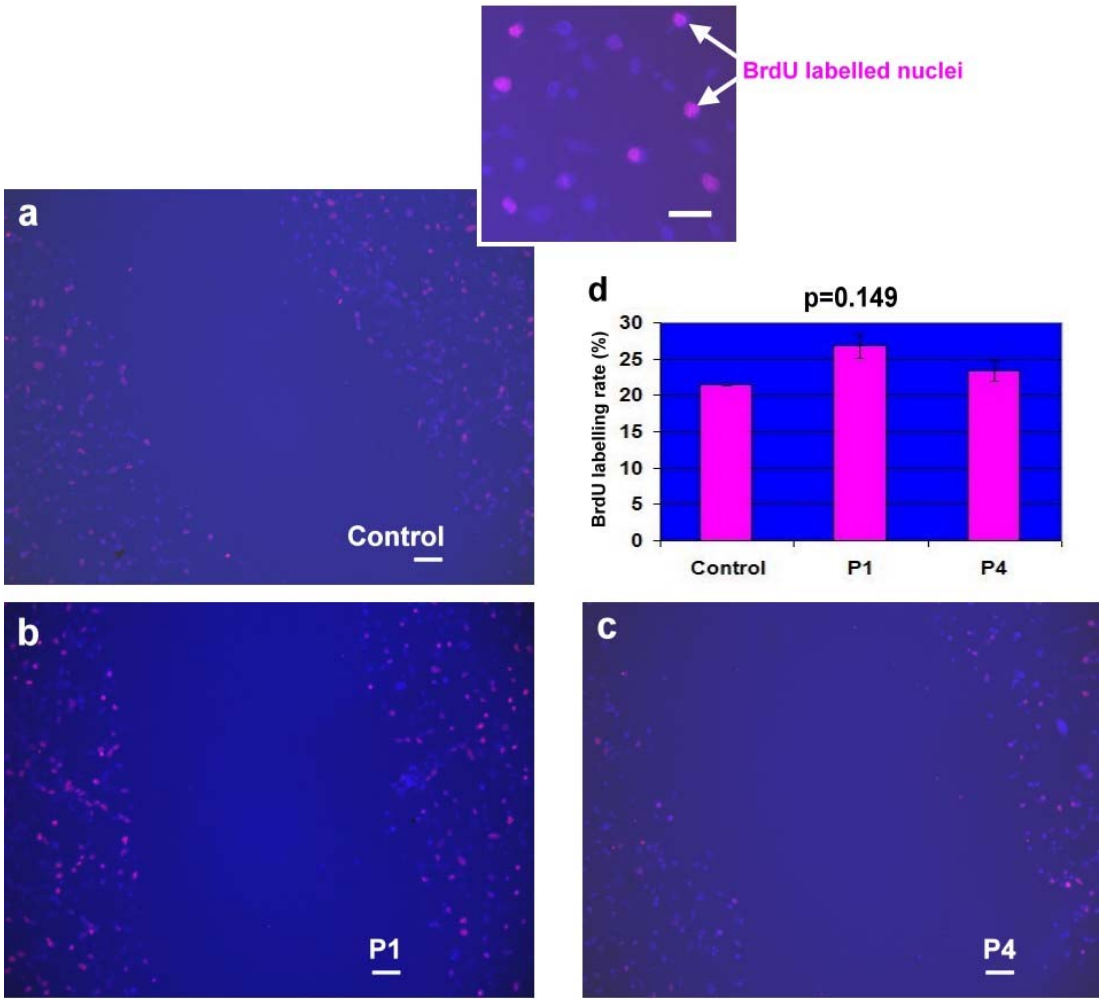

Figure 7-9 Proliferation does not affect the rate of wound closure. A BrdU incorporation assay was performed four hours after wounding in control (a), clone P1 (b) and clone P4 (c) cells. BrdU labelled cells showed pink nuclei (arrows) while unlabelled cells were counterstained by TO-PRO-3 (blue). Inset is to show more clearly the pink and blue nuclei. BrdU labelling rate was calculated and is plotted in panel (d). Control and clone P4 cells showed similar proliferation rates. Clone P1 seemed to exhibit a higher proliferation rate but the difference in the proliferation rate was not statistically significant (p=0.149 in one-way ANOVA). Scale bar = 50µm in a,b,c; 25µm in the inset.

7.3.4 *Dact2* knockdown cells form more jagged cysts in 3D collagen matrices

Based on the *Dact2* knockdown phenotypes in collective cell migration as demonstrated by a wound healing model, one step further towards understanding the function of *Dact2* in kidney development was to grow these cells in the 3D collagen matrix tubulogenesis model. When cultured in 3D collagen I gel, mIMCD-3 cells are

expected to form cysts during the first few days. These cysts are induced to generate branching tubules in the presence of HGF (Cantley et al., 1994). When I grew control and *Dact2* knockdown mIMCD-3 cells, their morphology was inspected daily by using a microscope. In the presence of HGF, cysts and branching tubules were all found in control, P1 and P4 cells because these cells were not synchronised when seeding. However, there seemed to be a subtle difference between control and *Dact2*-depleted cells. Most of the cysts formed by control cells showed round and smooth edges and were therefore termed as 'round cysts'. However, most cysts found in either P1or P4 cells exhibited uneven edges and were called as 'jagged cysts'. Forty cysts were picked randomly and counted in each clone of cells and the percentage of jagged cysts was calculated and plotted in Figure 7-10. When counting the cysts, the labels of the cells were masked so that the counting was done blind. In untransfected cells and cells expressing NC plasmid, jagged cysts accounted for only ~30% of the total cysts whilst in *Dact2*-depleted cells, the percentage of jagged cysts reached ~60%. This experiment was done only once due to the time available in my PhD project. The preliminary observation needs to be verified by repeating the 3D collagen gel culture and obtaining enough data for statistical analysis.

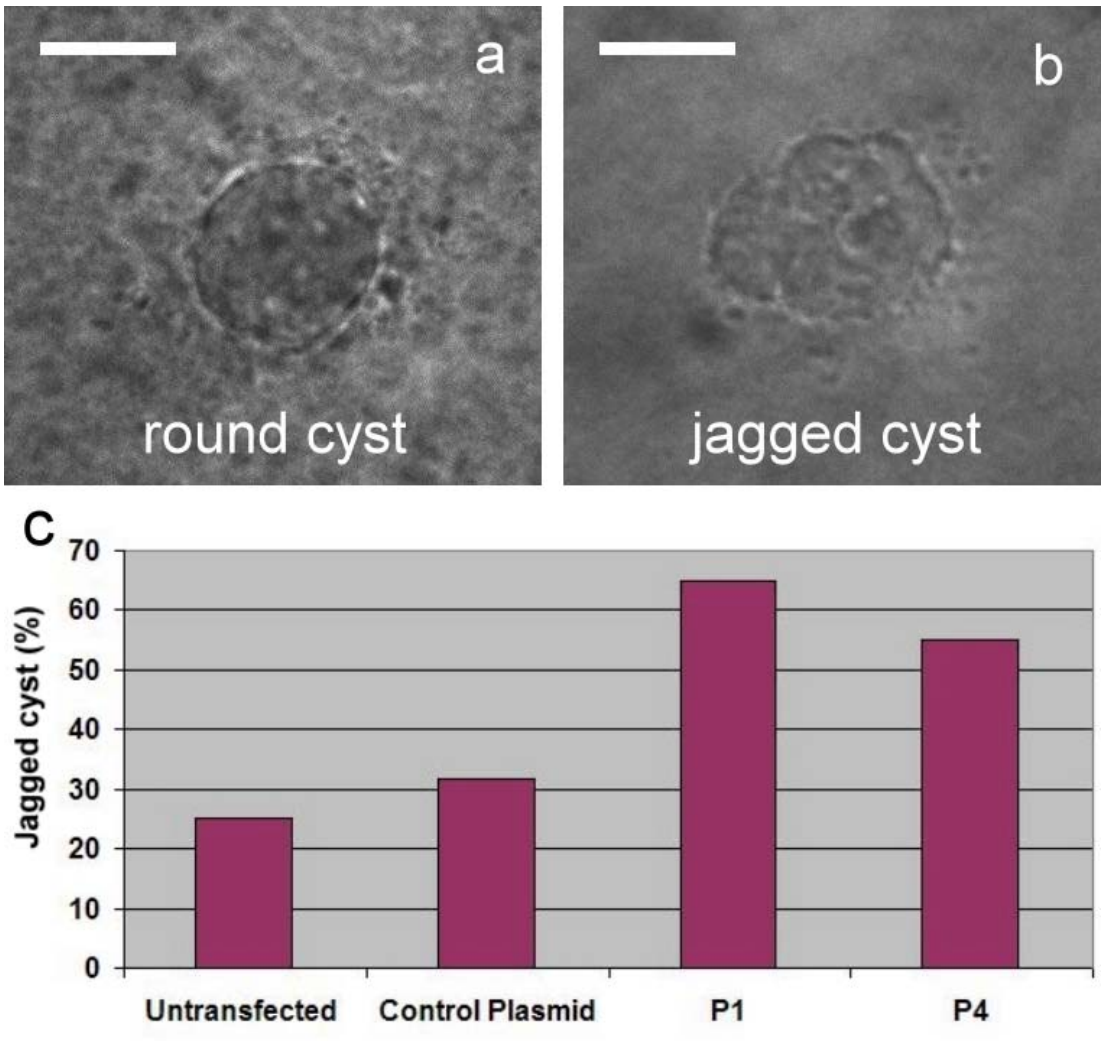

Figure 7-10 Cysts formed by mIMCD-3 cells in 3D collagen I matrices. Phase contrast photomicrographs showed a 'round cyst' (a) whose edge was smooth and a 'jagged cyst' (b) with its uneven contour. Both cysts could be found in control and *Dact2* knockdown cells. The percentage of the jagged cysts for each clone of mIMCD-3 cells is shown in panel (c). *Dact2* knockdown cells seemed to exhibit double amount of the jagged cysts. Scale bar = 20μm.

7.4 Discussion

7.4.1 A promising RNAi tool made to investigate branching morphogenesis

The stable mIMCD-3 cell lines expressing *Dact2* shRNA were promising tools to investigate *Dact2* functions in cell culture based models. They offered satisfactory *Dact2* knockdown efficiency (Figure 7-5) and were able to overcome problems encountered by siRNA-mediated RNAi such as low transfection efficiency in hard-to-transfect cell lines and the longevity of the silenced state. The longevity of the silenced state is critical when growing these cells in 3D matrices to investigate branching morphogenesis. The phenotypes of aberrant cell migration and increased jagged cyst formation were seen in both clones studied, though the latter was a preliminary observation. These different clones expressing distinct sequences of *Dact2* shRNA (P1 and P4) served as the multiplicity controls to confirm that these phenotypes were specific to *Dact2* depletion because it is barely possible for different shRNAs to cause the same off-target effects (Jackson et al., 2003). Similar strategies to look at epithelial morphogenesis have recently been reported in mIMCD-3 cells (Mai et al., 2005) and MDCK cells (Aijaz et al., 2007; Kim et al., 2007a). Mai *et al.* made stable mIMCD-3 cell lines expressing *Pkhd1* shRNA and showed that these cells exhibited impaired tubulogenesis in 3D culture. They then turned to 2D culture assays, including wound healing assay, to further investigate the possible mechanisms underlying the impaired tubulogenesis (Mai et al., 2005).

Two strategies in designing the constructs that may provide additional insights into this system include co-expression of reporter genes such as GFP or luciferase and the inducible expression of RNAi effectors like tetracycline-inducible promoter system (Gossen et al., 1995). The former allows tracking of the transfected cells and illustrating the transfection efficiency. The latter provides a major advantage to reverse the knockdown of the gene though may cause some level of leakiness, which may result in significant gene repression in the absence of induction (Lin et al., 2004).

7.4.2 *Dact2* and known molecules modulating collective cell migration

Dact2-depletion resulted in uncoordinated cell migration and amoeboid migration behaviour of individual cells (Figure 7-6, 7-8 and AVI movies in the attached CD) but the mechanisms are yet to be investigated. Clues may lie in the well-characterised wound healing model using another kidney-derived epithelial cell line, MDCK cells. (Fenteany et al., 2000). Following scratch wounding of MDCK epithelial cell monolayers, cells move in to close the gap as a continuous sheet while strictly maintaining cell–cell junctions. This wound closure is driven by cell migration, with active protrusive crawling in multiple rows of cells from the wound margin (Farooqui and Fenteany, 2005), rather than by purse-string contraction or cell proliferation (Fenteany et al., 2000; Sponsel et al., 1994). MDCK cell sheet migration depends on Rac and phosphoinositides (Fenteany et al., 2000), GSK3 (Farooqui et al., 2006), ADP-ribosylation factor 6 (ARF6) (Santy and Casanova, 2001), c-Jun-N-terminal kinase (Altan and Fenteany, 2004) and Raf kinase inhibitor protein (Zhu et al., 2005). Many of these molecules directly or indirectly affect actin filament reorganization, assembly and disassembly and thus affect the generation of the driving force of wound closure (Farooqui et al., 2006; Friedl and Wolf, 2003). Therefore, the future plans to investigate the mechanisms by which *Dact2* modulates collective cell migration in mIMCD-3 cells may include the examination of actin organisation and dynamics in *Dact2*-depleted cells and the interaction between *Dact2* and known molecules described in MDCK wound healing models.

Immediately before this thesis was compiled, a project student in this lab found impaired formation of perimarginal actin bundles only in those *Dact2*-depleted mIMCD-3 cells I made, but not in control cells (Ekiert, personal communication). In MDCK wound healing models, the formation of this perimarginal actin bundle depends on Rho activity (Fenteany et al., 2000). Hence, the encouraging finding of impaired actin bundle formation in *Dact2*-depleted cells suggests that research into the regulation between *Dact2* and Rho activity will be promising.

In addition to the force generation, the amoeboid migration observed in *Dact2*-depleted cells was reminiscent of migration of leukocytes and some tumour cells (Farina et al., 1998; Friedl et al., 2001). These cells show weakened adhesiveness for ECM due to their deregulated integrin expression (Jaspars et al., 1996; Kraus et al., 2002; Rintoul and Sethi, 2001). Hence the adhesion molecules including integrins in these *Dact2*-depleted mIMCD-3 cells also need to be examined. More importantly, a novel mechanism of cancer cell migration is described as collective amoeboid transition (CAT). Hegerfeldt *et al.* showed that in multicellular clusters that emanate from primary melanoma explants, anti-β1 integrin antibodies induce not only the loss of collective movement, but also the dissemination of individual cells that adopt β1-integrin-independent amoeboid migration (Hegerfeldt et al., 2002). As *Dact2* depletion was able to change the collective mIMCD-3 epithelial sheets into amoeboid cellular movements, *Dact2* might play a role in tumourigenesis and invasiveness. It is therefore critical to work out the mechanisms by which *Dact2* governs CAT.

7.4.3 From amoeboid movement to the formation of jagged cysts

In 3D culture, a single cell can proliferate and its clone will eventually form a hollow sphere that is lined by a monolayer of polarised epithelial cells. This structure, referred to as a cyst, can be induced to generate branching tubules by growth factors such as HGF (Cantley et al., 1994; Wang et al., 1990). Both cysts and tubules may represent the basic building blocks for the formation of more complex epithelial organs. Each cell in a well-developed cyst are polarised and have three types of cell surface domain: an apical surface domain that borders the lumen; a basal surface domain that attach to the ECM and a lateral surface domain that adheres to neighbouring cells. To form such an organised structure, cells need to proliferate, migrate and differentiate following an intrinsic mechanism that can precisely coordinate their individual behaviour. During the process of the cyst formation, cells often lack one or more surface domains. Cells lacking a lateral surface domain divide to generate a neighbour; cells lacking an apical surface domain create apical lumens; cells lacking a basal surface domain die. These cells differentiate further to attain

three types of surface domain and finally form a cyst with the apical surface facing the lumen (Lin et al., 1999; O'Brien et al., 2002). Disruptions in molecules modulating the arrangement of these three surface domains result in abnormal cyst formation. For example, O'Brien *et al.* showed that dominant negative Rac1 causes inverted apical polarity of the MDCK cells and thus forms cell arregates without lumens (O'Brien et al., 2001).

The underlying mechanisms for the *Dact2*-mediated jagged cyst formation are yet to be elucidated. The three surfaces rule in the generation of cysts (O'Brien et al., 2002) seems to offer some implications. Aijaz *et al.* showed that depletion of *Apg-2* in MDCK cells causes irregular cysts by retarding the recruitment of the junctional protein ZO-1, which affects the lateral surface of polarised epithelial cells in cysts (Aijaz et al., 2007). Following this three surfaces rule and taking into account my results of the wound healing assay seemed to offer implications on the possible mechanisms of the jagged cyst formation. The amoeboid migration observed in *Dact2*-depleted cells indicated potential errors in integrins, which are key factors defining the basal surfaces of the polarised epithelial cells (Zegers et al., 2003). Besides, *Dact2*-depleted cells showed impaired organisation of acitn (Ekiert, personal communication), which locates at the apical surfaces of polarised epithelial cells in a normal cyst (O'Brien et al., 2001; Verkoelen et al., 2000). Finally, the uncoordinated migration seen in a *Dact2*-depleted cell collective might reflect errors in the microfilament networks which connect cell-cell junctions. The reduced tension between cells might therefore cause the cells of the cyst to spread out when growing in 3D matrices. Staining of markers for each surface domain of epithelial cells in cysts, for example, gp135 for apical surface, ZO-1 for lateral surface and type IV collagen for the basal surface (Wang et al., 1990), will help to delineate the underlying mechanisms for the jagged cyst formation in the *Dact2*-depleted cells.

Notably, however, jagged cysts seemed to account for ~30% of the total cysts in both the wild type mIMCD-3 cells and the cells transfected with control plasmids. The presence of jagged cysts in wild type cells might indicate that jagged cyst was a stage prior to the round cyst stage in the development of tubules. *Dact2*-depleted cells

formed more jagged cysts (~60%) and might thus show delayed tubulogenesis. Analysis of the jagged cysts from both control and *Dact2*-depleted cells by polarisation markers may offer more insights. If the staining of the polarisation markers shows significant differences in these morphologically similar jagged cysts derived from control and *Dact2*-depleted cells, it indicates that *Dact2* modulates the polarisation of the normal cysts. If the analysis proves jagged cysts are the same in both control and *Dact2*-depleted cells, it implies that *Dact2* depletion causes delayed round cyst formation via mechanisms other than polarisation. In either case, *Dact2* depletion may result in more jagged cysts and thus delays tubulogenesis.

A major limitation of these experiments comes from the origin of the mIMCD-3 cells. Because these cells are derived from adult but not embryonic kidneys, the results obtained from this model system might not be very authentic when applied to the very complex processes in kidney morphogenesis. Embryonic kidney cell lines have been developed (Barasch et al., 1996; Sakurai et al., 1997a). These cell lines may be more suitable in this model system for shedding light on kidney development. Although the exact mechanism leading to the pronounced increase in the jagged cyst formation seen in *Dact2*-depleted cells remains to be elucidated, the results that I have shown in this chapter will help contribute to a better understanding of the processes involved in branching morphogenesis as well as the functions of *Dact2*.

Chapter 8

Conclusions

8.1 Experimental conclusions

Mammalian kidney development is controlled by a complex molecular network. In this thesis, I have presented two genes, *Dact1* and *Dact2*, in this network. I confirmed their expression in developing kidneys, described their temporospatial expression patterns and investigated their functions in various model systems for kidney development. All the results were previously unreported. The experimental conclusions are described below.

8.1.1 *Dact1* and *Dact2* have distinct expression profiles in the developing kidneys

Using quantitative real time PCR, I have shown that *Dact1* and *Dact2* exhibit distinct temporal expression profiles from embryonic to postnatal kidneys. *Dact1* was detected in kidneys at all embryonic stages tested (e.g. from E11.5 to E17.5) and was expressed at a very low level in adult kidneys. Among the embryonic stages I analysed, the level of *Dact2* in kidneys increased from E11.5, peaked at E17.5 and reduced postnatally. In adult kidneys, the *Dact2* expression level is comparable to that at E14.5. In addition to the different time-frame of expression, *Dact1* and *Dact2* showed a distinctive spatial pattern of expression in kidneys.

By using RNA *in situ* hybridisation, I have shown that *Dact1* was expressed by the metanephric mesenchyme. In kidneys at later developmental stages when renal stroma developed, *Dact1* was expressed predominantly by the medullary stroma. Many of the stromal cells die via apoptosis by birth (Coles et al., 1993). This is probably the reason that *Dact1* was hard to detect in adult kidneys by *in situ* hybridisation. The very low level of *Dact1* expression in adult kidneys was confirmed by quantitative real time PCR. The paralogous gene *Dact2* was expressed exclusively by the ureteric buds of the kidneys throughout the developmental stages. The distinct expression patterns of *Dact1* and *Dact2* suggest different functional roles in the kidney development.

8.1.2 *Dact1* negatively regulates cell proliferation and UB branching

To discover the functions of *Dact1* in kidney development, I used a siRNA approach to knockdown *Dact1* in a cell culture system. While verifying *Dact1* siRNA in conventional 2D cell cultures, I found differences in the growth rates between *Dact1* siRNA-treated and control groups of cells. In cells in which *Dact1* was knocked down, there was an increase in cell number and cell proliferation index. I therefore hypothesised that *Dact1* negatively regulated cell proliferation, designed sets of experiments to test this hypothesis and confirmed it.

Next, I moved from using a 2D cell culture to use a kidney organ culture which is more physiologically relevant than the 2D cell culture system. I found that knocking *Dact1* down by siRNA-mediated RNAi in kidney organ culture seemed to stimulate UB branching although the transfection efficiency was not very satisfactory. It is common for researchers to encounter difficulties when trying to deliver siRNAs into cultured kidneys using chemical-based delivery vehicles (e.g. siLentFect or Lipofectamine) (Vanio, personal communication). The problem of efficient delivery of RNAi effectors into kidneys growing in culture needs to be overcome. If a more satisfactory delivery efficiency can be achieved, I would like to test whether this increase in UB branching is indeed a phenotype caused by the depletion of *Dact1* in the kidneys. Caution has to be applied when drawing conclusions about the function of a gene based on analysing siRNA phenotypes. The conclusion would be stronger if the same phenotype (*i.e.* increased UB branching) were also observed when cultured kidneys were transfected by several individual *Dact1* siRNAs targeting different regions of *Dact1*. In addition, performing cell proliferation assays in the kidney organ culture which has been transfected with *Dact1* siRNA will help answer whether *Dact1* regulates UB branching by increased cell proliferation. This work will fill the gap between the cellular phenotype and kidney phenotype observed.

8.1.3 *Dact2* is required for renal epithelial sheet migration

By using stable mIMCD-3 cell lines, I have shown that *Dact2* is required for renal epithelial sheet migration. Cells lacking *Dact2* showed slow and amoeboid movements. This phenotype was confirmed by different clone of cells expressing shRNA targeting distinct *Dact2* sequences. Our preliminary observation of impaired formation of actin bundles in *Dact2*-depleted cells supported the observed cellular phenotype in the wound assay and opened the way to new research into the interplay between Dact2 and cytoskeletal systems. Additionally, the amoeboid movements seen in *Dact2*-depleted cells indicated errors in cell-cell and/or cell-matrix interaction. Both cell-cell and cell-matrix interactions are important factors for a normal round cyst formation. Therefore, the amoeboid movement seemed to support the interesting observation in the 3D gel tubulogenesis model where *Dact2* knockdown favoured the formation of jagged cysts. This observation need to be tested by repeating the experiments to obtain enough samples for statistics. This preliminary observation supported the idea that *Dact2* acts as an intrinsic factor to control branching morphogenesis.

8.1.4 *Dact* genes and kidney development

Mouse kidney development starts from the reciprocal induction between the metanephric mesenchyme and the ureteric buds. It was very interesting to study both *Dact* genes in one project because *Dact1* and *Dact2* happen to be expressed by each of the components of the developing kidneys. Understanding each of these *Dact* genes in developing kidneys is like understanding kidney development from two important angles.

Dact1 is expressed in the metanephric mesenchyme during early kidney development (E11.5 and E12.5) and is later detected in the renal stroma (E14.5). So far in the literature, most efforts made to the investigation of MET during kidney development have focused on the metanephrogenic mesenchyme. In my study, the temporospatial expression pattern of *Dact1* highlighted the heterogeneous nature of the metanephric

mesenchyme and the importance of renal stroma in kidney development. By using the siRNA approach to explore the potential functions of *Dact1* in an embryonic mesenchymal cell line, *Dact1* was found to be a negative regulator of cell proliferation. The finding that *Dact1* was expressed in the differentiated medullary stroma in developing kidneys and the results of being a negative regulator in cell culture suggested that *Dact1* might be a proliferation-to-differentiation switch of stromal mesenchyme in the developing kidneys. This feature somehow resembled a transcription factor, *Pbx1*, which is expressed by renal stroma. *Pbx1* deficient kidneys initiate nephrogenesis but exhibit sustained proliferation of the mesenchyme without subsequent differentiation (Schnabel et al., 2003). Notably, however, *Pbx1* regulates signals sending from stroma to control proliferation and differentiation of metanephrogenic mesenchyme whereas *Dact1* might regulate proliferation and differentiation of the stroma itself.

In addition, the discovery of *Dact1* to be a negative regulator of UB branching drew my attention from renal stroma to another compartment (*i.e.* the ureteric buds) of the developing kdineys. Distinct from the plausible link between stromal signals and *Ret* proposed by Batourina *et al.* (Batourina et al., 2001) (also reviewed briefly in section 1.4.4), this finding seemed to offer new insights into the regulatory role of renal stroma in UB branching.

Dact2 was identified as a UB marker and has addressed several intriguing questions on branching morphogenesis. It was not a critical factor for the collecting duct cells to survive but it was quite important for the normal migration movement of an epithelial sheet. Cells lacking *Dact2* seemed to dissociate with their neighbours and attempted to spread out from the epithelial sheet. When growing in 3D gels, *Dact2*-depleted cells seemed to spread out the smooth edges that they ought to form resulting in more jagged cysts observed. These results did demonstrate the biological functions of *Dact2* in collecting duct cells and also shed light on potential roles of *Dact2* in branching morphogenesis of kidneys. I might expect to see abnormal branching patterns of ureteric buds in kidneys where *Dact2* has been depleted.

8.2 Future perspectives

Although this thesis has addressed two main questions regarding the expressions and functions of both *Dact* genes in cell and kidney organ culture systems, inevitably many questions still remain. Some of the questions have already been discussed in each result chapter. However, many avenues remain to be explored. They are discussed below.

8.2.1 Potential signalling pathways regulated by *Dact1* to control cell proliferation in developing kidneys

Many signalling pathways, such as WNT, TGFβ, EGF, and Sonic Hedgehog (Shh), are known to control cell proliferation. To work out the signalling pathway by which DACT1 acts to control cell proliferation in developing kidneys, I would here try to narrow down the candidate pathways based on the literature and the results presented in this thesis. Among the proteins known to control cell proliferation in developing kidneys (as summarised in Table 1-1), the β-catenin downstream gene *N-myc* is proved to control metanephric mesenchymal cell proliferation (Bates et al., 2000). Like *Dact1*, *N-myc* is expressed by the metanephric mesenchyme (Shimono et al., 1999). DACT1 has been shown to directly bind to DVL (Cheyette et al., 2002) and has been implicated in WNT/β-catenin pathway in various developmental contexts as discussed. Therefore, it will be interesting to investigate whether DACT1 binds to DVL and acts as an antagonist of β-catenin leading to the repression of *N-myc*-modulated cell proliferation in the metanephric mesenchyme (Figure 8-1). This postulated pathway indicated that DACT1 regulates the size of the mesenchymal cell population. Experiments including BrdU incorporation assay and *N-myc* expression in *Dact1*-depleted kidney organ culture are required to test this hypothesis.

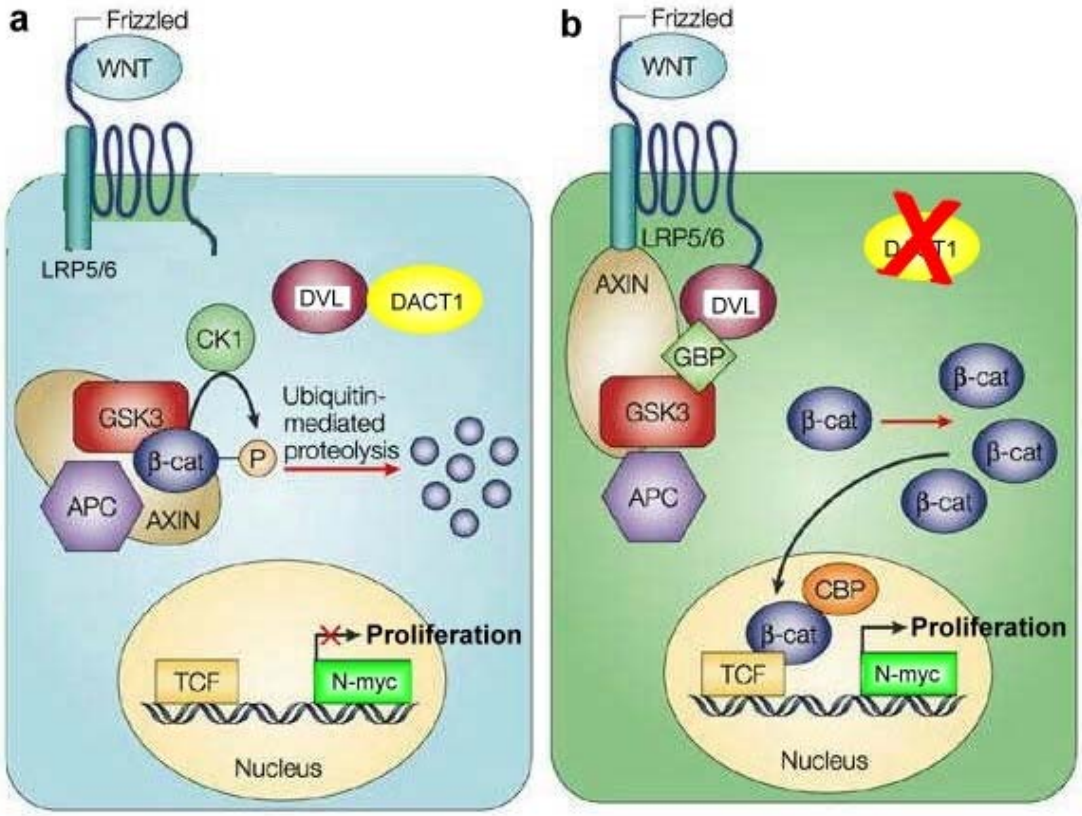

Figure 8-1 Proposed pathway for DACT1 in WNT/β-catenin/N-myc-mediated cell proliferation. In (a), DACT1 binds to DVL so that β-catenin is degraded by the destruction complex. The downstream gene N-myc is inactivated and the cell stops to proliferate. When DACT1 is depleted (b), DVL binds to the destruction complex in response to WNT signaling. β-catenin is stabilised and translocated into the nucleus to activate N-myc driving the cell to proliferate (Modified from Moon et al., 2004).

Interestingly, the pattern of the canonical WNT/β-catenin signalling activity seems to support the idea that DACT1 is a negative regulator of β-catenin in developing kidneys. By using β-catenin-responsive TCF/βGal reporter transgenic mice, Iglesias *et al.* demonstrated that intense canonical WNT signalling was evident in epithelia of the branching UB and in nephrogenic mesenchyme during its transition into renal tubules. Antibodies against active (nonphosphorylated) β-catenin were used to confirm that the transgene expression reflects endogenous canonical WNT/β-catenin signalling activity. As kidney development proceeds, the TCF signal is found only in the nephrogenic zone (Iglesias et al., 2007). The areas showing TCF signal are zones where cells undergo extensive proliferation. From my results, hardly any *Dact1* was expressed in these areas. On the contrary, in the medullary stroma, where cells do not

undergo much proliferation, cells express high levels of *Dact1* but exhibit undetectable canonical WNT/β-catenin signalling activity. Other factors known to control cell proliferation in many compartments of the developing kidneys (*i.e.* IGF I/II, RA, Glypican-3 as summarised in Table 1-1) might exert their effects by repressing DACT1 activity in developing kidneys. To examine this hypothesis, it will be desirable to use embryonic mesenchymal cell culture systems where no indirect effect from other compartment of developing kidneys can be found.

8.2.2 Functional roles of *Dact1* in the development of renal stroma

While I have already shown that *Dact1* was expressed by the medullary stroma at E14.5 (Figure 3-9) and have explored its functions in branching morphogenesis and nephrogenesis, the question on its role in the development of renal stroma remains. Finding the function of a gene in the development of renal stroma, which is less understood than the metanephrogenic mesenchyme and the ureteric buds, will be a new research area worthy of exploring.

The better characterised stromal marker, *Foxd1*, seems to be a promising target to investigate. *Foxd1* is strongly expressed in the nephrogenic zone whereas *Dact1* is expressed in the medullary stroma. Implicated from the complementary expression pattern of *Foxd1* and *Dact1*, it will be interesting to find out whether these two genes counteract each other to specify the fate of the mesenchymal cells. Mesenchymal cells that express high levels of *Foxd1* and low levels of *Dact1* might have the features of stromal progenitors and locate in the nephrogenic zone. On the other hand, mesenchymal cells that express high levels of *Dact1* and low levels of *Foxd1* might become differentiated medullary stroma cells. Using *Dact1* siRNA to silence *Dact1* at early stage kidneys growing in culture might therefore change the boundary between the nephrogenic and medullary zones. *Dact1* silencing might result in more mesenchymal cells expressing low levels of *Dact1* while maintaining high levels of *Foxd1* and eventually lead to a wider nephrogenic zone (Figure 8-2). This model can also be tested by generating *Dact1* mutant mice and comparing the width of the nephrogenic zone in mutant and wild type kidneys. Additionally, the *Dact1* mutant

mice are very likely to offer great understanding of the functional roles of *Dact1* in UB branching and nephrogenesis.

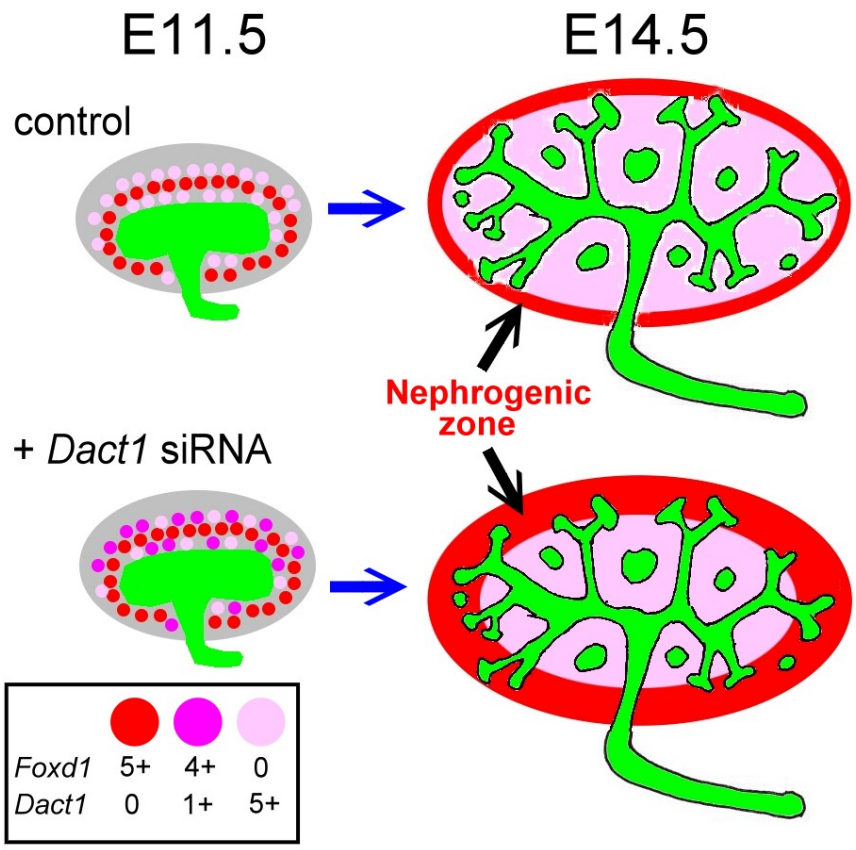

Figure 8-2 Proposed model for the interaction between *Foxd1* and *Dact1*. At E11.5, a group of mesenchymal cells express high levels of *Foxd1* (red ball) and another group of mesenchymal cells express high levels of *Dact1* (pale pink ball). When kidneys cultured in the presence of *Dact1* siRNA, *Dact1* is knocked down and *Foxd1* might be turned on (magenta ball). This eventually leads to a wider nephrogenic zone. The value and '+' are simply to indicate the possible relative expression levels of both genes.

Another interesting question is whether *Dact1* is involved in the retinoid-mediated stromal differentiation. Retinoids have been shown to modulate embryonic differentiation and cell identity determination (Means and Gudas, 1995). They are also involved in epithelial differentiation in mammalian developing kidneys (Gilbert, 2002; Moreau et al., 1998). In chapter 3 and 4, I have shown that *Dact1* was normally expressed by the differentiated medullary stroma (Figure 3-9) and this

expression pattern was further enhanced by the exogenous ATRA in organ culture (Figure 4-1 and 4-2), it might be possible that ATRA upregulate the *Dact1* expression in subsets of mesenchymal cells, which in turn differentiate into the medullary stroma. Difficulties in experiments for this hypothesis may lie in the choosing of the appropriate medullary stroma marker. According to the expression patterns, candidate markers may include the transcription factor *Pod1* (Quaggin et al., 1999) and the stromal nidogen extracellular matrix protein *Snep* (Leimeister et al., 2004), though the functions of these molecules in developing kidneys are yet to be characterised. In addition, these stromal markers on their own could be partner proteins that *Dact1* work with to control stromal development. This will also be a new area to be explored.

8.2.3 Can *Dact2* control cell migration through TGFβ signalling pathway?

In this project, I have shown that *Dact2* is required for the collective migration of collecting duct cells (described in details in section 7.3.3). An intriguing question following this result is to identify the intracellular signalling pathway in which *Dact2* is involved in regulating the migration of collecting duct cells. Implications from the MDCK cell wound healing model, including potential proteins with which *Dact2* may work, have been discussed in section 7.4.2. In addition, as DACT2 has been shown to antagonise Nodal activity by promoting the degradation of ALK4 and ALK5 receptors (Zhang et al., 2004), it will be interesting to explore whether *Dact2* controls cell migration through this pathway. TGFβ1 signals through ALK4 (Figure 1-4) and has been shown to inhibit the migration of human proximal tubular cells (Tian and Phillips, 2003). This may suggest a hypothesis that *Dact2* silencing enhances the inhibitory effect of TGFβ1 on the migration of renal epithelial cells. Although *Dact2* has been shown to antagonise Nodal activity in zebrafish, Nodal is not an ideal pathway to investigate until its expression in the developing kidneys is confirmed (as reviewed in section 1.4.3).

8.2.4 Is *Dact2* required for normal branching morphogenesis?

The promising observation that *Dact2*-depleted cells formed more jagged cysts in 3D tubulogenesis model suggested a role for *Dact2* in branching morphogenesis. Analysis of the markers for each surface domain of epithelial cells in cysts will offer valuable information on the function of *Dact2* in this tubulogenesis model (as discussed in the section 7.4.3). Furthermore, TGFβ1 is proved to inhibit UB branching in kidney organ culture (Bush et al., 2004; Ritvos et al., 1995) and is able to inhibit mIMCD-3 cells to branch in the 3D culture system (Sakurai and Nigam, 1997). Complementary to the wound healing assay on the *Dact2* and TGFβ1-ALK4 pathway, it would be sensible to use the 3D tubulogenesis model to test whether *Dact2* silencing increases the cellular sensitivity to TGFβ1 when the branching is being inhibited. Besides, if new methods (discussed in section 6.4.3) can offer better delivery of siRNA into kidney organ culture, experimenters will then be able to look for the embryonic kidney phenotype when *Dact2* is silenced. Alternatively, generation of *Dact2* mutant mice will offer considerable insights into the functional roles of *Dact2* in UB branching and probably in nephrogenesis and stroma development.

8.3 Summary

In summary, this thesis characterised the expression patterns of *Dact1* and *Dact2* in embryonic and postnatal mouse kidneys. The functions of both genes were investigated in various model systems. *Dact1* was expressed by the metanephric mesenchyme followed by the medullary stroma. It acted as a negative regulator of cell proliferation in 2D cell culture. It also seemed to be a negative regulator of UB branching in kidney organ culture but did not affect nephrogenesis. *Dact2* was expressed exclusively by the ureteric buds. It was required for the collective migration of renal epithelial cells. Silencing of *Dact2* seemed to generate more jagged cysts in the 3D tubulogenesis model. More work is required to investigate the underling mechanisms of the phenotypes observed and explore more functional roles they may have in mammalian kidney development.

Now may be the time to review the question list raised in section 1.6. Apparently this thesis answered some of these important questions. The remaining questions on the list and some interesting questions followed this study, which have already been discussed in this thesis, will be the future plans for the investigation of *Dact* genes in mammalian kidney development. I would use Table 8-1 as a summary of this thesis and the future plans.

Table 8-1 Summary of this thesis and the future plans.

1. When, where and how are *Dact* genes expressed in developing kidneys?

Answer: described in chapter 3. ✓

2. What developmental events of kidney development are *Dact* genes involved?

(a) UB induction
(b) UB branching
(c) Nephron induction
(d) Nephron differentiation
(e) Stromal development

Answer: b for *Dact1*; others need to be tested in the future. ✓

3. What cellular events are modulated by *Dact* genes?

(a) proliferation
(b) apoptosis
(c) migration
(d) differentiation

Answer: (a) for *Dact1* and (c) for *Dact2* in this thesis. ✓

4. What are the possible signalling pathways that *Dact* genes are involved in regulating kidney development?

Answer: discussed in chapter 8. ?

Chapter 9

References

Abrahamson, D.R., and Wang, R. (2003) Development of the glomerular capillary and its basement membrane. In: P.D., V., A.S., W., and Bard, J.B. (eds) The Kidney: from normal development to congenital disease. Academic Press, London, pp. 221-249.

Aijaz, S., Sanchez-Heras, E., Balda, M.S., and Matter, K. (2007) Regulation of tight junction assembly and epithelial morphogenesis by the heat shock protein Apg-2. BMC Cell Biol 8:49.

Airaksinen, M.S., Holm, L., and Hatinen, T. (2006) Evolution of the GDNF family ligands and receptors. Brain, behavior and evolution 68:181-190.

Ajioka, I., and Nakajima, K. (2005) Birth-date-dependent segregation of the mouse cerebral cortical neurons in reaggregation cultures. The European journal of neuroscience 22:331-342.

Altan, Z.M., and Fenteany, G. (2004) c-Jun N-terminal kinase regulates lamellipodial protrusion and cell sheet migration during epithelial wound closure by a gene expression-independent mechanism. Biochemical and biophysical research communications 322:56-67.

Amarzguioui, M., Rossi, J.J., and Kim, D. (2005) Approaches for chemically synthesized siRNA and vector-mediated RNAi. FEBS letters 579:5974-5981.

Andrews, K.L., Betsuyaku, T., Rogers, S., Shipley, J.M., Senior, R.M., and Miner, J.H. (2000) Gelatinase B (MMP-9) is not essential in the normal kidney and does not influence progression of renal disease in a mouse model of Alport syndrome. The American journal of pathology 157:303-311.

Anonymous (2003) Whither RNAi? Nature cell biology 5:489-490.

Araki, T., Hayashi, M., and Saruta, T. (2003) Cloning and characterization of a novel gene promoting ureteric bud branching in the metanephros. Kidney international 64:1968-1977.

Arar, M., Xu, Y.C., Elshihabi, I., Barnes, J.L., Choudhury, G.G., and Abboud, H.E. (2000) Platelet-derived growth factor receptor beta regulates migration and DNA synthesis in metanephric mesenchymal cells. J Biol Chem 275:9527-9533.

Barasch, J., Pressler, L., Connor, J., and Malik, A. (1996) A ureteric bud cell line induces nephrogenesis in two steps by two distinct signals. The American journal of physiology 271:F50-61.

Barasch, J., Qiao, J., McWilliams, G., Chen, D., Oliver, J.A., and Herzlinger, D. (1997) Ureteric bud cells secrete multiple factors, including bFGF, which rescue renal progenitors from apoptosis. The American journal of physiology 273:F757-767.

Barasch, J., Yang, J., Ware, C.B., Taga, T., Yoshida, K., Erdjument-Bromage, H., Tempst, P., Parravicini, E., Malach, S., Aranoff, T., and Oliver, J.A. (1999) Mesenchymal to epithelial conversion in rat metanephros is induced by LIF. Cell 99:377-386.

Bard, J.B. (2002) Growth and death in the developing mammalian kidney: signals, receptors and conversations. Bioessays 24:72-82.

Bard, J.B. (2003) The metanephros. In: Vize, P.D., Woolf, A.S., and Bard, J.B. (eds) The Kidney, from normal development to congenital disease. Academic Press, London, pp. 139-148.

Barros, E.J., Santos, O.F., Matsumoto, K., Nakamura, T., and Nigam, S.K. (1995) Differential tubulogenic and branching morphogenetic activities of growth factors: implications for epithelial tissue development. Proceedings of the National Academy of Sciences of the United States of America 92:4412-4416.

Bates, C.M., Kharzai, S., Erwin, T., Rossant, J., and Parada, L.F. (2000) Role of N-myc in the developing mouse kidney. Dev Biol 222:317-325.

Batourina, E., Gim, S., Bello, N., Shy, M., Clagett-Dame, M., Srinivas, S., Costantini, F., and Mendelsohn, C. (2001) Vitamin A controls epithelial/mesenchymal interactions through Ret expression. Nature genetics 27:74-78.

Bayle, J., Fitch, J., Jacobsen, K., Kumar, R., Lafyatis, R., and Lemaire, R. (2007) Increased Expression of Wnt2 and SFRP4 in Tsk Mouse Skin: Role of Wnt Signaling in Altered Dermal Fibrillin Deposition and Systemic Sclerosis. J Invest Dermatol.

Boivin, G.P., O'Toole, B.A., Orsmby, I.E., Diebold, R.J., Eis, M.J., Doetschman, T., and Kier, A.B. (1995) Onset and progression of pathological lesions in transforming growth factor-beta 1-deficient mice. The American journal of pathology 146:276-288.

Boutros, M., and Mlodzik, M. (1999) Dishevelled: at the crossroads of divergent intracellular signaling pathways. Mechanisms of development 83:27-37.

Brophy, P.D., Ostrom, L., Lang, K.M., and Dressler, G.R. (2001) Regulation of ureteric bud outgrowth by Pax2-dependent activation of the glial derived neurotrophic factor gene. Development (Cambridge, England) 128:4747-4756.

Bush, K.T., Sakurai, H., Steer, D.L., Leonard, M.O., Sampogna, R.V., Meyer, T.N., Schwesinger, C., Qiao, J., and Nigam, S.K. (2004) TGF-beta superfamily members modulate growth, branching, shaping, and patterning of the ureteric bud. Dev Biol 266:285-298.

Cacalano, G., Farinas, I., Wang, L.C., Hagler, K., Forgie, A., Moore, M., Armanini, M., Phillips, H., Ryan, A.M., Reichardt, L.F., Hynes, M., Davies, A., and Rosenthal, A. (1998) GFRalpha1 is an essential receptor component for GDNF in the developing nervous system and kidney. Neuron 21:53-62.

Cammas, L., Romand, R., Fraulob, V., Mura, C., and Dolle, P. (2007) Expression of the murine retinol dehydrogenase 10 (Rdh10) gene correlates with many sites of retinoid signalling during embryogenesis and organ differentiation. Dev Dyn 236:2899-2908.

Cano-Gauci, D.F., Song, H.H., Yang, H., McKerlie, C., Choo, B., Shi, W., Pullano, R., Piscione, T.D., Grisaru, S., Soon, S., Sedlackova, L., Tanswell, A.K., Mak, T.W., Yeger, H., Lockwood, G.A., Rosenblum, N.D., and Filmus, J. (1999) Glypican-3-deficient mice exhibit developmental overgrowth and some of the abnormalities typical of Simpson-Golabi-Behmel syndrome. The Journal of cell biology 146:255-264.

Cantley, L.G., Barros, E.J., Gandhi, M., Rauchman, M., and Nigam, S.K. (1994) Regulation of mitogenesis, motogenesis, and tubulogenesis by hepatocyte growth factor in renal collecting duct cells. The American journal of physiology 267:F271-280.

Carroll, T.J., Park, J.S., Hayashi, S., Majumdar, A., and McMahon, A.P. (2005) Wnt9b plays a central role in the regulation of mesenchymal to epithelial transitions underlying organogenesis of the mammalian urogenital system. Dev Cell 9:283-292.

Cebrian, C., Borodo, K., Charles, N., and Herzlinger, D.A. (2004) Morphometric index of the developing murine kidney. Dev Dyn 231:601-608.

Chen, L., and Al-Awqati, Q. (2005) Segmental expression of Notch and Hairy genes in nephrogenesis. American journal of physiology 288:F939-952.

Cheng, H.T., Kim, M., Valerius, M.T., Surendran, K., Schuster-Gossler, K., Gossler, A., McMahon, A.P., and Kopan, R. (2007) Notch2, but not Notch1, is required for proximal fate acquisition in the mammalian nephron. Development 134:801-811.

Cheyette, B.N., Waxman, J.S., Miller, J.R., Takemaru, K., Sheldahl, L.C., Khlebtsova, N., Fox, E.P., Earnest, T., and Moon, R.T. (2002) Dapper, a Dishevelled-associated antagonist of beta-catenin and JNK signaling, is required for notochord formation. Dev Cell 2:449-461.

Cho, E.A., and Dressler, G.R. (2003) Formation and development of nephrons. In: P.D., V., A.S., W., and Bard, J.B. (eds) The Kidney: from normal development to congenital disease. Academic Press, London, pp. 195-210.

Cho, E.A., Patterson, L.T., Brookhiser, W.T., Mah, S., Kintner, C., and Dressler, G.R. (1998) Differential expression and function of cadherin-6 during renal epithelium development. Development 125:803-812.

Christiansen, J.H., Dennis, C.L., Wicking, C.A., Monkley, S.J., Wilkinson, D.G., and Wainwright, B.J. (1995) Murine Wnt-11 and Wnt-12 have temporally and spatially restricted expression patterns during embryonic development. Mechanisms of development 51:341-350.

Coles, H.S., Burne, J.F., and Raff, M.C. (1993) Large-scale normal cell death in the developing rat kidney and its reduction by epidermal growth factor. Development 118:777-784.

Cullen-McEwen, L.A., Caruana, G., and Bertram, J.F. (2005) The where, what and why of the developing renal stroma. Nephron Exp Nephrol 99:e1-8.

Davies, J., Lyon, M., Gallagher, J., and Garrod, D. (1995) Sulphated proteoglycan is required for collecting duct growth and branching but not nephron formation during kidney development. Development 121:1507-1517.

Davies, J.A. (2003) Development of the ureteric bud. In: P.D., V., A.S., W., and Bard, J.B. (eds) The Kidney: from normal development to congenital disease. Academic Press, London, pp. 165-179.

Davies, J.A. (2005) Cell migration. Mechanisms of morphogenesis: the creation of biological form. Academic Press, London, pp. 93-196.

Davies, J.A. (2006) Branching morphogenesis in mammalian kidneys. In: Davies, J.A. (ed) Branching morphogenesis. Landes Bioscience, Georgetown, pp. 143-159.

Davies, J.A., and Bard, J.B. (1998) The development of the kidney. Current topics in developmental biology 39:245-301.

Davies, J.A., and Fisher, C.E. (2002) Genes and proteins in renal development. Experimental nephrology 10:102-113.

Davies, J.A., and Garrod, D.R. (1995) Induction of early stages of kidney tubule differentiation by lithium ions. Dev Biol 167:50-60.

Davies, J.A., Ladomery, M., Hohenstein, P., Michael, L., Shafe, A., Spraggon, L., and Hastie, N. (2004) Development of an siRNA-based method for repressing specific genes in renal organ culture and its use to show that the Wt1 tumour suppressor is required for nephron differentiation. Human molecular genetics 13:235-246.

Davies, J.A., Millar, C.B., Johnson, E.M., Jr., and Milbrandt, J. (1999) Neurturin: an autocrine regulator of renal collecting duct development. Developmental genetics 24:284-292.

Donovan, M.J., Natoli, T.A., Sainio, K., Amstutz, A., Jaenisch, R., Sariola, H., and Kreidberg, J.A. (1999) Initial differentiation of the metanephric mesenchyme is independent of WT1 and the ureteric bud. Developmental genetics 24:252-262.

Dudley, A.T., Godin, R.E., and Robertson, E.J. (1999) Interaction between FGF and BMP signaling pathways regulates development of metanephric mesenchyme. Genes & development 13:1601-1613.

Dudley, A.T., Lyons, K.M., and Robertson, E.J. (1995) A requirement for bone morphogenetic protein-7 during development of the mammalian kidney and eye. Genes & development 9:2795-2807.

Dudley, A.T., and Robertson, E.J. (1997) Overlapping expression domains of bone morphogenetic protein family members potentially account for limited tissue defects in BMP7 deficient embryos. Dev Dyn 208:349-362.

Duester, G. (2000) Families of retinoid dehydrogenases regulating vitamin A function: production of visual pigment and retinoic acid. European journal of biochemistry / FEBS 267:4315-4324.

Duxbury, M.S., and Whang, E.E. (2004) RNA interference: a practical approach. The Journal of surgical research 117:339-344.

Ekblom, P., and Weller, A. (1991) Ontogeny of tubulointerstitial cells. Kidney international 39:394-400.

Elliott, D.J., and Grellscheid, S.N. (2006) Alternative RNA splicing regulation in the testis. Reproduction (Cambridge, England) 132:811-819.

Esquela, A.F., and Lee, S.J. (2003) Regulation of metanephric kidney development by growth/differentiation factor 11. Dev Biol 257:356-370.

Farina, K.L., Wyckoff, J.B., Rivera, J., Lee, H., Segall, J.E., Condeelis, J.S., and Jones, J.G. (1998) Cell motility of tumor cells visualized in living intact primary tumors using green fluorescent protein. Cancer Res 58:2528-2532.

Farooqui, R., and Fenteany, G. (2005) Multiple rows of cells behind an epithelial wound edge extend cryptic lamellipodia to collectively drive cell-sheet movement. Journal of cell science 118:51-63.

Farooqui, R., Zhu, S., and Fenteany, G. (2006) Glycogen synthase kinase-3 acts upstream of ADP-ribosylation factor 6 and Rac1 to regulate epithelial cell migration. Experimental cell research 312:1514-1525.

Feifel, E., Krall, M., Geibel, J.P., and Pfaller, W. (1997) Differential activities of H+ extrusion systems in MDCK cells due to extracellular osmolality and pH. The American journal of physiology 273:F499-506.

Fenteany, G., Janmey, P.A., and Stossel, T.P. (2000) Signaling pathways and cell mechanics involved in wound closure by epithelial cell sheets. Curr Biol 10:831-838.

Fisher, C.E., Michael, L., Barnett, M.W., and Davies, J.A. (2001) Erk MAP kinase regulates branching morphogenesis in the developing mouse kidney. Development 128:4329-4338.

Fisher, D.A., Kivimae, S., Hoshino, J., Suriben, R., Martin, P.M., Baxter, N., and Cheyette, B.N. (2006) Three Dact gene family members are expressed during embryonic development and in the adult brains of mice. Dev Dyn 235:2620-2630.

Friedl, P., Borgmann, S., and Brocker, E.B. (2001) Amoeboid leukocyte crawling through extracellular matrix: lessons from the Dictyostelium paradigm of cell movement. Journal of leukocyte biology 70:491-509.

Friedl, P., Hegerfeldt, Y., and Tusch, M. (2004) Collective cell migration in morphogenesis and cancer. The International journal of developmental biology 48:441-449.

Friedl, P., and Wolf, K. (2003) Tumour-cell invasion and migration: diversity and escape mechanisms. Nat Rev Cancer 3:362-374.

Gailit, J., and Ruoslahti, E. (1988) Regulation of the fibronectin receptor affinity by divalent cations. J Biol Chem 263:12927-12932.

Ghosh, D. (2000) Object-oriented transcription factors database (ooTFD). Nucleic acids research 28:308-310.

Gilbert, S.F. (2006) Paraxial and intermediate mesoderm In: Gilbert, S.F. (ed) Developmental biology. Sinauer Sssociates, Inc., Sunderland.

Gilbert, T. (2002) Vitamin A and kidney development. Nephrol Dial Transplant 17 Suppl 9:78-80.

Gill, S.E., Pape, M.C., and Leco, K.J. (2006) Tissue inhibitor of metalloproteinases 3 regulates extracellular matrix--cell signaling during bronchiole branching morphogenesis. Dev Biol 298:540-554.

Godin, R.E., Takaesu, N.T., Robertson, E.J., and Dudley, A.T. (1998) Regulation of BMP7 expression during kidney development. Development 125:3473-3482.

Goodyer, P., Kurpad, A., Rekha, S., Muthayya, S., Dwarkanath, P., Iyengar, A., Philip, B., Mhaskar, A., Benjamin, A., Maharaj, S., Laforte, D., Raju, C., and

Phadke, K. (2007) Effects of maternal vitamin A status on kidney development: a pilot study. Pediatric nephrology (Berlin, Germany) 22:209-214.

Gordon, M.D., and Nusse, R. (2006) Wnt signaling: multiple pathways, multiple receptors, and multiple transcription factors. J Biol Chem 281:22429-22433.

Gossen, M., Freundlieb, S., Bender, G., Muller, G., Hillen, W., and Bujard, H. (1995) Transcriptional activation by tetracyclines in mammalian cells. Science 268:1766-1769.

Goumans, M.J., and Mummery, C. (2000) Functional analysis of the TGFbeta receptor/Smad pathway through gene ablation in mice. The International journal of developmental biology 44:253-265.

Grobstein, C. (1953) Inductive epitheliomesenchymal interaction in cultured organ rudiments of the mouse. Science 118:52-55.

Gupta, I.R., Piscione, T.D., Grisaru, S., Phan, T., Macias-Silva, M., Zhou, X., Whiteside, C., Wrana, J.L., and Rosenblum, N.D. (1999) Protein kinase A is a negative regulator of renal branching morphogenesis and modulates inhibitory and stimulatory bone morphogenetic proteins. J Biol Chem 274:26305-26314.

Hammes, A., Guo, J.K., Lutsch, G., Leheste, J.R., Landrock, D., Ziegler, U., Gubler, M.C., and Schedl, A. (2001) Two splice variants of the Wilms' tumor 1 gene have distinct functions during sex determination and nephron formation. Cell 106:319-329.

Hannon, G.J. (2002) RNA interference. Nature 418:244-251.

Hannon, G.J., and Rossi, J.J. (2004) Unlocking the potential of the human genome with RNA interference. Nature 431:371-378.

Hatini, V., Huh, S.O., Herzlinger, D., Soares, V.C., and Lai, E. (1996) Essential role of stromal mesenchyme in kidney morphogenesis revealed by targeted disruption of Winged Helix transcription factor BF-2. Genes & development 10:1467-1478.

Hegerfeldt, Y., Tusch, M., Brocker, E.B., and Friedl, P. (2002) Collective cell movement in primary melanoma explants: plasticity of cell-cell interaction, beta1-integrin function, and migration strategies. Cancer Res 62:2125-2130.

Hellmich, H.L., Kos, L., Cho, E.S., Mahon, K.A., and Zimmer, A. (1996) Embryonic expression of glial cell-line derived neurotrophic factor (GDNF) suggests multiple developmental roles in neural differentiation and epithelial-mesenchymal interactions. Mechanisms of development 54:95-105.

Heuckeroth, R.O., Enomoto, H., Grider, J.R., Golden, J.P., Hanke, J.A., Jackman, A., Molliver, D.C., Bardgett, M.E., Snider, W.D., Johnson, E.M., Jr., and Milbrandt, J. (1999) Gene targeting reveals a critical role for neurturin in the development and maintenance of enteric, sensory, and parasympathetic neurons. Neuron 22:253-263.

Holen, T., Amarzguioui, M., Wiiger, M.T., Babaie, E., and Prydz, H. (2002) Positional effects of short interfering RNAs targeting the human coagulation trigger Tissue Factor. Nucleic acids research 30:1757-1766.

Hoppler, S., and Kavanagh, C.L. (2007) Wnt signalling: variety at the core. Journal of cell science 120:385-393.

Horton, C., and Maden, M. (1995) Endogenous distribution of retinoids during normal development and teratogenesis in the mouse embryo. Dev Dyn 202:312-323.

Hugo, H., Ackland, M.L., Blick, T., Lawrence, M.G., Clements, J.A., Williams, E.D., and Thompson, E.W. (2007) Epithelial--mesenchymal and mesenchymal--epithelial transitions in carcinoma progression. Journal of cellular physiology 213:374-383.

Huppi, K., Martin, S.E., and Caplen, N.J. (2005) Defining and assaying RNAi in mammalian cells. Mol Cell 17:1-10.

Igarashi, P., Vanden Heuvel, G.B., Payne, J.A., and Forbush, B., 3rd (1995) Cloning, embryonic expression, and alternative splicing of a murine kidney-specific Na-K-Cl cotransporter. The American journal of physiology 269:F405-418.

Iglesias, D.M., Hueber, P.A., Chu, L., Campbell, R., Patenaude, A.M., Dziarmaga, A.J., Quinlan, J., Mohamed, O., Dufort, D., and Goodyer, P.R. (2007) Canonical WNT signaling during kidney development. American journal of physiology 293:F494-500.

Itaranta, P., Chi, L., Seppanen, T., Niku, M., Tuukkanen, J., Peltoketo, H., and Vainio, S. (2006) Wnt-4 signaling is involved in the control of smooth muscle cell fate via Bmp-4 in the medullary stroma of the developing kidney. Dev Biol 293:473-483.

Itaranta, P., Lin, Y., Perasaari, J., Roel, G., Destree, O., and Vainio, S. (2002) Wnt-6 is expressed in the ureter bud and induces kidney tubule development in vitro. Genesis 32:259-268.

Jackson, A.L., Bartz, S.R., Schelter, J., Kobayashi, S.V., Burchard, J., Mao, M., Li, B., Cavet, G., and Linsley, P.S. (2003) Expression profiling reveals off-target gene regulation by RNAi. Nature biotechnology 21:635-637.

Jaspars, L.H., Bonnet, P., Bloemena, E., and Meijer, C.J. (1996) Extracellular matrix and beta 1 integrin expression in nodal and extranodal T-cell lymphomas. The Journal of pathology 178:36-43.

Kanwar, Y.S., Liu, Z.Z., Kumar, A., Wada, J., and Carone, F.A. (1995) Cloning of mouse c-ros renal cDNA, its role in development and relationship to extracellular matrix glycoproteins. Kidney international 48:1646-1659.

Karavanova, I.D., Dove, L.F., Resau, J.H., and Perantoni, A.O. (1996) Conditioned medium from a rat ureteric bud cell line in combination with bFGF induces complete differentiation of isolated metanephric mesenchyme. Development 122:4159-4167.

Katoh, M., and Katoh, M. (2003) Identification and characterization of human DAPPER1 and DAPPER2 genes in silico. Int J Oncol 22:907-913.

Kim, D., and Dressler, G.R. (2007) PTEN modulates GDNF/RET mediated chemotaxis and branching morphogenesis in the developing kidney. Dev Biol 307:290-299.

Kim, M., Datta, A., Brakeman, P., Yu, W., and Mostov, K.E. (2007a) Polarity proteins PAR6 and aPKC regulate cell death through GSK-3beta in 3D epithelial morphogenesis. Journal of cell science 120:2309-2317.

Kim, S.E., Lee, W.J., and Choi, K.Y. (2007b) The PI3 kinase-Akt pathway mediates Wnt3a-induced proliferation. Cellular signalling 19:511-518.

Kispert, A., Vainio, S., and McMahon, A.P. (1998) Wnt-4 is a mesenchymal signal for epithelial transformation of metanephric mesenchyme in the developing kidney. Development 125:4225-4234.

Kispert, A., Vainio, S., Shen, L., Rowitch, D.H., and McMahon, A.P. (1996) Proteoglycans are required for maintenance of Wnt-11 expression in the ureter tips. Development 122:3627-3637.

Kitamoto, Y., Tokunaga, H., and Tomita, K. (1997) Vascular endothelial growth factor is an essential molecule for mouse kidney development: glomerulogenesis and nephrogenesis. The Journal of clinical investigation 99:2351-2357.

Kitisin, K., Saha, T., Blake, T., Golestaneh, N., Deng, M., Kim, C., Tang, Y., Shetty, K., Mishra, B., and Mishra, L. (2007) Tgf-Beta signaling in development. Sci STKE 2007:cm1.

Kittler, R., Pelletier, L., Ma, C., Poser, I., Fischer, S., Hyman, A.A., and Buchholz, F. (2005) RNA interference rescue by bacterial artificial chromosome transgenesis in mammalian tissue culture cells. Proceedings of the National Academy of Sciences of the United States of America 102:2396-2401.

Kloth, S., Gmeiner, T., Aigner, J., Jennings, M.L., Rockl, W., and Minuth, W.W. (1998) Transitional stages in the development of the rabbit renal collecting duct. Differentiation 63:21-32.

Kobayashi, A., Kwan, K.M., Carroll, T.J., McMahon, A.P., Mendelsohn, C.L., and Behringer, R.R. (2005) Distinct and sequential tissue-specific activities of the LIM-class homeobox gene Lim1 for tubular morphogenesis during kidney development. Development 132:2809-2823.

Koseki, C., Herzlinger, D., and al-Awqati, Q. (1992) Apoptosis in metanephric development. The Journal of cell biology 119:1327-1333.

Kraus, A.C., Ferber, I., Bachmann, S.O., Specht, H., Wimmel, A., Gross, M.W., Schlegel, J., Suske, G., and Schuermann, M. (2002) In vitro chemo- and radio-resistance in small cell lung cancer correlates with cell adhesion and constitutive activation of AKT and MAP kinase pathways. Oncogene 21:8683-8695.

Kreidberg, J.A., Donovan, M.J., Goldstein, S.L., Rennke, H., Shepherd, K., Jones, R.C., and Jaenisch, R. (1996) Alpha 3 beta 1 integrin has a crucial role in kidney and lung organogenesis. Development 122:3537-3547.

Kreidberg, J.A., Sariola, H., Loring, J.M., Maeda, M., Pelletier, J., Housman, D., and Jaenisch, R. (1993) WT-1 is required for early kidney development. Cell 74:679-691.

Lassus, P., Rodriguez, J., and Lazebnik, Y. (2002) Confirming specificity of RNAi in mammalian cells. Sci STKE 2002:PL13.

Lee, K.Y., Jeong, J.W., Wang, J., Ma, L., Martin, J.F., Tsai, S.Y., Lydon, J.P., and DeMayo, F.J. (2007) Bmp2 is critical for the murine uterine decidual response. Molecular and cellular biology 27:5468-5478.

Lee, W.C., Berry, R., Hohenstein, P., and Davies, J.A. (2008) siRNA as a tool for investigating organogenesis – the pitfalls and the promises. Organogenesis in press.

Lee, W.C., and Davies, J.A. (2006) Dapper1 and Dapper2 are expressed in distinct parts of developing metanephroi. Nephrol Dial Transplant 21:18-19.

Lee, W.C., and Davies, J.A. (2007) Dact1 is a novel target of retinoic acid in renal organogenesis. Nephrol Dial Transplant 22:3.

Leimeister, C., Schumacher, N., Diez, H., and Gessler, M. (2004) Cloning and expression analysis of the mouse stroma marker Snep encoding a novel nidogen domain protein. Dev Dyn 230:371-377.

Lelongt, B., Trugnan, G., Murphy, G., and Ronco, P.M. (1997) Matrix metalloproteinases MMP2 and MMP9 are produced in early stages of kidney morphogenesis but only MMP9 is required for renal organogenesis in vitro. The Journal of cell biology 136:1363-1373.

Levinson, R., and Mendelsohn, C. (2003a) Stromal progenitors are important for patterning epithelial and mesenchymal cell types in the embryonic kidney. Semin Cell Dev Biol 14:225-231.

Levinson, R., and Mendelsohn, C. (2003b) Stromal progenitors are important for patterning epithelial and mesenchymal cell types in the embryonic kidney. Seminars in Cell & Developmental Biology 14:225.

Li, X., Hyink, D.P., Polgar, K., Gusella, G.L., Wilson, P.D., and Burrow, C.R. (2005) Protein kinase X activates ureteric bud branching morphogenesis in developing mouse metanephric kidney. J Am Soc Nephrol 16:3543-3552.

Lin, H.H., Yang, T.P., Jiang, S.T., Yang, H.Y., and Tang, M.J. (1999) Bcl-2 overexpression prevents apoptosis-induced Madin-Darby canine kidney simple epithelial cyst formation. Kidney international 55:168-178.

Lin, X., Yang, J., Chen, J., Gunasekera, A., Fesik, S.W., and Shen, Y. (2004) Development of a tightly regulated U6 promoter for shRNA expression. FEBS letters 577:376-380.

Lin, Y., Liu, A., Zhang, S., Ruusunen, T., Kreidberg, J.A., Peltoketo, H., Drummond, I., and Vainio, S. (2001) Induction of ureter branching as a response to Wnt-2b signaling during early kidney organogenesis. Dev Dyn 222:26-39.

Lindahl, P., Hellstrom, M., Kalen, M., Karlsson, L., Pekny, M., Pekna, M., Soriano, P., and Betsholtz, C. (1998) Paracrine PDGF-B/PDGF-Rbeta signaling controls mesangial cell development in kidney glomeruli. Development 125:3313-3322.

Lindenbergh-Kortleve, D.J., Rosato, R.R., van Neck, J.W., Nauta, J., van Kleffens, M., Groffen, C., Zwarthoff, E.C., and Drop, S.L. (1997) Gene expression of the insulin-like growth factor system during mouse kidney development. Molecular and cellular endocrinology 132:81-91.

Little, M.H., Brennan, J., Georgas, K., Davies, J.A., Davidson, D.R., Baldock, R.A., Beverdam, A., Bertram, J.F., Capel, B., Chiu, H.S., Clements, D., Cullen-McEwen, L., Fleming, J., Gilbert, T., Herzlinger, D., Houghton, D., Kaufman, M.H., Kleymenova, E., Koopman, P.A., Lewis, A.G., McMahon, A.P., Mendelsohn, C.L., Mitchell, E.K., Rumballe, B.A., Sweeney, D.E., Valerius, M.T., Yamada, G., Yang, Y., and Yu, J. (2007) A high-resolution anatomical ontology of the developing murine genitourinary tract. Gene Expr Patterns 7:680-699.

Liu, L., Dunn, S.T., Christakos, S., Hanson-Painton, O., and Bourdeau, J.E. (1993) Calbindin-D28k gene expression in the developing mouse kidney. Kidney international 44:322-330.

Liu, Z.Z., Kumar, A., Ota, K., Wallner, E.I., and Kanwar, Y.S. (1997) Developmental regulation and the role of insulin and insulin receptor in metanephrogenesis. Proceedings of the National Academy of Sciences of the United States of America 94:6758-6763.

Loughna, S., Landels, E., and Woolf, A.S. (1996) Growth factor control of developing kidney endothelial cells. Experimental nephrology 4:112-118.

Luo, G., Hofmann, C., Bronckers, A.L., Sohocki, M., Bradley, A., and Karsenty, G. (1995) BMP-7 is an inducer of nephrogenesis, and is also required for eye development and skeletal patterning. Genes & development 9:2808-2820.

Lyons, K.M., Hogan, B.L., and Robertson, E.J. (1995) Colocalization of BMP 7 and BMP 2 RNAs suggests that these factors cooperatively mediate tissue interactions during murine development. Mechanisms of development 50:71-83.

Maeshima, A., Vaughn, D.A., Choi, Y., and Nigam, S.K. (2006) Activin A is an endogenous inhibitor of ureteric bud outgrowth from the Wolffian duct. Dev Biol 295:473-485.

Maeshima, A., Zhang, Y.Q., Furukawa, M., Naruse, T., and Kojima, I. (2000) Hepatocyte growth factor induces branching tubulogenesis in MDCK cells by modulating the activin-follistatin system. Kidney international 58:1511-1522.

Mai, W., Chen, D., Ding, T., Kim, I., Park, S., Cho, S.Y., Chu, J.S., Liang, D., Wang, N., Wu, D., Li, S., Zhao, P., Zent, R., and Wu, G. (2005) Inhibition of Pkhd1 impairs tubulomorphogenesis of cultured IMCD cells. Molecular biology of the cell 16:4398-4409.

Martinez, G., Mishina, Y., and Bertram, J.F. (2002) BMPs and BMP receptors in mouse metanephric development: in vivo and in vitro studies. The International journal of developmental biology 46:525-533.

McCright, B., Gao, X., Shen, L., Lozier, J., Lan, Y., Maguire, M., Herzlinger, D., Weinmaster, G., Jiang, R., and Gridley, T. (2001) Defects in development of the kidney, heart and eye vasculature in mice homozygous for a hypomorphic Notch2 mutation. Development (Cambridge, England) 128:491-502.

McManus, M.T., and Sharp, P.A. (2002) Gene silencing in mammals by small interfering RNAs. Nature reviews 3:737-747.

Means, A.L., and Gudas, L.J. (1995) The roles of retinoids in vertebrate development. Annual review of biochemistry 64:201-233.

Mendelsohn, C., Batourina, E., Fung, S., Gilbert, T., and Dodd, J. (1999) Stromal cells mediate retinoid-dependent functions essential for renal development. Development 126:1139-1148.

Mendelsohn, C., Lohnes, D., Decimo, D., Lufkin, T., LeMeur, M., Chambon, P., and Mark, M. (1994) Function of the retinoic acid receptors (RARs) during development (II). Multiple abnormalities at various stages of organogenesis in RAR double mutants. Development 120:2749-2771.

Mercado-Pimentel, M.E., Hubbard, A.D., and Runyan, R.B. (2007) Endoglin and Alk5 regulate epithelial-mesenchymal transformation during cardiac valve formation. Dev Biol 304:420-432.

Merkel, C.E., Karner, C.M., and Carroll, T.J. (2007) Molecular regulation of kidney development: is the answer blowing in the Wnt? Pediatric nephrology (Berlin, Germany) 22:1825-1838.

Meyer, T.N., Schwesinger, C., Sampogna, R.V., Vaughn, D.A., Stuart, R.O., Steer, D.L., Bush, K.T., and Nigam, S.K. (2006) Rho kinase acts at separate steps in ureteric bud and metanephric mesenchyme morphogenesis during kidney development. Differentiation 74:638-647.

Michael, L., and Davies, J.A. (2004) Pattern and regulation of cell proliferation during murine ureteric bud development. Journal of anatomy 204:241-255.

Michael, L., Sweeney, D.E., and Davies, J.A. (2007) The lectin Dolichos biflorus agglutinin is a sensitive indicator of branching morphogenetic activity in the developing mouse metanephric collecting duct system. Journal of anatomy 210:89-97.

Milbrandt, J., de Sauvage, F.J., Fahrner, T.J., Baloh, R.H., Leitner, M.L., Tansey, M.G., Lampe, P.A., Heuckeroth, R.O., Kotzbauer, P.T., Simburger, K.S., Golden, J.P., Davies, J.A., Vejsada, R., Kato, A.C., Hynes, M., Sherman, D., Nishimura, M., Wang, L.C., Vandlen, R., Moffat, B., Klein, R.D., Poulsen, K., Gray, C., Garces, A., Johnson, E.M., Jr., and et al. (1998) Persephin, a novel neurotrophic factor related to GDNF and neurturin. Neuron 20:245-253.

Mildner, M., Ballaun, C., Stichenwirth, M., Bauer, R., Gmeiner, R., Buchberger, M., Mlitz, V., and Tschachler, E. (2006) Gene silencing in a human organotypic skin model. Biochemical and biophysical research communications 348:76-82.

Miyazaki, Y., Oshima, K., Fogo, A., Hogan, B.L., and Ichikawa, I. (2000) Bone morphogenetic protein 4 regulates the budding site and elongation of the mouse ureter. The Journal of clinical investigation 105:863-873.

Miyazaki, Y., Oshima, K., Fogo, A., and Ichikawa, I. (2003) Evidence that bone morphogenetic protein 4 has multiple biological functions during kidney and urinary tract development. Kidney international 63:835-844.

Monte, J.C., Sakurai, H., Bush, K.T., and Nigam, S.K. (2007) The developmental nephrome: systems biology in the developing kidney. Current opinion in nephrology and hypertension 16:3-9.

Montesano, R., Schaller, G., and Orci, L. (1991) Induction of epithelial tubular morphogenesis in vitro by fibroblast-derived soluble factors. Cell 66:697-711.

Moon, R.T., Kohn, A.D., De Ferrari, G.V., and Kaykas, A. (2004) WNT and beta-catenin signalling: diseases and therapies. Nature reviews 5:691-701.

Moore, M.W., Klein, R.D., Farinas, I., Sauer, H., Armanini, M., Phillips, H., Reichardt, L.F., Ryan, A.M., Carver-Moore, K., and Rosenthal, A. (1996) Renal and neuronal abnormalities in mice lacking GDNF. Nature 382:76-79.

Moreau, E., Vilar, J., Lelievre-Pegorier, M., Merlet-Benichou, C., and Gilbert, T. (1998) Regulation of c-ret expression by retinoic acid in rat metanephros: implication in nephron mass control. The American journal of physiology 275:F938-945.

Moser, M., Pscherer, A., Roth, C., Becker, J., Mucher, G., Zerres, K., Dixkens, C., Weis, J., Guay-Woodford, L., Buettner, R., and Fassler, R. (1997) Enhanced apoptotic cell death of renal epithelial cells in mice lacking transcription factor AP-2beta. Genes & development 11:1938-1948.

Muller, U., Wang, D., Denda, S., Meneses, J.J., Pedersen, R.A., and Reichardt, L.F. (1997) Integrin alpha8beta1 is critically important for epithelial-mesenchymal interactions during kidney morphogenesis. Cell 88:603-613.

Nagata, M., Nakauchi, H., Nakayama, K., Nakayama, K., Loh, D., and Watanabe, T. (1996) Apoptosis during an early stage of nephrogenesis induces renal hypoplasia in bcl-2-deficient mice. The American journal of pathology 148:1601-1611.

Nakai, S., Sugitani, Y., Sato, H., Ito, S., Miura, Y., Ogawa, M., Nishi, M., Jishage, K., Minowa, O., and Noda, T. (2003) Crucial roles of Brn1 in distal tubule formation and function in mouse kidney. Development 130:4751-4759.

Narita, T., Nishimatsu, S., Wada, N., and Nohno, T. (2007) A Wnt3a variant participates in chick apical ectodermal ridge formation: distinct biological activities of Wnt3a splice variants in chick limb development. Development, growth & differentiation 49:493-501.

Natoli, T.A., Liu, J., Eremina, V., Hodgens, K., Li, C., Hamano, Y., Mundel, P., Kalluri, R., Miner, J.H., Quaggin, S.E., and Kreidberg, J.A. (2002) A mutant

form of the Wilms' tumor suppressor gene WT1 observed in Denys-Drash syndrome interferes with glomerular capillary development. J Am Soc Nephrol 13:2058-2067.

Niederreither, K., Fraulob, V., Garnier, J.M., Chambon, P., and Dolle, P. (2002) Differential expression of retinoic acid-synthesizing (RALDH) enzymes during fetal development and organ differentiation in the mouse. Mechanisms of development 110:165-171.

Nieman, M.T., Prudoff, R.S., Johnson, K.R., and Wheelock, M.J. (1999) N-cadherin promotes motility in human breast cancer cells regardless of their E-cadherin expression. The Journal of cell biology 147:631-644.

Nishinakamura, R., Matsumoto, Y., Nakao, K., Nakamura, K., Sato, A., Copeland, N.G., Gilbert, D.J., Jenkins, N.A., Scully, S., Lacey, D.L., Katsuki, M., Asashima, M., and Yokota, T. (2001) Murine homolog of SALL1 is essential for ureteric bud invasion in kidney development. Development 128:3105-3115.

Nobes, C.D., and Hall, A. (1999) Rho GTPases control polarity, protrusion, and adhesion during cell movement. The Journal of cell biology 144:1235-1244.

O'Brien, L.E., Jou, T.S., Pollack, A.L., Zhang, Q., Hansen, S.H., Yurchenco, P., and Mostov, K.E. (2001) Rac1 orientates epithelial apical polarity through effects on basolateral laminin assembly. Nature cell biology 3:831-838.

O'Brien, L.E., Zegers, M.M., and Mostov, K.E. (2002) Opinion: Building epithelial architecture: insights from three-dimensional culture models. Nat Rev Mol Cell Biol 3:531-537.

Orellana, S.A., and Avner, E.D. (1998) Cell and molecular biology of kidney development. Seminars in nephrology 18:233-243.

Osta, W.A., Chen, Y., Mikhitarian, K., Mitas, M., Salem, M., Hannun, Y.A., Cole, D.J., and Gillanders, W.E. (2004) EpCAM is overexpressed in breast cancer and is a potential target for breast cancer gene therapy. Cancer Res 64:5818-5824.

Oxburgh, L., Chu, G.C., Michael, S.K., and Robertson, E.J. (2004) TGFbeta superfamily signals are required for morphogenesis of the kidney mesenchyme progenitor population. Development 131:4593-4605.

Pachnis, V., Mankoo, B., and Costantini, F. (1993) Expression of the c-ret proto-oncogene during mouse embryogenesis. Development 119:1005-1017.

Palfi, A., Ader, M., Kiang, A.S., Millington-Ward, S., Clark, G., O'Reilly, M., McMahon, H.P., Kenna, P.F., Humphries, P., and Farrar, G.J. (2006) RNAi-

based suppression and replacement of rds-peripherin in retinal organotypic culture. Human mutation 27:260-268.

Park, C.E., Lee, D., Kim, K.H., and Lee, K.A. (2006) Establishment of ovarian reconstruction system in culture for functional genomic analysis. Journal of bioscience and bioengineering 102:396-401.

Paroo, Z., Liu, Q., and Wang, X. (2007) Biochemical mechanisms of the RNA-induced silencing complex. Cell research 17:187-194.

Partanen, A.M. (1990) Epidermal growth factor and transforming growth factor-alpha in the development of epithelial-mesenchymal organs of the mouse. Current topics in developmental biology 24:31-55.

Pepicelli, C.V., Kispert, A., Rowitch, D.H., and McMahon, A.P. (1997) GDNF induces branching and increased cell proliferation in the ureter of the mouse. Dev Biol 192:193-198.

Perantoni, A.O., Dove, L.F., and Karavanova, I. (1995) Basic fibroblast growth factor can mediate the early inductive events in renal development. Proceedings of the National Academy of Sciences of the United States of America 92:4696-4700.

Perez-Pomares, J.M., Mironov, V., Guadix, J.A., Macias, D., Markwald, R.R., and Munoz-Chapuli, R. (2006) In vitro self-assembly of proepicardial cell aggregates: an embryonic vasculogenic model for vascular tissue engineering. The anatomical record 288:700-713.

Persengiev, S.P., Zhu, X., and Green, M.R. (2004) Nonspecific, concentration-dependent stimulation and repression of mammalian gene expression by small interfering RNAs (siRNAs). RNA (New York, N.Y 10:12-18.

Pichel, J.G., Shen, L., Sheng, H.Z., Granholm, A.C., Drago, J., Grinberg, A., Lee, E.J., Huang, S.P., Saarma, M., Hoffer, B.J., Sariola, H., and Westphal, H. (1996) Defects in enteric innervation and kidney development in mice lacking GDNF. Nature 382:73-76.

Piscione, T.D., Yager, T.D., Gupta, I.R., Grinfeld, B., Pei, Y., Attisano, L., Wrana, J.L., and Rosenblum, N.D. (1997) BMP-2 and OP-1 exert direct and opposite effects on renal branching morphogenesis. The American journal of physiology 273:F961-975.

Plisov, S.Y., Yoshino, K., Dove, L.F., Higinbotham, K.G., Rubin, J.S., and Perantoni, A.O. (2001) TGF beta 2, LIF and FGF2 cooperate to induce nephrogenesis. Development 128:1045-1057.

Porteous, S., Torban, E., Cho, N.P., Cunliffe, H., Chua, L., McNoe, L., Ward, T., Souza, C., Gus, P., Giugliani, R., Sato, T., Yun, K., Favor, J., Sicotte, M.,

Goodyer, P., and Eccles, M. (2000) Primary renal hypoplasia in humans and mice with PAX2 mutations: evidence of increased apoptosis in fetal kidneys of Pax2(1Neu) +/- mutant mice. Human molecular genetics 9:1-11.

Pozzi, A., Coffa, S., Bulus, N., Zhu, W., Chen, D., Chen, X., Mernaugh, G., Su, Y., Cai, S., Singh, A., Brissova, M., and Zent, R. (2006) H-Ras, R-Ras, and TC21 differentially regulate ureteric bud cell branching morphogenesis. Molecular biology of the cell 17:2046-2056.

Qiao, J., Cohen, D., and Herzlinger, D. (1995) The metanephric blastema differentiates into collecting system and nephron epithelia in vitro. Development 121:3207-3214.

Qiao, J., Uzzo, R., Obara-Ishihara, T., Degenstein, L., Fuchs, E., and Herzlinger, D. (1999) FGF-7 modulates ureteric bud growth and nephron number in the developing kidney. Development 126:547-554.

Quaggin, S.E., Schwartz, L., Cui, S., Igarashi, P., Deimling, J., Post, M., and Rossant, J. (1999) The basic-helix-loop-helix protein pod1 is critically important for kidney and lung organogenesis. Development 126:5771-5783.

Quinlan, J., Kaplan, F., Sweezey, N., and Goodyer, P. (2007) LGL1, a novel branching morphogen in developing kidney, is induced by retinoic acid. American journal of physiology 293:F987-993.

Rauchman, M.I., Nigam, S.K., Delpire, E., and Gullans, S.R. (1993) An osmotically tolerant inner medullary collecting duct cell line from an SV40 transgenic mouse. The American journal of physiology 265:F416-424.

Reya, T., and Clevers, H. (2005) Wnt signalling in stem cells and cancer. Nature 434:843-850.

Ribes, D., Fischer, E., Calmont, A., and Rossert, J. (2003) Transcriptional control of epithelial differentiation during kidney development. J Am Soc Nephrol 14 Suppl 1:S9-15.

Rintoul, R.C., and Sethi, T. (2001) The role of extracellular matrix in small-cell lung cancer. The lancet oncology 2:437-442.

Ritvos, O., Tuuri, T., Eramaa, M., Sainio, K., Hilden, K., Saxen, L., and Gilbert, S.F. (1995) Activin disrupts epithelial branching morphogenesis in developing glandular organs of the mouse. Mechanisms of development 50:229-245.

Rosowski, M., Falb, M., Tschirschmann, M., and Lauster, R. (2006) Initiation of mesenchymal condensation in alginate hollow spheres--a useful model for understanding cartilage repair? Artificial organs 30:775-784.

Sainio, K. (2003a) Development of the mesonephric kidney In: P.D., V., A.S., W., and Bard, J.B. (eds) The Kidney:from normal development to congenital disease. Academic Press, London, pp. 75-86.

Sainio, K. (2003b) Experimental methods for studying urogenital development. In: P.D., V., A.S., W., and Bard, J.B. (eds) The Kidney: from normal development to congenital disease. Academic Press, London, pp. 327-342.

Sainio, K., Suvanto, P., Davies, J., Wartiovaara, J., Wartiovaara, K., Saarma, M., Arumae, U., Meng, X., Lindahl, M., Pachnis, V., and Sariola, H. (1997) Glial-cell-line-derived neurotrophic factor is required for bud initiation from ureteric epithelium. Development 124:4077-4087.

Sakai, T., Larsen, M., and Yamada, K.M. (2003) Fibronectin requirement in branching morphogenesis. Nature 423:876-881.

Sakurai, H., Barros, E.J., Tsukamoto, T., Barasch, J., and Nigam, S.K. (1997a) An in vitro tubulogenesis system using cell lines derived from the embryonic kidney shows dependence on multiple soluble growth factors. Proceedings of the National Academy of Sciences of the United States of America 94:6279-6284.

Sakurai, H., and Nigam, S.K. (1997) Transforming growth factor-beta selectively inhibits branching morphogenesis but not tubulogenesis. The American journal of physiology 272:F139-146.

Sakurai, H., Tsukamoto, T., Kjelsberg, C.A., Cantley, L.G., and Nigam, S.K. (1997b) EGF receptor ligands are a large fraction of in vitro branching morphogens secreted by embryonic kidney. The American journal of physiology 273:F463-472.

Sampogna, R.V., and Nigam, S.K. (2004) Implications of gene networks for understanding resilience and vulnerability in the kidney branching program. Physiology (Bethesda, Md 19:339-347.

Sanchez, M.P., Silos-Santiago, I., Frisen, J., He, B., Lira, S.A., and Barbacid, M. (1996) Renal agenesis and the absence of enteric neurons in mice lacking GDNF. Nature 382:70-73.

Santy, L.C., and Casanova, J.E. (2001) Activation of ARF6 by ARNO stimulates epithelial cell migration through downstream activation of both Rac1 and phospholipase D. The Journal of cell biology 154:599-610.

Sariola, H., Aufderheide, E., Bernhard, H., Henke-Fahle, S., Dippold, W., and Ekblom, P. (1988) Antibodies to cell surface ganglioside GD3 perturb inductive epithelial-mesenchymal interactions. Cell 54:235-245.

Sariola, H., Sainio, K., and Bard, J.B. (2003a) Fates of the metanephric mesenchyme. In: P.D., V., A.S., W., and Bard, J.B. (eds) The Kidney:from normal development to congenital disease. Academic Press, London, pp. 181-193.

Sariola, H., Sainio, K., and Bard, J.B. (2003b) Fates of the metanephric mesenchyme. In: Vize, P.D., Woolf, A.S., and Bard, J.B. (eds) The kidney, from normal development to congenital disease. Academic Press, London, pp. 181-193.

Sarov, M., and Stewart, A.F. (2005) The best control for the specificity of RNAi. Trends in biotechnology 23:446-448.

Saxen, L. (1987) Organogenesis of the kidney. Cambridge University Press, Cambridge.

Scacheri, P.C., Rozenblatt-Rosen, O., Caplen, N.J., Wolfsberg, T.G., Umayam, L., Lee, J.C., Hughes, C.M., Shanmugam, K.S., Bhattacharjee, A., Meyerson, M., and Collins, F.S. (2004) Short interfering RNAs can induce unexpected and divergent changes in the levels of untargeted proteins in mammalian cells. Proceedings of the National Academy of Sciences of the United States of America 101:1892-1897.

Schmidt-Ott, K.M., Yang, J., Chen, X., Wang, H., Paragas, N., Mori, K., Li, J.Y., Lu, B., Costantini, F., Schiffer, M., Bottinger, E., and Barasch, J. (2005) Novel regulators of kidney development from the tips of the ureteric bud. J Am Soc Nephrol 16:1993-2002.

Schnabel, C.A., Godin, R.E., and Cleary, M.L. (2003) Pbx1 regulates nephrogenesis and ureteric branching in the developing kidney. Dev Biol 254:262-276.

Schuchardt, A., D'Agati, V., Larsson-Blomberg, L., Costantini, F., and Pachnis, V. (1994) Defects in the kidney and enteric nervous system of mice lacking the tyrosine kinase receptor Ret. Nature 367:380-383.

Schuetz, C.S., Bonin, M., Clare, S.E., Nieselt, K., Sotlar, K., Walter, M., Fehm, T., Solomayer, E., Riess, O., Wallwiener, D., Kurek, R., and Neubauer, H.J. (2006) Progression-specific genes identified by expression profiling of matched ductal carcinomas in situ and invasive breast tumors, combining laser capture microdissection and oligonucleotide microarray analysis. Cancer Res 66:5278-5286.

Semenov, M.V., and Snyder, M. (1997) Human dishevelled genes constitute a DHR-containing multigene family. Genomics 42:302-310.

Semizarov, D., Frost, L., Sarthy, A., Kroeger, P., Halbert, D.N., and Fesik, S.W. (2003) Specificity of short interfering RNA determined through gene expression signatures. Proceedings of the National Academy of Sciences of the United States of America 100:6347-6352.

Shah, M.M., Sampogna, R.V., Sakurai, H., Bush, K.T., and Nigam, S.K. (2004) Branching morphogenesis and kidney disease. Development 131:1449-1462.

Shakya, R., Watanabe, T., and Costantini, F. (2005) The role of GDNF/Ret signaling in ureteric bud cell fate and branching morphogenesis. Dev Cell 8:65-74.

Shimono, A., Okuda, T., and Kondoh, H. (1999) N-myc-dependent repression of ndr1, a gene identified by direct subtraction of whole mouse embryo cDNAs between wild type and N-myc mutant. Mechanisms of development 83:39-52.

Shiomi, N., Cui, X.M., Yamamoto, T., Saito, T., and Shuler, C.F. (2006) Inhibition of SMAD2 expression prevents murine palatal fusion. Dev Dyn 235:1785-1793.

Sledz, C.A., Holko, M., de Veer, M.J., Silverman, R.H., and Williams, B.R. (2003) Activation of the interferon system by short-interfering RNAs. Nature cell biology 5:834-839.

Smith, C., and Mackay, S. (1991) Morphological development and fate of the mouse mesonephros. Journal of anatomy 174:171-184.

Song, Y., Zhang, Z., Yu, X., Yan, M., Zhang, X., Gu, S., Stuart, T., Liu, C., Reiser, J., Zhang, Y., and Chen, Y. (2006) Application of lentivirus-mediated RNAi in studying gene function in mammalian tooth development. Dev Dyn 235:1334-1344.

Sorenson, C.M., Rogers, S.A., Korsmeyer, S.J., and Hammerman, M.R. (1995) Fulminant metanephric apoptosis and abnormal kidney development in bcl-2-deficient mice. The American journal of physiology 268:F73-81.

Sponsel, H.T., Breckon, R., Hammond, W., and Anderson, R.J. (1994) Mechanisms of recovery from mechanical injury of renal tubular epithelial cells. The American journal of physiology 267:F257-264.

Stamm, S., Riethoven, J.J., Le Texier, V., Gopalakrishnan, C., Kumanduri, V., Tang, Y., Barbosa-Morais, N.L., and Thanaraj, T.A. (2006) ASD: a bioinformatics resource on alternative splicing. Nucleic acids research 34:D46-55.

Stark, K., Vainio, S., Vassileva, G., and McMahon, A.P. (1994) Epithelial transformation of metanephric mesenchyme in the developing kidney regulated by Wnt-4. Nature 372:679-683.

Stuart, R.O., Bush, K.T., and Nigam, S.K. (2001) Changes in global gene expression patterns during development and maturation of the rat kidney. Proceedings of the National Academy of Sciences of the United States of America 98:5649-5654.

Stuart, R.O., Bush, K.T., and Nigam, S.K. (2003) Changes in gene expression patterns in the ureteric bud and metanephric mesenchyme in models of kidney development. Kidney international 64:1997-2008.

Su, Y., Zhang, L., Gao, X., Meng, F., Wen, J., Zhou, H., Meng, A., and Chen, Y.G. (2007) The evolutionally conserved activity of Dapper2 in antagonizing TGF-beta signaling. Faseb J 21:682-690.

Suriben, R., Fisher, D.A., and Cheyette, B.N. (2006) Dact1 presomitic mesoderm expression oscillates in phase with Axin2 in the somitogenesis clock of mice. Dev Dyn 235:3177-3183.

Tang, M.J., Worley, D., Sanicola, M., and Dressler, G.R. (1998) The RET-glial cell-derived neurotrophic factor (GDNF) pathway stimulates migration and chemoattraction of epithelial cells. The Journal of cell biology 142:1337-1345.

Teebken, O.E., Bader, A., Steinhoff, G., and Haverich, A. (2000) Tissue engineering of vascular grafts: human cell seeding of decellularised porcine matrix. Eur J Vasc Endovasc Surg 19:381-386.

Tian, Y.C., and Phillips, A.O. (2003) TGF-beta1-mediated inhibition of HK-2 cell migration. J Am Soc Nephrol 14:631-640.

Torban, E., Eccles, M.R., Favor, J., and Goodyer, P.R. (2000) PAX2 suppresses apoptosis in renal collecting duct cells. The American journal of pathology 157:833-842.

Trzpis, M., Popa, E.R., McLaughlin, P.M., van Goor, H., Timmer, A., Bosman, G.W., de Leij, L.M., and Harmsen, M.C. (2007) Spatial and Temporal Expression Patterns of the Epithelial Cell Adhesion Molecule (EpCAM/EGP-2) in Developing and Adult Kidneys. Nephron Exp Nephrol 107:e119-e131.

Tufro, A. (2000) VEGF spatially directs angiogenesis during metanephric development in vitro. Dev Biol 227:558-566.

Uehara, Y., Minowa, O., Mori, C., Shiota, K., Kuno, J., Noda, T., and Kitamura, N. (1995) Placental defect and embryonic lethality in mice lacking hepatocyte growth factor/scatter factor. Nature 373:702-705.

Veis, D.J., Sorenson, C.M., Shutter, J.R., and Korsmeyer, S.J. (1993) Bcl-2-deficient mice demonstrate fulminant lymphoid apoptosis, polycystic kidneys, and hypopigmented hair. Cell 75:229-240.

Verkoelen, C.F., Van Der Boom, B.G., and Romijn, J.C. (2000) Identification of hyaluronan as a crystal-binding molecule at the surface of migrating and proliferating MDCK cells. Kidney international 58:1045-1054.

Vilar, J., Gilbert, T., Moreau, E., and Merlet-Benichou, C. (1996) Metanephros organogenesis is highly stimulated by vitamin A derivatives in organ culture. Kidney international 49:1478-1487.

Voet, D., Voet, J.G., and Pratt, C.W. (2002) Fundamentals of biochemistry. Wiley, New York.

Vrljicak, P., Myburgh, D., Ryan, A.K., van Rooijen, M.A., Mummery, C.L., and Gupta, I.R. (2004) Smad expression during kidney development. American journal of physiology 286:F625-633.

Vukicevic, S., Kopp, J.B., Luyten, F.P., and Sampath, T.K. (1996) Induction of nephrogenic mesenchyme by osteogenic protein 1 (bone morphogenetic protein 7). Proceedings of the National Academy of Sciences of the United States of America 93:9021-9026.

Wagner, B., Ricono, J.M., Gorin, Y., Block, K., Arar, M., Riley, D., Choudhury, G.G., and Abboud, H.E. (2007) Mitogenic Signaling via Platelet-Derived Growth Factor beta in Metanephric Mesenchymal Cells. J Am Soc Nephrol 18:2903-2911.

Wang, A.Z., Ojakian, G.K., and Nelson, W.J. (1990) Steps in the morphogenesis of a polarized epithelium. I. Uncoupling the roles of cell-cell and cell-substratum contact in establishing plasma membrane polarity in multicellular epithelial (MDCK) cysts. Journal of cell science 95 (Pt 1):137-151.

Wang, C., and Roy, S.K. (2006) Expression of growth differentiation factor 9 in the oocytes is essential for the development of primordial follicles in the hamster ovary. Endocrinology 147:1725-1734.

Waxman, J.S., Hocking, A.M., Stoick, C.L., and Moon, R.T. (2004) Zebrafish Dapper1 and Dapper2 play distinct roles in Wnt-mediated developmental processes. Development 131:5909-5921.

Welham, S.J., Riley, P.R., Wade, A., Hubank, M., and Woolf, A.S. (2005) Maternal diet programs embryonic kidney gene expression. Physiological genomics 22:48-56.

Weller, A., Sorokin, L., Illgen, E.M., and Ekblom, P. (1991) Development and growth of mouse embryonic kidney in organ culture and modulation of development by soluble growth factor. Dev Biol 144:248-261.

Wellik, D.M., Hawkes, P.J., and Capecchi, M.R. (2002) Hox11 paralogous genes are essential for metanephric kidney induction. Genes & development 16:1423-1432.

Wharton, K.A., Jr. (2003) Runnin' with the Dvl: proteins that associate with Dsh/Dvl and their significance to Wnt signal transduction. Dev Biol 253:1-17.

Widenfalk, J., Nosrat, C., Tomac, A., Westphal, H., Hoffer, B., and Olson, L. (1997) Neurturin and glial cell line-derived neurotrophic factor receptor-beta (GDNFR-beta), novel proteins related to GDNF and GDNFR-alpha with specific cellular patterns of expression suggesting roles in the developing and adult nervous system and in peripheral organs. J Neurosci 17:8506-8519.

Wilkinson, D.G. (1992) Whole mount in situ hybridization of vertebrate embryos. In: Wilkinson, D.G. (ed) In Situ Hybridization: A Practical Approach IRL Press, Oxford, pp. 75-83.

Wilson, J.G., and Warkany, J. (1948) Malformations in the genito-urinary tract induced by maternal vitamin A deficiency in the rat. The American journal of anatomy 83:357-407.

Winyard, P.J., Nauta, J., Lirenman, D.S., Hardman, P., Sams, V.R., Risdon, R.A., and Woolf, A.S. (1996) Deregulation of cell survival in cystic and dysplastic renal development. Kidney international 49:135-146.

Woolf, A.S., Kolatsi-Joannou, M., Hardman, P., Andermarcher, E., Moorby, C., Fine, L.G., Jat, P.S., Noble, M.D., and Gherardi, E. (1995) Roles of hepatocyte growth factor/scatter factor and the met receptor in the early development of the metanephros. The Journal of cell biology 128:171-184.

Woolf, A.S., and Welham, S.J. (2002) Cell turnover in normal and abnormal kidney development. Nephrol Dial Transplant 17 Suppl 9:2-4.

Xu, P.X., Adams, J., Peters, H., Brown, M.C., Heaney, S., and Maas, R. (1999) Eya1-deficient mice lack ears and kidneys and show abnormal apoptosis of organ primordia. Nature genetics 23:113-117.

Xu, P.X., Zheng, W., Huang, L., Maire, P., Laclef, C., and Silvius, D. (2003) Six1 is required for the early organogenesis of mammalian kidney. Development 130:3085-3094.

Yau, T.O., Chan, C.Y., Chan, K.L., Lee, M.F., Wong, C.M., Fan, S.T., and Ng, I.O. (2005) HDPR1, a novel inhibitor of the WNT/beta-catenin signaling, is frequently downregulated in hepatocellular carcinoma: involvement of methylation-mediated gene silencing. Oncogene 24:1607-1614.

Yin, J., Xu, K., Zhang, J., Kumar, A., and Yu, F.S. (2007) Wound-induced ATP release and EGF receptor activation in epithelial cells. Journal of cell science 120:815-825.

Yuan, H.T., Suri, C., Landon, D.N., Yancopoulos, G.D., and Woolf, A.S. (2000) Angiopoietin-2 is a site-specific factor in differentiation of mouse renal vasculature. J Am Soc Nephrol 11:1055-1066.

Yun, M.S., Kim, S.E., Jeon, S.H., Lee, J.S., and Choi, K.Y. (2005) Both ERK and Wnt/beta-catenin pathways are involved in Wnt3a-induced proliferation. Journal of cell science 118:313-322.

Zegers, M.M., O'Brien, L.E., Yu, W., Datta, A., and Mostov, K.E. (2003) Epithelial polarity and tubulogenesis in vitro. Trends in cell biology 13:169-176.

Zeng, Y., Yi, R., and Cullen, B.R. (2003) MicroRNAs and small interfering RNAs can inhibit mRNA expression by similar mechanisms. Proceedings of the National Academy of Sciences of the United States of America 100:9779-9784.

Zhan, Y., Fujino, A., MacLaughlin, D.T., Manganaro, T.F., Szotek, P.P., Arango, N.A., Teixeira, J., and Donahoe, P.K. (2006) Mullerian inhibiting substance regulates its receptor/SMAD signaling and causes mesenchymal transition of the coelomic epithelial cells early in Mullerian duct regression. Development 133:2359-2369.

Zhang, L., Zhou, H., Su, Y., Sun, Z., Zhang, H., Zhang, L., Zhang, Y., Ning, Y., Chen, Y.G., and Meng, A. (2004) Zebrafish Dpr2 inhibits mesoderm induction by promoting degradation of nodal receptors. Science 306:114-117.

Zhu, S., Mc Henry, K.T., Lane, W.S., and Fenteany, G. (2005) A chemical inhibitor reveals the role of Raf kinase inhibitor protein in cell migration. Chemistry & biology 12:981-991.

Zhu, X.H., Wang, C.H., and Tong, Y.W. (2007) Growing tissue-like constructs with Hep3B/HepG2 liver cells on PHBV microspheres of different sizes. Journal of biomedical materials research 82:7-16.